IDENTIFICATION OF MINK1 IN MODULATING ANTI-TUMOR IMMUNITY IN HEPATOCELLULAR CARCINOMA USING AN *IN VIVO* KINOME CRISPR SCREEN

CHU CHIN NGOK

MPhil

The Hong Kong Polytechnic University

2023

The Hong Kong Polytechnic University
Department of Applied Biology and Chemical Technology

Identification of MINK1 in modulating anti-tumor immunity in hepatocellular carcinoma using an *in vivo* kinome CRISPR screen

CHU CHIN NGOK

A thesis submitted in partial fulfilment of the requirements for the degree of Master of Philosophy

Aug 2023

Certificate of Originality

I hereby declare that this thesis is my own work and that, to the best of my knowledge and belief, it reproduces no material previously published or written, nor material that has been accepted for the award of any other degree or diploma, except where due acknowledgement has been made in the text.

___ _____ (Signed)

__CHU CHIN NGOK_____ (Name of student)

Abstract

HCC is the third most lethal cancer and sixth most commonly diagnosed cancer worldwide. Emerging trends in immunotherapy, which have shown higher efficiency and better patient survival, have revolutionized the clinical management of HCC. Despite advances in therapeutic strategies, the low response rate to immune checkpoint inhibitors (ICI) remains a major hurdle in HCC treatment. Therefore, there is an urgent need to study the mechanisms of cancer–immune evasion.

Kinase inhibitors are a popular treatment option for patients with cancer. The focus of kinase inhibitors has recently shifted from targeting pathways related to tumor proliferation to pathways related to immune regulation, as an increasing number of studies have reported the role of kinases in immune escape and ICI resistance. Therefore, we hypothesized that kinase inhibitors would enhance anti-tumor immune responses in HCC. Using an *in vivo* CRISPR knockout screening approach, we injected RIL-175 cells transduced with a kinome-pooled library into immunocompetent wildtype (WT) mice and immunodeficient Rag1-KO mice, and identified protein kinases crucial for immune modulation in HCC. Of all the protein kinases identified, MINK1 (Misshapen Like Kinase 1) showed the most significant result, with all RIL-175 cells with Mink1 knockout depleted in immunocompetent mice. The clinical relevance of MINK1 in HCC was confirmed by analysis of TCGA-LIHC and GEO cohorts, showing that overexpression of MINK1 promotes poor prognosis in HCC patients. Moreover, the TIDE web-based tool suggested that MINK1 overexpression was positively correlated with T cell dysfunction in patients with HCC. To functionally characterize the role of MINK1 in HCC, subcutaneous mouse models with Mink1 knockout have been developed. We observed tumor growth in immunocompetent mice, but not in immunodeficient mice, in Mink1 knockout mouse models.

We further elucidated the mechanisms by which MINK1 affects the immune environment in HCC by a Mink1 overexpression mouse model. Using bulk RNA sequencing analysis, we observed enrichment in inflammation-related pathways and inflammatory factors *Il-6* and *Csf3*, in addition to the downregulation of gene sets linked to T cells, suggesting that Mink1 overexpression may induce changes in gene networks associated with immune microenvironment remodeling and a robust inflammatory response. Mink1 contributes to the immunosuppressive TME, as evidenced by a reduction in $CD8^+$ T cells and a substantial increase in neutrophil infiltration in our Mink1 overexpression model. We performed single-cell RNA sequencing (scRNA-seq) to gain comprehensive insight into the interactions between tumors and neutrophils. Neutrophil increases in tumors belong to the Mmp9-expressing and Pd-l1-expressing populations. Moreover, we observed increased Pd-1 and Pd-l1 expression in T cells and neutrophils. GSEA analysis showed the IL6/JAK/STAT3 pathway was upregulated in the neutrophil population in the Mink1 overexpression sample.

In summary, this study identified Mink1 as a novel regulator of HCC immune evasion and revealed the mechanism by which Mink1 regulates HCC immune evasion is driven by IL-6- and CSF3-induced neutrophil recruitment and suppression of T cell function through PD-1 and PD-L1 interactions between neutrophils and T cells. Increased MMP9 expression may be regulated by the IL6/JAK/STAT3 pathway in neutrophils.

(492 words)

Acknowledgement

First, I would like to thank my esteemed supervisor, Professor Terence Lee Kin Wah. His insightful suggestion on my research topic and direction is the cornerstone of this journey. I am grateful for being supervised by such an enthusiastic and erudite scientist. His relentless pursuit of knowledge ignited my passion for research and cancer study. Despite his busy schedule in managing administrative and department tasks, he generously devoted time to support the whole TLEE team and always prioritized teammates' needs. Throughout my study, his invaluable supervision and unwavering support fostered my academic growth and allowed me to be better equipped for future challenges. I sincerely wish that TLEE team will continue to flourish.

I am grateful for joining the TLEE lab and meeting all my lovely lab mates who provided an environment that I feel valued and supported. I would like to thank Dr. Carmen Leung Oi Ning. Her guidance and detailed teaching of various laboratory techniques have been invaluable. I am truly thankful for her patience and help so that I can overcome struggle to continue experiments. I would also like to thank Dr. Sara Ying Fan, my adventure buddy, for her encouragement and help during my study. Her positive vibes and ideas for organizing awesome hiking trips have kept me motivated. I would like to thank Dr. Sherry Xue Qian Wu for her assistance with mouse experiments. I would also like to thank Dr-to-be Martina Lei Mang Leng for being my guiding light during the study time. Her willingness to share insights has enriched my lab experience in countless ways and her dedication to both scientific excellence and fostering a supportive lab environment has encouraged me to overcome many obstacles. I am grateful to have had my buddy, Ms. Rainbow Leung Wing Hei and Ms. Catherine Gu Yu Jia by my side. Thank you for their warm support both inside and outside the lab, making each day in the lab enjoyable. Great thank also goes to my other lab mates

Ms. Wing Ki Chau, Mr. Gregory Kenneth Muliawan, Ms. Mandy Sze Man Chan, Dr. Shakeel Khan, and my previous lab mate Dr. Etienne Mok Ho Kit.

I would like to express my gratitude to the experimental design advice provided by Professor Stephanie Ma and Dr. Nickolas Teo from The University of Hong Kong. Great thanks to Dr. Johnson Ng Kai Yu for his expertise, generous guidance, and advice on my project.

A special thanks to Haruichi Furudate for creating the inspiring manga "Haikyuu!!" and to Production I.G to bring this story to animation. During the challenging times of my study, "Haikyuu!!" has been a constant source of motivation and inspiration.

Lastly, I would like to express my sincere thanks to my family and friends. Thank you for always supporting me and bear with me for skipping your gatherings for these two years.

Publications

1. **Chu CN**, Lee TKW^. Targeting protein kinases in cancer stem cells. Essays Biochem; 2022;66(4):399-412.

2. Khan SA, Ying F, **Chu CN**, Lee TKW. Network Pharmacology and Molecular Docking Combined with Experiments Reveal Benzoxazinone Derivatives as Potential Therapeutics for Hepatocellular Carcinoma; submitted.

Conference Presentations and Awards

1. **Chu CN**, Lee TKW. An *in vivo* kinome CRISPR-Cas9 screen identifies MINK1 as a modulator of immune evasion in hepatocellular carcinoma. 3rd ABCT Research Postgraduate Symposium in the Biology Discipline 2023 (Poster Presentation Award)

2. **Chu CN**, Leung CON, Gurung S, Chung KPS, Lee TKW. Adipocyte derived FABP4 promotes non alcoholic fatty liver disease induced hepatocellular carcinoma by driving Wnt β catenin signaling cascade. EACR 2023 Congress (EACR 2023 Congress Travel Grant)

Content

List of Figures

List of Tables

List of Abbreviations

AASLD	American association for the study of liver diseases
ADT	Adoptive cell transfer
AKT	Protein kinase B
APC	Adenomatous polyposis coli
APC	antigen presentation cell
ARG1	Arginase 1
ARID2	AT-rich interaction domain 2
ATP	Adenosine triphosphate
ATR	Ataxia telangiectasia and Rad3 related protein
β-cat	Beta-catenin
BCLC	Barcelona clínic liver cancer
CCL	Chemokine (C-C motif) ligand
CDC7	Cell division cycle 7
CDK8	Cyclin dependent kinase 8
CDKN2A	Cyclin-dependent kinase inhibitor 2A
CGC	Cancer Gene Census
CIK cell	Cytokine-induced killer cell
CM	Conditioned medium
CRISPR	Clustered regularly interspaced short palindromic repeats
CSF1	Colony stimulating factor 1
CSF1R	Colony stimulating factor 1 receptor
CSF3	Colony-stimulating factor 3
CTL	Cytotoxic T cell
CTLA-4	Cytotoxic T-lymphocyte-associated protein 4
CTNNB1	Catenin beta 1
CX3CL1	Fractalkine
CXCL	Chemokine (C-X-C motif) ligand
CXCR	CXC chemokine receptor
DC	Dendritic cell
DDLT	Deceased donor liver transplantation
DEG analysis	Differential expression analysis
DMEM	Dulbecco's Modified Eagle Medium
EASL	European association for the study of the liver
EGFR	Epidermal growth factor receptor
ELISA	Enzyme-linked immunosorbent assay
FACS	Fluorescence-activated cell sorting
FAK	Focal adhesion kinase

FC	Fold change
FDA	Food and drug administration
FDR	False discovery rate
FOXP3	Forkhead box P3
GCK	Glucokinase
GEO	Gene Expression Omnibus
GM-CSF	Granulocyte-macrophage colony-stimulating factor
GO	Gene Ontology
GR	Glucocorticoid receptor
GSEA	Gene Set Enrichment Analysis
GW	Gateway
HBV	Hepatitis B virus
HCC	Hepatocellular carcinoma
HCV	Hepatitis C virus
HSC	Hematopoietic stem cell
HTVI	Hydrodynamic tail vein injection
ICAM-1	Intercellular Adhesion Molecule 1
ICI	Immune checkpoint inhibitor
IDO	indoleamine 2,3-dioxygenase
IFN-y	Interferon gamma
Ils	interleukin
iNOS	Inducible nitric oxide synthase
JAK1	Janus kinase 1
JNK	c-Jun N-terminal kinase
KC	kupffer cell
KEGG	Kyoto Encyclopedia of Genes and Genomes
KO	Knock out
KRAS	Ki-ras2 Kirsten rat sarcoma viral oncogene homolog
LAG3	Lymphocyte activating 3
LATS1	Large tumor suppressor kinase 1
LDLT	living donor liver transplantation
LSEC	Liver sinusoidal endothelial cell
LY6C	Lymphocyte antigen 6 family member C
LY6G	Lymphocyte antigen 6 family member G
MAGeCK	Model-based Analysis of Genome-wide CRISPR/Cas9 Knockout
MAP4K6	Mitogen-activated protein kinase kinase kinase kinase 6
MAPK	Mitogen-activated protein kinase
MC	Milan criteria

MDSC	Myeloid-derived suppressor cell
MEK	Mitogen-activated protein kinase kinase
MHC	Major histocompatibility complex
MINK1	Misshapen Like Kinase 1
M-MDSC	Monocytic myeloid derived suppressor cells
MMP9	Matrix metallopeptidase 9
MOI	Multiplicity of infection
MST1/2	Macrophage stimulating 1
NAFLD	Nonalcoholic fatty liver disease
NASH	Nonalcoholic steatohepatitis
NET	Neutrophil extracellular traps
NFE2L2	NFE2 like BZIP transcription factor 2
NF-κB	Nuclear factor kappa B
NK	Natural killer cell
NKT	Natural killer t cell
NLR	Neutrophil-to-lymphocyte ratio
NLRP3	NLR family pyrin domain containing 3
NRK	Nik-related protein kinase
NRTK	Non-receptor tyrosine kinase
OE	Overexpression
OS	Overall survival
PAK3	p21-activated kinase 2
PCA	Principal component analysis
PD-1	Programmed cell death protein 1
PDGFR	Platelet-derived growth factor receptor
PD-L1	Programmed death-ligand 1
PEI	Percutaneous ethanol
PFS	Progression-free survival
PGE2	Prostaglandin E2
PGE2	Prostaglandin E2
PI3K	Phosphoinositide 3-kinases
PIP5K1C	Phosphatidylinositol-4-phosphate 5-Kinase type 1
PKCi	Protein kinase C iota
PMN-MDSC	Polymorphonucler myeloid-derived suppressor cell
QPCTL	Glutaminyl-peptide cyclotransferase-like protein
RAG1	Recombination activating gene 1
RFA	Radiofrequency ablation
ROS	ROS Proto-Oncogene

RPMI	Roswell Park Memorial Institute
RPS6KA3	Ribosomal protein s6 kinase A3
RTK	Receptor tyrosine kinase
SB	Sleeping beauty
sgRNA	Single guide RNA
SIK2	Salt-inducible kinase 2
SMAD2	SMAD Family Member 2
STAT3	Signal transducer and activator of transcription 3
STK	Serine/threonine kinase
SVR	Sustained virological response
TACE	Transarterial chemoembolization
TAM	Tumor-associated macrophage
TAN	Tumor associated neutrophils
TCGA	The Cancer Genome Atlas
Teff	Effector T cell
TERT	Telomerase reverse transcriptase
TGF-β	Transforming growth factor beta
Th17	T helper 17 cell
TIE2	TEK tyrosine kinase
TIL	Tumor-infiltrating lymphocyte
TIM	Timeless
TKI	Tyrosine kinase inhibitor
TLR	Toll-like receptor
TME	Tumor microenvironment
TNF-a	Tumor necrosis factor alpha
TNIK	TRAF2 and NCK-interacting protein kinase
TP53	Tumor protein 53
Treg	Regulatory T cell
TYRO3	TYRO3 Protein Tyrosine Kinase
UMAP	Uniform manifold approximation and projection
UMI	Unique molecular identifiers
VEGF	Vascular endothelial growth factor
VEGFR	VEGF receptor
Wnt	Wingless-related integration site
WT	Wild type

Chapter 1 Introduction

1.1 Hepatocellular carcinoma (HCC)

1.1.1 Epidemiology and etiology of HCC

Hepatocellular carcinoma (HCC) is the most frequent primary liver cancer, accounts for 85-90% of cases. The incidence of HCC has tripled over the last 30 years. Despite being the sixth most commonly diagnosed cancer worldwide, HCC is the third most lethal cancer in 2020, which leads to a relatively high mortality rate with a 5-year overall survival rate of approximately 20% in HCC patients (Llovet et al., 2021).This is due to the poor prognosis resulting from late diagnosis, and the high recurrence rate of HCC in men is 34.8/100,000 persons in 2021, which is three times higher than that in women (Sung et al., 2021). Such disparity of HCC occurrence in terms of sex could be a result of a higher probability of men being exposed to various risk factors and differences in sex hormones.

Developing countries, particularly in Asia and Africa, contribute significantly to the global burden of HCC, (Zhou et al., 2020). However, in recent years, the incidence of HCC in developing countries has significantly decreased due to successful virus prevention strategies. Meanwhile in Europe and the United States, efforts in raising awareness of HCC continue, and HCC has been reported to be the fastest-growing cause of cancer-related deaths in the United States. In Hong Kong, liver cancer is the third leading cause of cancer-related deaths with 1530 deaths reported in 2020 (Census and Statistics Department, 2022). Furthermore, a similar high mortality rate in males was observed when compared to females (31.9 in male vs 9.8 in female per 100,000 persons/individuals), which is consistent with global trends.

Hepatitis B virus (HBV) and hepatitis C virus (HCV) infections, obesity, alcohol abuse, and nonalcoholic steatohepatitis (NASH) are important risk factors for HCC

development (Gomes et al., 2013). In addition, aflatoxin exposure, diabetes mellitus, and smoking can contribute to the development of HCC (Figure 1.1). These risk factors may cause acute or chronic liver disease, which accounts for more than 90% of all HCC cases. Chronic liver disease, hepatic inflammation, and dysregulation of liver regeneration may lead to cirrhosis, which favors genetic and epigenetic alterations that eventually result in the initiation and progression of HCC (Fig. 1) (Weber et al., 2011).

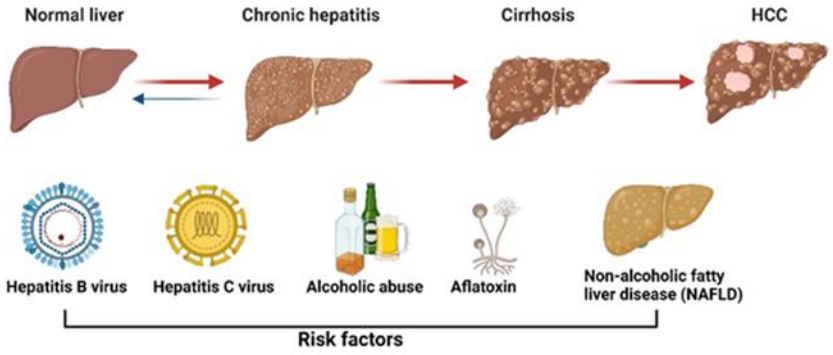

Figure 1.1 Illustration of the mechanisms of HCC development

HBV and HCV infections and other notable risk factors cause genetic and epigenetic aberrations in the liver, leading to acute or chronic liver damage by dysregulation of liver regeneration and the hepatocyte cell cycle.

HBV and HCV infections are the most common etiologies of HCC in developing countries, and are responsible for approximately 60% of HCC cases in Asia (Llovet et al., 2021). HBV is a DNA virus that works via oncogenic activation through viral genome integration into the host cell genome. However, HCV is unable to integrate into the host genome, which poses a risk of HCC that is mainly restricted to individuals with cirrhosis or chronic liver damage. The prevalence of chronic viral infections has significantly decreased in recent decades owing to the widespread implementation of universal HBV vaccination and direct-acting antiviral agents against HCV to increase sustained virological response (SVR) in patients with HCC (Villanueva, 2019).

However, a recent report indicated a delay in the viral hepatitis elimination plan in both developed and developing countries, with a high proportion of patients from the least developed countries, which are yet to be tested for viral infection due to the COVID-19 pandemic (Kondili et al., 2022).

Recently, the attention on viral-induced HCC has shifted towards non-viral-related factors, primarily non-alcoholic fatty liver disease (NAFLD), due to an increase in cases of NASH in Western countries. Meanwhile, an unhealthy diet and lifestyle leads to an increasing prevalence of obesity, knowing that it is the precursor of NAFLD. Unhealthy eating habits and lifestyles lead to an increasing prevalence of obesity, which acts as a precursor of NAFLD. Approximately 20-30% of patients with NAFLD progress to NASH, and approximately 20% of NASH patients would suffer from continuous progression towards cirrhosis (Loomba & Adams, 2019).

1.1.2 Molecular profile of HCC

HCC is a highly heterogeneous malignancy that is believed to stem from a variety of factors, including etiological diversity, genetic alterations, microenvironment complexity, and dysregulation of signaling pathways (Bruix et al., 2014). Recent advances in next-generation sequencing technologies have greatly enhanced our understanding of the pathogenesis of HCC. Through an in-depth understanding of the genome-wide landscape of HCC, various genetic and epigenetic alterations have been reported. Although consensus in terms of predicting or identifying driver genes has not been extensive, most studies have asserted that such driver genes undergo regular mutations in patients with HCC, which ultimately alters several pathways related to HCC (Alqahtani et al., 2019; Rebouissou & Nault, 2020).

(1) Telomere maintenance pathway: Increased telomerase expression that allows unlimited proliferation of cancer cells is detected in the majority of patients with HCC. Key events that lead to telomerase reactivation include telomerase reverse transcriptase (TERT) promoter mutations (54-60%), TERT amplification (5-6%), viral insertions in the promoter (10-15%), and chromosome translocation (Lee et al., 2016; Nault et al., 2013; Totoki et al., 2014). **(2) The cell cycle pathway**: tumor protein 53 (TP53) is mainly involved in the initiation of cell cycle arrest, apoptosis, and DNA repair. This tumor suppressor gene is ranked as the second most frequently mutated gene in HCC (12-48%) and predominantly occurs as a missense mutation within the DNA-binding domain (Guichard et al., 2012; Hsu et al., 1991). Apart from TP53, alteration of cyclin-dependent kinase inhibitor 2A (CDKN2A) was reported in 8% of HCC cases (Guichard et al., 2012); **(3) WNT/β-catenin pathway:** Genes encoding the three key components of this pathway, Catenin Beta 1 (CTNNB1), axis inhibition protein 1 (AXIN1), and adenomatous polyposis coli protein (APC), were found to be frequently mutated in HCC cases (11-35%; 5-15%; and 1.6%, respectively). In particular, CTNNB1 phospho-site mutants lead to constitutive activation of β-catenin, which contributes the most to tumor progression (de La Coste et al., 1998; Satoh et al., 2000). **(4) Epigenetic dysregulation:** Epigenetic changes can lead to aberrant DNA methylation patterns and histone modifications that affect chromatin structure, gene accessibility, and modulation of non-coding RNAs, all of which have profound effects on the development of HCC. For instance, the loss of function of epigenetic drivers, namely ARID1A and ARID2, is involved in chromatin remodeling, which was reported in 18% of HCC cases (Fujimoto et al., 2015). Interestingly, many epigenetic mutants, including ARID1A, are involved in modulating the immune microenvironment of HCC tumors (Feng et al., 2022); **(5) Ras/MAPK signaling pathway:** The MAPK signaling pathway is discovered to be activated in over half of the HCC cases. Surprisingly, activating

mutations in the major regulators of this pathway, RAS and RAF, are rarely found in HCC, which may suggest alternative mechanisms and regulators behind the dysregulation of this pathway in HCC (Zucman-Rossi et al., 2015). Other frequent mutations also occured in PTEN, NFE2L2, and MYC. Considering the highly heterogeneous genomic aberrations in HCC, studies related to the molecular profile of HCC may facilitate disease management for HCC patients by grouping patients into relatively homogeneous subtypes in addition to using the traditional staging system.

Table 1.1 list of the most frequently mutated genes in HCC identified in genome-wide studies

Gene	Mutation frequency (%)	Function
TERT	60.0	Telomere maintenance
TP53	29.2	Tumor suppressor
CTNNB1	27.4	Transcriptional regulator
ARID1A	10.0	Chromatin remodeling
ARID2	9.5	Chromatin remodeling
JAK1	7.7	Kinase
AXIN1	7.5	Signal transducer
NFE2L2	5.1	Transcriptional regulator
RPS6KA3	4.6	Kinase
CDKN2A	4.1	Cell cycle regulator
APC	1.6	Signal transducer
MYC	11	Oncogenic transcriptional regulator

Note. The table is modified from [The mutational landscape of hepatocellular carcinoma] (Lee, 2015)

1.1.3 Current treatments for HCC

The treatment options for HCC are determined based on the stage of cancer diagnosis according to the Barcelona Clinic Liver Cancer (BCLC) staging system (Figure 1.2)(Llovet et al., 2021). This system has been widely adopted and endorsed by both the American Association for the Study of Liver Diseases (AASLD) and the European Association for the Study of the Liver (EASL), and serves as a guide for selecting

appropriate treatment strategies for HCC by classifying HCC patients into 5-stages. Patients with early stage HCC (BCLC 0/A) can undergo resection, local ablation, or liver transplantation and have an excellent prognosis. However, due to the asymptomatic nature of the early stages of HCC, most patients are diagnosed at intermediate or advanced stages. In addition, the recurrence rate of HCC in patients has been reported to reach 70–80% following resection over a 5-year period (Saito et al., 2021). Transarterial chemoembolization (TACE) is the standard treatment for intermediate-stage HCC (BCLC-B). Systemic therapies comprising oral tyrosine kinase inhibitors (TKIs) and immune checkpoint inhibitors (ICIs) have become the treatment of choice for patients with advanced-stage HCC (BCLC-C). Sorafenib and lenvatinib are widely known as major first-line treatment options for patients with advanced-stage HCC (Torimura & Iwamoto, 2022). For patients in the terminal stage (BCLC-D), the sole option is best supportive care (Reig et al., 2022).

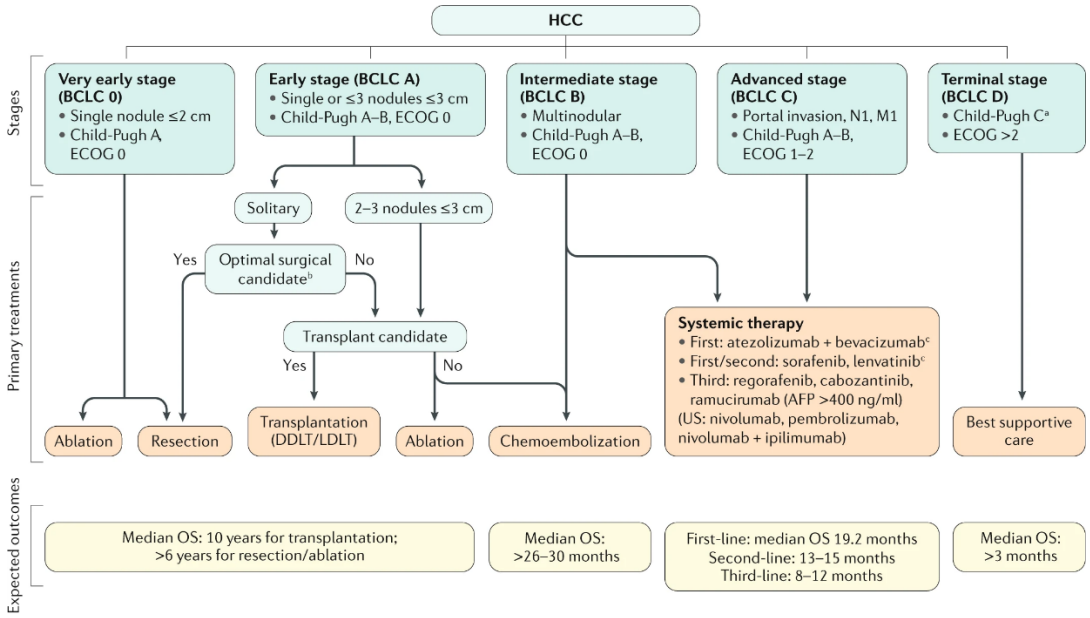

Figure 1.2 BCLC staging system with treatment strategies for HCC patients

The BCLC staging system categorizes hepatocellular carcinoma (HCC) into five distinct stages based on tumor size and patient health status.

Note. The figure is modified from [Hepatocellular carcinoma] (Llovet et al., 2021)

1.1.3.1 Hepatic resection

Hepatic resection is the preferred treatment for HCC in patients meeting the Milan criteria (MC) (HCC tumor up to three lesions < 3 cm or a single lesion < 5 cm, with well-preserved liver function without vascular invasion) (Mazzaferro et al., 1996). Post-surgerical management with a precise assessment of the hepatic reserve is crucial. In patients with concurrent liver cirrhosis, particularly those with portal hypertension, liver resection is not recommended as a first-line treatment option because of the high risk of postoperative liver failure (Bruix et al., 2021). Liver resection offers patients meeting the Milan criteria a significant improvement in the 5-year survival rate of up to 70%. Despite these benefits, HCC recurrence remains high following resection; therefore, combination therapies are often recommended.

1.1.3.2 Liver transplantation

Liver transplantation is the only curative therapeutic approach used to treat patients with HCC in the early stages of cirrhosis, when patients are not suitable for resection. Liver transplantation is usually performed by replacing the entire liver with either a deceased or a living donor. While deceased donor liver transplantation (DDLT) has significantly alleviated the organ shortage challenge, studies have reported higher tumor recurrence rates in HCC patients who underwent DDLT than in those who underwent living donor liver transplantation (LDLT) (Kulik et al., 2012).

Liver transplantation decision is made based on MC, with restriction of patients to possess a single tumor below 5 cm in diameter or up to three tumors less than 3 cm in diameter without vascular invasion (Mazzaferro et al., 1996). Liver transplantation has demonstrated high efficacy, with a 5-year survival rate of approximately 70% and tumor recurrence rate of approximately 10-15%. years, with a 5-year survival rate of 70% and

recurrence rate of 10-15% (Franssen et al., 2014). However, patients who are not eligible for LT require bridging therapies such as TACE and radiofrequency ablation (RFA) to reduce the HCC burden until they are suitable for transplantation procedures. Due to the shortage of donor livers and prolonged waiting time, intrinsic oncogenesis allows patients to be at a high risk of developing a range of health problems, including metabolic and cardiovascular diseases, as well as other types of cancer.

1.1.3.3 Liver ablation

Liver ablation is regarded as a non-surgical treatment for early-stage liver cancer in patients who have preserved liver function and are unable to meet the criteria for either resection or LT (Azab et al., 2011). Two common techniques are percutaneous ethanol injection (PEI), which involves ethanol injection that results in cell dehydration and protein denaturation, leading to tumor necrosis. RFA utilizes electromagnetic energy to heat up and destroy tumor tissue. RFA is generally more effective than PEI and has a complete response rate of > 90%, with a 5-year survival rate of 40-70% (Heimbach et al., 2018). On the other hand, PEI is better suited for smaller tumors and has a complete tumor necrosis rate of 60-100%. Azab and his colleagues (2011) have reported combining RFA with PEI to yield better treatment outcomes than single RFA treatment (Lin et al., 2005).

1.1.3.4 Transarterial chemoembolization (TACE)

TACE is a well-established first-line treatment for intermediate-stage HCC patients with multiple nodules that have not spread to other parts of the body or those who are unable to respond to previous therapeutic modalities. Conventional TACE procedure involves drugs carried by Lipiodol (Lencioni et al., 2005). TACE induces ischemic necrosis by selectively blocking tumor blood vessels and combines the cytotoxic effects

of drugs with tumor starvation. An alternative method to TACE with drug-eluting beads (DEBs) involves the ion exchange mechanism. This approach has shown promising results with a mean patient survival of > 2 years. However, the 3-year survival rate has dropped sharply to approximately 18.1% (Machairas et al., 2021). Recently, the combined approach of TACE followed by RFA has been established as one of the most commonly used methods in HCC treatment, demonstrating a significant overall survival (OS) rate and relapse-free survival rate compared to RFA alone (W. Liu et al., 2020).

1.1.3.5 Systematic therapy

HCC patients show resistance to conventional chemotherapy, with response rates of less than 20% (Deng et al., 2015). Therefore, systemic therapies that interfere with specific signaling pathways involved in HCC regulation, such as Wnt, PI3K-AKT-mTOR, and Vascular endothelial growth factor (VEGF), by blocking crucial components of cellular processes, have become popular and have demonstrated clinical efficacy (Llovet et al., 2021). The combined use of systemic therapies comprising oral TKIs and immune checkpoint inhibitors (ICIs) is an innovative approach that can be applied to HCC patients.

The serine/threonine and tyrosine kinase inhibitor sorafenib was the first FDA-approved first-line treatment for advanced HCC. Sorafenib targets Raf, B-Raf, vascular endothelial growth factor receptors (VEGFRs), and platelet-derived growth factor receptor (PDGFR), which are capable of reducing HCC proliferation and angiogenesis (Kudo et al., 2018). However, sorafenib only provides modest survival benefits compared to placebo in patients with advanced HCC with 3 months prolonged overall survival (NCT00105443) (Llovet et al., 2008). In addition, a low response rate of 2%

and adverse side effects have been reported in clinical trials. Therefore, apart from dosage reduction, treatment strategies that employ combination therapy are suggested to improve treatment outcomes. Recent research indicates that combining sorafenib with hepatic resection leads to improved overall survival in patients with advanced HCC, with a median survival of 15.0 months, compared to 8.0 months in patients who received sorafenib alone (Zhu et al., 2019).

In 2018, another FDA-approved TKI, lenvatinib, specifically targeted VEGFR, PDGFRα, and FGFR to suppress HCC proliferation and angiogenesis, as an alternative to sorafenib as a first-line treatment for unresectable HCC. This drug has a better response rate (40.6% vs. 12.4%) and median progression-free survival (7.3 months vs. 3.6 months) than sorafenib (NCT01761266) (Kudo et al., 2018). A study reported a noticeable trend in favor of lenvatinib over sorafenib for HBV-positive patients, with 59% of HBV cases showing favorable outcomes with lenvatinib (Casadei-Gardini et al., 2022).

In recent years, other multi-TKIs and ICIs have displayed favorable efficacy in patients with advanced-stage HCC, such as regorafenib, which targets VEGFs, c-KIT, and TIE2, and Ramucirumab, which targets VEGFR2, providing more treatment options in the future. In 2020, a combination of bevacizumab, an anti-VEGF antibody, and atezolizumab, an anti-PD-L1 antibody, as first-line treatment for unresectable HCC, was approved by the FDA (Finn, Qin, et al., 2020). Treatments combining ICIs with other agents have become a promising therapeutic approach for HCC, and a detailed discussion of immunotherapy, including ICIs, is included in Section 1.2.3.

1.2 Immunology of HCC and immunotherapy

1.2.1 Mechanism balance tolerance and immunity in normal liver

The liver is an important metabolic and immunological organ constantly exposed to antigen-rich blood from the gastrointestinal tract via the portal vein (Rossetto et al., 2019). The liver immune microenvironment is maintained by a complex cytokine milieu, with both pro-inflammatory and anti-inflammatory cytokines playing a role (Fabregat et al., 2016; Sachdeva et al., 2015). Within the liver sinusoids, a diverse array of immune cells actively survey and eliminate invading pathogens and endotoxins through cytokine- and chemokine-mediated inflammatory activation (Heymann & Tacke, 2016). Briefly, hepatic innate lymphocytes recognize ligands on cells with viral infections and produce a variety of inflammatory cytokines to regulate immune responses. Natural killer T cells (NKTs) can directly kill target cells but have dual functions in modulating immune responses, as these cells secrete both pro- and anti-inflammatory molecules, including IFN-γ, IL-4, and IL-17 (Figure 1.3). In addition to lymphocytes, liver sinusoidal endothelial cells (LSECs), hepatic stellate cells (HSCs), and hepatocytes express toll-like receptors (TLRs), which are classic pattern recognition receptors that activate the immune system (Crispe, 2009; Matsumura et al., 2000).

To maintain a harmonious intrahepatic immune response, a balance between intrinsic liver tolerogenic mechanisms via the innate and adaptive immune responses in the uninflamed liver prevents chronic inflammation and organ autoimmune damage (Bottcher et al., 2011). Simultaneous preservation of the liver's ability to sustain effective responses against pathogens and toxins is required. Facilitated by the cell adhesion molecules ICAM-1 and VCAM-1, antigen presenting cells (APC), including LSECs, HSCs, and DCs, express a wide range of pattern-recognition receptors as they

are able to interact with T cells to promote immune tolerance (Cast et al., 2015; Schildberg et al., 2011). Studies have also reported the role of LSECs in inducing apoptosis of $CD4^+$ T cells and inhibiting the cytotoxic effect of $CD8^+$ T cells by cross-tolerance (Carambia et al., 2013; Limmer et al., 2005). Kupffer cells (KCs) are predominant macrophages in the liver and play a central role in pathogen clearance. Considering their highly plastic phenotype, these cells also employ Tregs to release anti-inflammatory cytokines in response to bacterial endotoxins (Ormandy et al., 2005). Furthermore, IL-10, TGF-β, and arginase produced by myeloid-derived suppressor cells (MDSCs) suppress T-cell activation (Sinha et al., 2007).

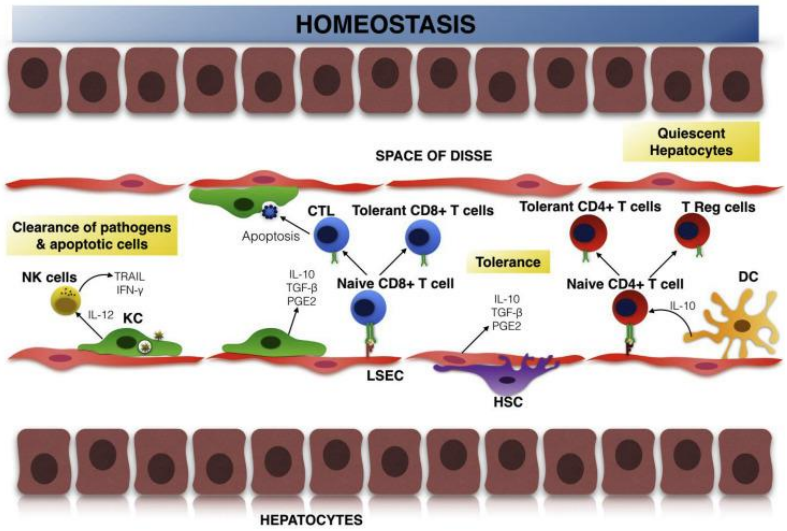

Figure 1.3 Immune cell composition in liver tolerance and homeostasis

Note. The figure is adopted from [Immune cell regulation of liver regeneration and repair] (Li & Hua, 2017)

1.2.2 Hepatocellular Carcinoma Immune Landscape

Liver tolerogenic responses are protective against harmless antigens and autoimmune damage yet detrimental when HCC tumors utilize these innate mechanisms. Mounting evidence has shown that dysregulation of immunological mechanisms by changes in immune cell composition in the tumor microenvironment (TME), elevated expression

of immune checkpoints, and an immunosuppressive tumor microenvironment mediated by cytokines contributes greatly to HCC tumorigenesis and progression (Hato et al., 2014). The TME of HCC consists of hepatocytes, tumor cells, immune cell subsets, immune receptors and ligands, and tumor-associated fibroblasts. This complex cellular interaction with one another through cell–cell interaction and cytokine and chemokine signals, is a critical regulator of tumor immune evasion (Figure 1.4) (Ma et al., 2009; Murakami, 2004; Wu et al., 2009). The immune cell landscape in HCC is discussed below.

1.2.2.1 Innate immune system

A lower frequency of DCs has been reported in HCC patient tissue samples than in healthy controls. Moreover, the same study indicated that these DCs are incapable of infiltrating cancer nodules, thus preventing the priming of $CD8^+$ T cells and anti-tumor immune cell recruitment (Gerner et al., 2008). The functional defect in DCs may be due to dysregulation of tumor antigens and various mediators (e.g., reduction in IL-12 production and increased release of VEGF, IL-10, and TGF-β) in the tumor or stromal cells in the TME (Kakumu et al., 2000; Matsui et al., 2002; Ninomiya et al., 1999). In addition, dysregulation of mature DCs leads to uncontrolled recruitment of Tregs. Recently, a new subset of DCs called $CD14^+$ cytotoxic T-lymphocyte-associated protein DCs expressing PD-1 was observed in patients with HCC (Han et al., 2014).

Similar to DCs, the functionality of NK cells is compromised in HCC. Studies have reported a significant reduction in NK cell subsets in the peripheral blood of HCC patients compared to healthy individuals, where these cell subsets exhibit lower levels of IFN-γ production and cytotoxic potential compared to non-tumor regions (Cai et al., 2008; B. Gao et al., 2009). Impaired NK cell function is caused by exhaustion,

dysregulation of inhibitory and activating receptors on NK cells, and infiltration of immature NK cells (Muhanna et al., 2008; Zecca et al., 2022). Severe hypoxia within the TME, in addition to exposure to immunomodulatory molecules, such as prostaglandin E2 (PGE2) and indoleamine 2,3-dioxygenase (IDO), contributes to the dysfunction of NK cells in the TME of HCC (Hoechst et al., 2009; Li et al., 2012).

An increased number of tumor-associated macrophages (TAMs) in HCC is associated with an unfavorable prognosis (Zhang et al., 2016). Macrophages, one of the most abundant tumor-infiltrating immune cell types, tend to differentiate into oncogenic M2 phenotypes upon tumor infiltration. Characterized by the expression of IL-10 and TGF-β as well as reduced antigen presentation capacity, TAMs promote tumor initiation, progression, and metastasis through various pathways involving the TLR4/STAT3, TLR4/ NF-κB, Wnt/β-catenin signaling pathways (Z. Li et al., 2019; Wang et al., 2014). TAMs enhance the recruitment and generation of Tregs by stimulating the activation of the T helper type 2 immune response. Moreover, interactions between TAMs, MDSCs, and Tregs lead to changes in chemokine production, expression of major histocompatibility complex class (MHC) I and II molecules, subsequent immunosuppression, and development of HCC (C. Lu et al., 2019).

MDSCs are a heterogeneous population consisting of early myeloid progenitors and immature granulocytes that possess immunosuppressive functions within the cancer context. There are two main subtypes of MDSCs, monocytic MDSCs (M-MDSCs) and polymorphonuclear MDSCs (PMN-MDSCs). M-MDSCs exhibit morphological characteristics similar to those of monocytes, whereas PMN-MDSCs resemble neutrophils. In patients with HCC, M-MDSCs accumulate and contribute to the establishment of an immunosuppressive TME by recruiting Tregs and suppressing NK

cells (Li et al., 2017; L. C. Lu et al., 2019). MDSC-mediated immunosuppression involves the production of various factors including iNOS, ROS, TGF-β, IL-10, IDO, and arginase (ARG1) (Bronte et al., 2003). Depletion of L-arginine by ARG1 leads to cell cycle arrest in tumor-infiltrating T cells. Moreover, the increased production of nitric oxide (NO) by iNOS and elevated levels of ROS contribute to the downregulation and desensitization of the T-cell receptor. In addition, IL-10 and TGF-β enable MDSCs to inhibit T cell proliferation, hinder DCs development, and impair the functionality of T and NK cells (Ostrand-Rosenberg et al., 2012).

Tumor-associated neutrophils (TANs) are unfavorable prognostic factors for patients with HCC (Arvanitakis et al., 2021). Similar to TAMs, TANs can exhibit either an anti-tumor N1 phenotype or a pro-tumor N2 phenotype. In HCC, TANs mediate immunosuppression and sorafenib resistance by recruiting TAMs and Tregs (Zhou et al., 2016). Clinical analysis of HCC samples implied a decrease in the number of T cells in samples with TANs infiltration and PD-L1 overexpression (He et al., 2015). The activation and modulation of TANs involve various molecules, including IL-17, CXCL1, CXCL2, and CXCL5 (McFarlane et al., 2021).

1.2.2.2 Adaptive immune system

$CD4^+$ and $CD8^+$ T lymphocytes (TILs) are the primary tumor-infiltrating lymphocyte subsets that function as anti-tumor elements. The activation of IFN-γ-producing $CD8^+$ T cells following the recognition of tumor antigens by APCs via MHC class I molecules is crucial for the surveillance of tumor cells in HCC (Sachdeva et al., 2015). A decrease in the number and increased exhaustion of these subsets have been observed in patients with liver cirrhosis and HCC (Fu et al., 2007). Clinical data has shown improved OS and favorable prognosis in human HCC patients with increasing $CD8^+$ TILs (Zhang et

al., 2018). Depletion of $CD4^+$ T cells in an HCC mouse model promoted an immunosuppressive TME (Ma et al., 2016). Moreover, MDSCs upregulate PD-L1 expression, causing functional exhaustion of effector T cells and subsequent inhibition of B-cell maturation through reduction of IL-21 secretion in HCC (Wu et al., 2009).

Infiltration of Tregs in patients with HCC is associated with poor prognosis (Zhou et al., 2009). The activation of Tregs is mediated by T-cell receptor (TCR) interactions, as well as signaling pathways involving IL-10 and TGF-β. Tregs, characterized by $Foxp3^+$ expression, blocks the release of perforin and granzymes and suppress key cytokines required for $CD8^+$ T cell activation (Rudensky, 2011; Sakaguchi et al., 2008). Clinical sample analysis further confirmed the reduced infiltration of $CD8^+$ T cells in tumor regions due to the accumulation of Tregs (Fu et al., 2007). The imbalance in T cell populations, with a decreased ratio of helper T cells to Tregs in the peripheral blood of patients with HCC, contributes to immune suppression (Lan et al., 2017). Recent studies have also indicated that an imbalance in the proportion of Th17 cells and Tregs promotes cancer progression, but further studies are required to gain mechanistic insight.

NKT cells, characterized by the expression of both TCR and NK cell receptors, exhibit potent cytokine production, including IL-4, IFN-γ, and TNF-α (Sachdeva et al., 2015). Their role in cancer is complex, acting as a double-edged sword by promoting anti-tumor responses through Teffs activation while simultaneously enhancing immune suppressor cell populations and inducing immune tolerance (Berzofsky & Terabe, 2009). In murine HCC models, Sachdeva et al. reported that the interaction between CXCR6 on NKT cells and its ligand CXCL16 on LSECs attracted NKT cells to the liver to suppress tumor growth (Ma et al., 2018). Although the frequency of NKT cells

is increased in patients with HCC, the influence of this subset on patient prognosis remains uncertain.

1.2.2.3 Interleukins and Chemokines

Cytokines play a crucial role in regulating the immune cell microenvironment in HCC by exerting both supportive and inhibitory effects through diverse signaling pathways. Immune suppression in the liver is primarily mediated by a balance between pro-inflammatory and anti-inflammatory cytokines (Sachdeva et al., 2015).

The Th1/Th2 balance is a strong determinant of anti-tumor immunity (Woo et al., 2008). Naïve $CD4^+$ cells differentiate into Th1 cells and activate $CD8^+$ cells in the presence of IL-12 and IFN-γ, whereas IL-4 drives the differentiation of $CD4^+$ T cells into Th2 cells (Akiba et al., 2001; Ikeguchi & Hirooka, 2005). The expression of Th1 cytokines in tumor tissues is associated with a favorable prognosis. However, liver cancer cells often exhibit a Th2 cytokine profile characterized by increased levels of anti-inflammatory cytokines, decreased levels of pro-inflammatory cytokines, and inhibition of tumor-specific $CD8^+$ T cell responses (Saxena & Kaur, 2015). The anti-inflammatory cytokines, IL-6 and IL-10, are often elevated in HCC and have been extensively studied. These interleukins inhibit T cell activation by suppressing the production of pro-inflammatory cytokines, promoting Treg differentiation, and impairing NKs (Beckebaum et al., 2004; Giannitrapani et al., 2002; Wong et al., 2009). Elevated serum TNF-α levels have also been observed in patients with HCC. TNF-α upregulates the expression of PD-L1 in macrophages, which suppresses the anti-tumor immune response mediated by $CD8^+$ T cells (Kuang et al., 2009). Additionally, TNF-α is induced by NF-κB in a positive feedback loop, which contributes to its immunosuppressive effects in HCC. Studies have indicated that both IL-1β and IL37 may stimulate the

production of cytokines to initiate immune processes in HCC (Sachdeva et al., 2015).

Chemokines are small soluble proteins that play a critical role in directing the recruitment of white blood cells, including lymphocytes, to HCC through their chemokine receptors (Yoong et al., 1999). These chemokines are involved in various events such as Th1/Th2 development. Several well-studied chemokine ligand-chemokine receptor axes, including CXCL12-CXCR4 and CCL20-CCR6, are associated with tumor progression by promoting tumor growth, invasion, and metastasis (Rubie et al., 2006; Sutton et al., 2007). Higher expression levels of CXCR3 have been reported in tumor-infiltrating cells than in peripheral lymphocytes (Oo et al., 2012). Additionally, the expression levels of chemokine receptors, such as CCR5 and CCR6, in the peripheral lymphocytes of HCC patients were also reduced, while their expression in tumor-infiltrating cells was elevated (Liu et al., 2004; Zahran et al., 2020). This suggests a role for these chemokine receptors in controlling the trafficking of Teffs to tumor regions. Studies have also suggested a role for fractalkine (CX3CL1) and its receptor ,CX3CR1, in HCC immune response regulation (Matsubara et al., 2007).

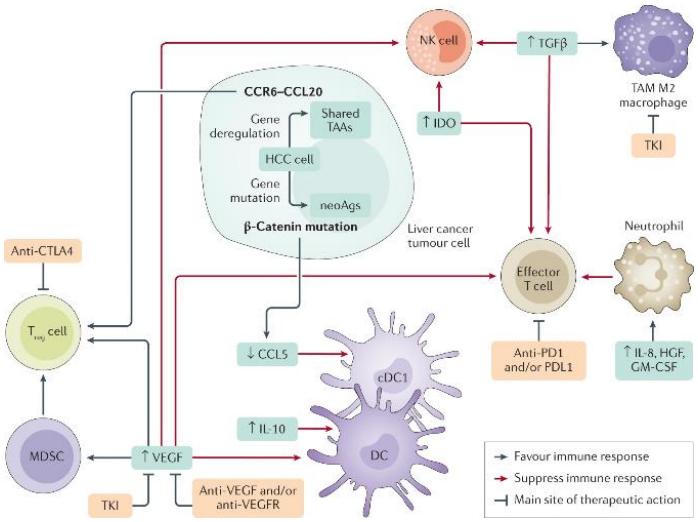

Figure 1.4 The landscape of immunosuppressive TME of HCC

Crosstalk between the TME and HCC cells is critical for cancer immune evasion because it promotes the

activation of immunosuppressive cells while inhibiting the regulation of immune surveillance.
Note. The figure is adopted from [Advances in immunotherapy for hepatocellular carcinoma] (Sangro et al., 2021)

1.2.3 Current immunotherapeutic

A great breakthrough has been made in understanding tumor immune surveillance using newly developed immunotherapies, revolutionizing the clinical management of HCC. The inhibition of ICIs in cancer therapy has been proven effective in disrupting the immune evasion mechanisms employed by HCC (El-Khoueiry et al., 2017; Qin et al., 2020). Apart from ICIs, different therapeutic strategies targeting impaired presentation of antigens, dysfunction of Teffs, promotion of Treg and MDSCs proliferation, and dysregulation of cytokine profiles have been investigated.

1.2.3.1. Immune checkpoint inhibitors (ICI)

Immune checkpoint components play a critical role in regulating the activation and tolerance of various immune cells. Well-known immune checkpoints (ICs) include CTLA-4, which regulates Teff and Treg, PD1 that regulate T cell exhaustion; T cell immunoglobulin and mucin domain containing-3 (TIM3); and lymphocyte-activation gene 3 (LAG3). These ICs function as co-inhibitory molecules that prevent the hyperactivation of the immune response to maintain immune homeostasis (Agdashian et al., 2019; Q. Gao et al., 2009; Liu et al., 2018). However, HCC and other cancers exploit this regulatory mechanism by expressing the corresponding ligands on tumor and stromal cells, thereby facilitating tumor immune evasion (Rabinovich et al., 2007). Immune checkpoint inhibitors (ICIs) have been developed to counteract this immune evasion strategy. ICIs are monoclonal antibodies that suppress the immune response against tumors by blocking the interaction between immune checkpoint proteins and their ligands (Sangro et al., 2021). By inhibiting inhibitory signals, ICIs restore the

activation and proliferation of T cells, enhance cytotoxic activity, and promote the release of pro-inflammatory mediators (Ribas & Wolchok, 2018).

Accumulating studies and trials have assessed the safety and efficacy of ICIs alone or in combination with other therapies to enhance anti-tumor immune responses in HCC (Table 1.2). To date, combined treatment with ICIs targeting CTLA-4, PD-1, or its ligand PD-L1, as well as other reagents, have been approved by the FDA for HCC treatment, resulting in better outcomes than sorafenib treatments (Finn, Qin, et al., 2020; Qin et al., 2019; Yau et al., 2022).

Table 1.2 Summary of clinical studies investigating immune checkpoint inhibitor in HCC

Treatment	Target	Clinical trial phrase (Patients number)	Clinical trial number	References
Monotherapy				
Nivolumab	PD-1	I/II (262)	NCT01658878	(El-Khoueiry et al., 2017)
Pembrolizumab	PD-1	II (104)	NCT02702414	(Zhu et al., 2018)
Camrelizumab	PD-1	II (220)	NCT02989922	(Qin et al., 2020)
Tislelizumab	PD-1	III (674)	NCT03412773	(Qin et al., 2019)
Durvulumab	PD-L1	I/II (1022)	NCT01693562	(Garon et al., 2023)
Tremelimumab	CTLA-4	II (21)	NCT01008358	(Sangro et al., 2013)
Cabolimab	Tim-3	I (369)	NCT02817633	(G. Li et al., 2019)
ICI + ICI				
Tremelimumab + Durvalumab	CTLA-4 PD-L1	III (1504)	NCT03298451	(Okusaka & Ikeda, 2018)
Nivolumab +	PD-1	I/II (148)	NCT01658878	(Yau et al.,

Ipilimumab	CTLA-4			2020)
Nivolumab + Ipilimumab	PD-1 CTLA-4	II (30)	NCT03222076	(Okusaka & Ikeda, 2018)
ICI + angiogenesis inhibitor				
Atezolizumab + Bevacizumab	PD-L1 VEGF	III (480)	NCT03434379	(Finn, Qin, et al., 2020)
Lenvatinib + Pembrolizumab	VEGFR PD-1	Ib (104)	NCT03006926	(Finn, Ikeda, et al., 2020)
Levantinib + pembrolizumab	VEGFR PD-1	III (750)	NCT03713593	(Sachdeva et al., 2015)
Camrelizumab + Apatinib	PD-1 VEGFR2	I (14)	NCT02942329	(Xu et al., 2019)
Avelumab+ Axitinib	PD-L1 VEGF	I (22)	NCT03289533	(Leone et al., 2021)

Early phase clinical trials assessing the efficacy of anti-PD-1/PD-L1 and anti-CTLA-4 monotherapies have shown encouraging outcomes in terms of survival and safety. The CheckMate 040 trial (NCT01658878) reported objective responses for 17 months, a median objective response rate of 15%, and a median overall survival of 15.6 months with nivolumab (anti-PD-L1 antibody) (El-Khoueiry et al., 2017). In the KENYOTE-224 trial (NCT02702414), pembrolizumab (anti-PD-1 antibody) demonstrated an objective response rate of 17% but had a progression-free survival of only 4.9 months (Zhu et al., 2018). These results have led to the accelerated approval by the FDA of nivolumab and pembrolizumab for the treatment of hepatocellular carcinoma (HCC) in 2017 and 2018, respectively. Camrelizumab, evaluated in a phase II trial (NCT02989922), exhibited a similar response rate of 14.7% and 6-month overall survival probability of 74.4% (Qin et al., 2020). Tremelimumab also led to significant tumor reduction in patients with HCC and HCV infection, as suggested by the reduction in Tregs within the tumor (Sangro et al., 2013). Ongoing clinical trials are investigating

the efficacy of other ICIs, such as tislelizumab and durvulumab, for the treatment of HCC (Garon et al., 2023; Qin et al., 2019). Despite promising preliminary results in terms of safety, anti-tumor effects, and anti-hepatitis viral effects of ICIs as monotherapy, phase III trials have been unable to replicate these findings. The CheckMate459 trial compared nivolumab with sorafenib as a first-line treatment but did not demonstrate a statistically significant survival advantage (Yau et al., 2022). Similarly, as reported by the KEYNOTE-240 trial, pembrolizumab did not improve overall survival (OS) or progression-free survival (PFS) when used as a second-line treatment following sorafenib therapy (Kudo et al., 2021).

Considering the efficacy of single-agent ICIs, therapeutic strategies have shifted toward combining agents to enhance therapeutic outcomes by targeting multiple immune pathways simultaneously or by combining ICIs with other treatment methods, such as TKIs or radiation therapy. The rationale behind these combinations is to achieve synergistic effects, overcome resistance mechanisms, and improve survival.

In 2020, the FDA approved the combination of nivolumab (an anti-PD-1 antibody) and ipilimumab (an anti-CTLA-4 antibody) as second-line treatment for HCC (NCT02477826) (Iinuma et al., 2022). Preliminary results from such drug combinations demonstrated a robust median patient overall survival of 22.8 months. As HCC is associated with intense vascularization, the rationale for ICIs with therapies targeting vascular endothelial growth factor (VEGF) has been raised. Studies have shown that this strategy is successful because VEGF blockade enhances the efficacy of ICIs in preclinical HCC models (Finn, Qin, et al., 2020). The combination of bevacizumab (anti-VEGF antibody) and atezolizumab (anti-PD-L1 antibody) as a first-line treatment for unresectable HCC was approved by the FDA. The combination treatment resulted

in durable clinical responses, significant increases in overall survival compared with sorafenib (84.8% vs. 72.2% over 6 months), and improved progression-free survival (54.5% vs. 37.2%) (NCT03434379) (Fig. 1.5) (Finn, Qin, et al., 2020). These clinical results proved that ICI combination therapy may become a new standard of care for HCC patients, and future studies and clinical trials should focus on optimizing the immunotherapeutic approach by examining the efficacy of different ICI-ICI or ICI-other therapy combinations. Nevertheless, a low response rate has been reported in clinical trials, including a phase 3 trial of bevacizumab plus atezolizumab treatment (30% objective response with 8% complete response) (NCT03434379) and a phase 3 trial of nivolumab (15% objective response with 4% complete response) (NCT02576509), resulting in an urgent need to study the detailed mechanisms of cancer–immune evasion to improve the response rate and efficacy of immunotherapy agents (Finn, Qin, et al., 2020; Yau et al., 2022).

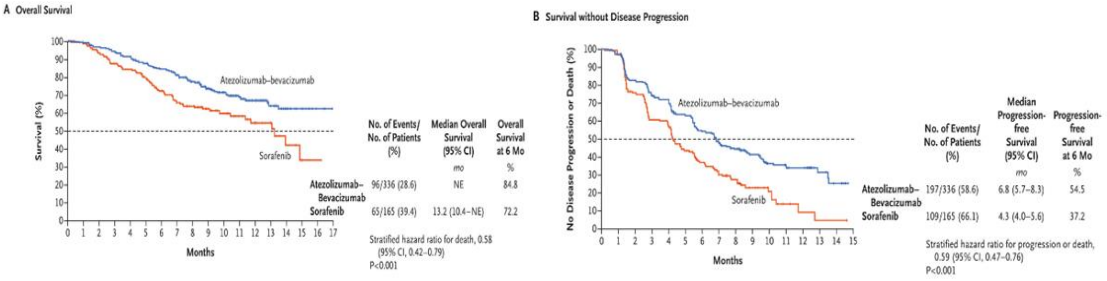

Figure 1.5 Kaplan-Meier curves of (A) overall survival and (B) progression-free survival of HCC patients treated with atezolizumab/bevacizumab

Note. The figure is adopted from [Atezolizumab plus Bevacizumab in Unresectable Hepatocellular Carcinoma] (Finn, Qin, et al., 2020)

1.2.3.2 Other HCC immunotherapies

Adoptive cell transfer (ACT) therapy involves the expansion and infusion of autologous anti-tumor T-cells to enhance the immune response against tumor cells. The effector cells used in ACT therapy include CIK cells, TILs, NK cells, and LAK cells (Zhang et al., 2019). It was believed that ACT would be challenging to apply to HCC until clinical trials have shown positive results in terms of PFS and OS, particularly with CIK-based infusions (D. Shi et al., 2020; Zhou et al., 2019). Future investigations should explore combination therapies involving ACT to maximize their efficacy in patients with HCC. Therapeutic vaccines aim to generate potent tumor-specific immune responses to overcome the immunosuppressive TME by introducing tumor-associated antigens (TAAs) into patients (Reparaz et al., 2022). Combination therapy with ICIs or ACT is recommended. In HCC, vaccines targeting AFP-derived peptides, glypican 3 (GPC3), and telomerase peptides have been evaluated because of their high expression in HCC (Nakagawa et al., 2017; D. Shi et al., 2020; Tornesello et al., 2022). Another strategy that involves the use of neoantigens has been identified by analyzing mutations, gene expression, and immune-related factors. However, the limited immunogenicity of the existing vaccines has hampered this progress.

1.3 Protein Kinase

1.3.1 Introduction to protein kinase superfamily

The protein kinase superfamily has been classified into three groups: serine/threonine kinases (STKs), tyrosine kinases (TKs), and dual-specificity kinases that act as both STKs and TKs based on the phosphorylated hydroxy-amino-acid target (Ardito et al., 2017). Tyrosine kinases are further categorized into receptor tyrosine kinases (RTKs), which are located on the cellular membrane, and non-receptor tyrosine kinases (NRTKs), which are found in the cytosol (Siveen et al., 2018). Kinases contain a catalytic domain of approximately 250-300 amino acids. Briefly, a typical protein kinase consists of a conserved core composed of a smaller N-terminal lobe containing mainly β-sheets involved in adenosine triphosphate (ATP) binding and substrate orientation and a larger C-terminal lobe containing mainly α-helices for catalytic activity and regulation (Figure 1.6A) (McClendon et al., 2014). The sequences and structures of protein kinases have been studied extensively, leading to the identification of conserved residues and motifs that are important for kinase function. In the early 1980s, the kinase domain was first sequenced, and subsequent sequencing revealed highly conserved residues presumed to be critical for kinase activity (Shoji et al., 1981). In 1995, Hanks and Hunter divided the kinase domain into 12 subdomains (I-XII), providing a framework for analyzing kinase sequence variations (Hanks & Hunter, 1995). The N-terminal lobe, comprising subdomains I-IV, contains a glycine-rich loop (GxGxΦG) that is important for ATP binding and an αC helix that undergoes conformational changes upon kinase activation (Hemmer et al., 1997). The interaction between β3-strand lysine and αC helix glutamate plays a crucial role in the formation of an activated state (McSkimming et al., 2017). The C-terminal lobe contains subdomains VI-XII and includes catalytic and activation segments. Additionally, a lysine residue within the catalytic loop forms ionic interactions with the γ-phosphate of

ATP, thereby facilitating catalysis (Knighton et al., 1991). The C-terminal region of the DFG motif is an activated kinase segment. In inactive kinases, an activation loop obstructs the kinase active site, thereby preventing substrate phosphorylation (Nolen et al., 2004). Following phosphorylation, the loop binds to the catalytic core, thereby exposing the active site for substrate-binding.

In the early 2000s, studies discovered that protein kinases catalyze phosphorylation by transferring γ-phosphate from ATP to the hydroxyl group of a serine, threonine, or tyrosine residue of substrate proteins (Figure 1.6B) (Matte et al., 1998). Subsequent research on mitogen-activated protein kinase (MAPK) cascades has revealed the capacity of kinases to function as both catalysts and substrates, suggesting a signal amplification function of kinases (Pearson et al., 2001). Sequential phosphorylation events in kinases enable efficient and faster transmission of signals to multiple target proteins, triggering coordinated cellular responses, and facilitating complex cellular processes. Protein phosphorylation can be reversed by phosphatase enzymes, which are powerful regulatory mechanisms that enable precise control of protein activity, localization, and signaling for dynamic cellular processes (Miller et al., 1996).

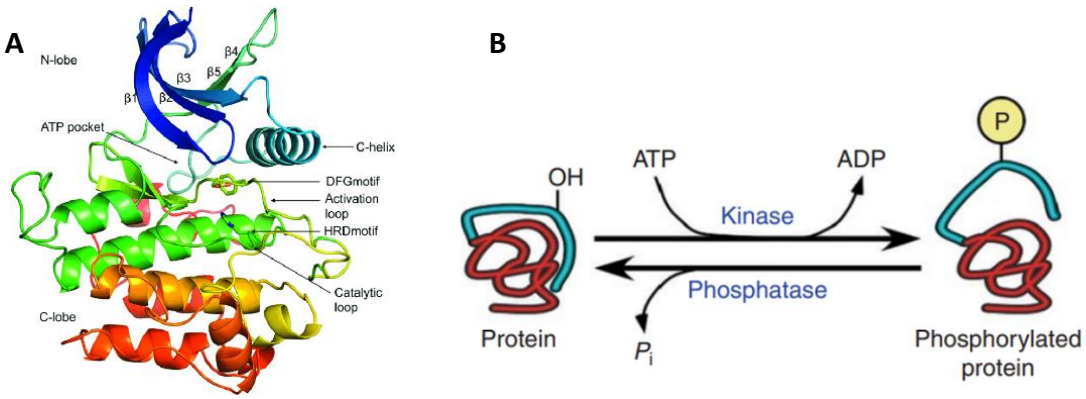

Figure 1.6 (A) Structure of a typical protein kinase domain, including ATP-binding sites and conserved structures. **(B)** The mechanism of protein phosphorylation

regulated by protein kinases and phosphatase.

Note. The figure is adopted from [Defining a new nomenclature for the structures of active and inactive kinases] (Modi & Dunbrack, 2019)

1.3.2 Role of protein kinase in cancer regulation and potential roles of kinase inhibitors in immunotherapies

To date, over one-third of the human proteins have been reported to be modified by kinase activity (Ardito et al., 2017). Advancements in proteomic technologies and high-throughput gene function analysis have facilitated the study of kinome profiles in human cancers, offering valuable insights into the dysregulation of protein kinases in various types of cancers. The Cancer Gene Census (CGC) revealed that a significant proportion of cancer genes encode the protein kinase domain, with approximately 10% of cancer genes being protein kinases (Futreal et al., 2004). Furthermore, approximately 12% of non-kinase cancer driver genes are substrates of kinase cancer driver genes, which underscores the significance of kinase-regulated pathways in cancer (Fleuren et al., 2016). Kinase drivers are found across various kinase subgroups, with a notable prevalence of tyrosine kinases, accounting for approximately 40% of this superfamily (Fleuren et al., 2016). Because of the critical role of protein kinases in signaling mechanisms that control cell growth, proliferation, and survival, where most oncogenes are recognized as kinases, kinases are one of the major therapeutic targets in cancer. Moreover, small-molecule kinase inhibitors can target specific protein kinases and show mild side effects compared with cytotoxic chemotherapy. However, in addition to the well-known role of kinases in cell proliferation, some studies have also reported the immunosuppressive properties of oncogenic kinases and proved that kinase inhibition elicits anti-tumor immune responses (Bancerek et al., 2013; Palacios et al., 2015; Symeonides et al., 2017; Zhang et al., 2012). An increasing number of studies have demonstrated that kinase inhibitors can affect the expression of immunosuppressive

cytokines, chemokines, and angiogenic factors in the TME through various pathways. Considering the advantage of targeting tumor-associated immune cells, as they are more genetically stable and less likely to develop resistance mutations against kinase inhibitors compared to cancer cells, more studies have focused on the role of these therapeutic drugs in cancer immune evasion. Two approaches have been adopted to study kinase inhibitors in cancer immunity, either by directly targeting immune system-associated kinases or by investigating kinase inhibitors that modulate the sensitivity of cancer to immunotherapy (Gross et al., 2015). The highlights of some of these studies are discussed below:

The TAM family of receptor tyrosine kinases (RTKs), including AXL, TYRO3, and MER, play a regulatory role in the inflammation cycle by employing various mechanisms, such as inhibiting the JAK-STAT pathway and facilitating the final differentiation of NK cells (Caraux et al., 2006; Rankin & Giaccia, 2016). AXL inhibition restored TKI sensitivity in *in vivo* models of erlotinib-resistant non-small cell lung cancer (NSCLC) (Zhang et al., 2012). Clinical trials are underway to explore the reversal of tumor immunosuppression through TAM kinase blockade, specifically with the use of the first AXL-targeted inhibitor, BGB324, in combination with erlotinib, for NSCLC treatment (Sang et al., 2022). Colony-stimulating factor 1 (CSF1) expressed on the cell surface of macrophages regulates macrophage polarization from pro-inflammatory M1 to anti-inflammatory M2 states. The CSF1R inhibitor BLZ945 impedes the tumor-promoting functions of TAM, leading to improved survival rates in glioblastoma mouse models (Guo et al., 2020). Another promising target, CDK8, enhances NK cell-mediated tumor control by phosphorylating STAT1 at S727 (Bancerek et al., 2013). In addition, CDK8 inhibitors have been shown to augment the secretion of IL-10 from activated DCs, potentially serving as a strategy to reduce tumor

microenvironment inflammation (Johannessen et al., 2017). Furthermore, inhibition of AKT, the major component of the PI3K-AKT-mTOR pathway, has been shown to limit the differentiation of MDSCs *in vitro* and reduce their infiltration into breast cancer tissue in mouse models, while enhancing the infiltration of $CD8^+$ T cells (Tohumeken et al., 2020). PI3Kδ signaling promotes B cell proliferation. The PI3Kγ isoform has been implicated in the inhibition of Treg activity. Inhibition of PI3Kγ with TG100-115 has been shown to enhance T-cell activity and improve its efficacy when combined with anti-PD1 immunotherapy (Yang et al., 2015). Treatment with another PI3Kγ inhibitor, IPI-549, also showed promising results in increasing the sensitivity to immunotherapy and remodeling of the TME in breast cancer mouse models (Seton-Rogers, 2017). In 2018, IPI-549 in combination with the anti-PD1 antibody nivolumab was evaluated for advanced solid tumors in phase I clinical trials, which suggested that IPI-549 can modulate cancer immunity by upregulating IFNg-responsive factors (Anderson et al., 2021; Jiang et al., 2020). In squamous cell carcinoma (SCC), oncogenic FAK upregulates the transcription of chemokine ligands and receptors. Studies have demonstrated that FAK inhibitors restored sensitivity to immunotherapy in pancreatic cancer models by reducing Treg levels, thus promoting $CD8^+$ T cell-mediated anti-tumor immunity (Symeonides et al., 2017). In addition, inhibition of MEK in a colon cancer model protected $CD8^+$ T cells from stimulation-induced death (Zheng et al., 2023). Combining MEK inhibition with anti-PD-L1 treatment has shown significant long-term tumor regression and surpasses the effects of single-agent treatment alone (Ruggieri et al., 2022). In contrast, mutant EGFR remodels the TME, which promotes immune escape and induces PDL1 expression (Li et al., 2018).

Other kinase oncogenes have also been implicated in HCC immune evasion, with different studies reporting the use of FDA-approved TKIs for HCC to enhance anti-

tumor immunity by sensitizing resistant cancers to immunotherapies such as ICIs (Table 1.3). For instance, *in vivo* and *in vitro* studies have demonstrated that sorafenib, the first-line treatment for HCC, enhances anti-tumor immunity by promoting the infiltration of immature dendritic cells, MDSCs, and Tregs after VEGFR inhibition (Cabrera et al., 2013; Cao et al., 2011). Kimura et al. (2018) reported increased number of $CD8^+$ T cells in lenvatinib-treated HCC mouse model. In the same study, a higher response rate was obtained with a combined treatment of lenvatinib and anti-PD-1 antibody compared with either treatment alone in immunocompetent mice. However, the molecular mechanisms underlying the improved response rate following combinatorial treatment with kinase inhibitors remain unclear. A better understanding of the role of protein kinases in immune modulation in HCC may provide insights into immunotherapy resistance and improve immunotherapy effectiveness.

Table 1.3 Summary of kinase inhibitors approved by the FDA for treatment of HCC

Studies demonstrating the regulatory roles of TKIs in tumor immunogenicity and immune responses.

Drugs	Kinase targets	Studies	Immunomodulation
Sorafenib	VEGFR1-3, PDGFR, FGFR, RAF, KIT, FLT-3	(Cao et al., 2011)	Reduces Tregs and MDSC in HCC mouse model.
		(Cabrera et al., 2013)	Restores Teff cell responses in peripheral mononuclear cells collected from HCC patients
		(Hage et al., 2019)	Reduces MHCI expression and trigger NK cell response
Lenvatinib	VEGFR1-3, PDGFR, FGFR1-4, RET, KIT	(Kimura et al., 2018)	Increases $CD8^+$ T cell populations in HCC mouse model
		(J. Zhu et al., 2021)	Increases CTLs and reduces PD-1 and TIM-3 level in mononuclear cells collected from HCC patients
		(Yi et al., 2021)	Reduces PD-L1 level and Treg cell differentiation in HCC cells
Regorafenib	VEGFR1-3, PDGFR, FGFR, RAF RET, KIT	(Qiu et al., 2018)	Reduces PD-L1 level in HCC mouse model
		(Shigeta et al., 2020)	Activation of CTL in HCC mouse model treated with αPD-1 antibody plus regorafenib
		(Ou et al., 2021)	Activation of $CD8^+$ T cells and suppression of M2 macrophage polarization
Cabozantinib	c-Met, VEGFR1/2/3, AXL, RET, ROS1, KIT	(Esteban-Fabro et al., 2022)	Decrease Treg and PD-1^+ T cell population. Increases neutrophil infiltration in HCC mouse model

1.4 Hypothesis and objectives of the study

Hypothesis

We hypothesized that protein kinases contribute to HCC development via immune-regulatory pathways. In this study, we aimed to identify a subset of kinases involved in immune modulation in HCC by employing an *in vivo* kinome-wide clustered regularly interspaced short palindromic repeat (CRISPR) screen and HCC mouse models.

Objectives of the study

1. To establish a kinome-wide mouse CRISPR knockout library by transduction of Cas9 expressing RIL-175 cell were transduced with a lentiviral gRNA expression vector.
2. To identify the protein kinases crucial for immune modulation in HCC by *in vivo* CRISPR screening in an HCC tumor mouse model derived from B and T cell-deficient Rag1-KO and immune-competent wild-type mice by deep sequencing.
3. To functionally characterize the identified protein kinases in immune modulation in HCC by knockout or overexpression of kinase genes using *the in vivo* CRISPR knockout and Sleeping Beauty (SB) transposon system.
4. To elucidate the molecular mechanisms of the candidate protein kinases involved in immune evasion using a single-cell RNA sequencing approach.

Chapter 2 Materials and Methodology

2.1 Materials

Table 2.1. Cell lines used in this study.

Cell line	Growth medium	Characteristics	Source
RIL-175	RPMI1640	Gift from Prof. Stephanie Ma (HKU, Hong Kong)	Mouse HCC
Hep55.1c	DMEM	Cell Line Service (Eppelheim, Germany)	Mouse HCC

Table 2.2. Primers for qPCR and deep sequencing of sgRNA library.

qPCR		
Gene	Forward (5'-3')	Reverse (5'-3')
Mink1 (sgRNA1)	AACCGAAACCGTGTGGGA	TGAGCAACACAAAGTCTG
Mink1 (sgRNA2)	AGAGACAGCTGCAGCAGGA	CCCCGACCGTAATGATACAG
Deep sequencing		
P5 primers		
Name	Sequence (5' – 3')	
P5 0 nt stagger	AATGATACGGCGACCACCGAGATCTACACTCTTTCCCTACACGACGCTCTTCCGATCTTTGTGGAAAGGACGAAACACCG	
P5 1 nt stagger	AATGATACGGCGACCACCGAGATCTACACTCTTTCCCTACACGACGCTCTTCCGATCTCTTGTGGAAAGGACGAAACACCG	
P5 2 nt stagger	AATGATACGGCGACCACCGAGATCTACACTCTTTCCCTACACGACGCTCTTCCGATCTGCTTGTGGAAAGGACGAAACACCG	
P5 3 nt stagger	AATGATACGGCGACCACCGAGATCTACACTCTTTCCCTACACGACGCTCTTCCGATCTAGCTTGTGGAAAGGACGAAACACCG	
P5 4 nt stagger	AATGATACGGCGACCACCGAGATCTACACTCTTTCCCTACACGACGCTCTTCCGATCTCAACTTGTGGAAAGGACGAAACACCG	
P5 6 nt stagger	AATGATACGGCGACCACCGAGATCTACACTCTTTCCCTACACGACGCTCTTCCGATCTTGCACCTTGTGGAAAGGACGAAACACCG	
P5 7 nt stagger	AATGATACGGCGACCACCGAGATCTACACTCTTTCCCTACACGACGCTCTTCCGATCTACGCAACTTGTGGAAAGGACGAAACACCG	
P5 8 nt	AATGATACGGCGACCACCGAGATCTACACTCTTTCCCTACAC	

stagger	GACGCTCTTCCGATCTGAAGACCCTTGTGGAAAGGACGAAACACCG
P7 primers	
Name	Sequence (5’ – 3’)
P7 index 1	CAAGCAGAAGACGGCATACGAGATGCTGGATTGTGACTGGAGTTCAGACGTGTGCTCTTCCGATCTCCAATTCCCACTCCTTTCAAGACCT
P7 index 2	CAAGCAGAAGACGGCATACGAGATTAACTCGGGTGACTGGAGTTCAGACGTGTGCTCTTCCGATCTCCAATTCCCACTCCTTTCAAGACCT
P7 index 3	CAAGCAGAAGACGGCATACGAGATCGGTGACCGTGACTGGAGTTCAGACGTGTGCTCTTCCGATCTCCAATTCCCACTCCTTTCAAGACCT
P7 index 4	CAAGCAGAAGACGGCATACGAGATTACAGAGGGTGACTGGAGTTCAGACGTGTGCTCTTCCGATCTCCAATTCCCACTCCTTTCAAGACCT
P7 index 5	CAAGCAGAAGACGGCATACGAGATATTGTCAAGTGACTGGAGTTCAGACGTGTGCTCTTCCGATCTCCAATTCCCACTCCTTTCAAGACCT

Table 2.3. sgRNA sequences.

Name	Sequence (5’ – 3’)
Mink_sgRNA1	GAGCGGAACCGAAACCGTGT
Mink_sgRNA2	GCCCCGACCGTAATGATACAG
Non-target control_sgRNA	GAATTCTGAGATTCCGCGGCT

Table 2.4. Antibodies used for western blot, immune profiling and IHC.

Western blot			
Antibodies	Condition	Catalogue number	Vendor
β-actin	1:5000	#A5316	MilliporeSigma (Massachusetts, USA)
α-Tubulin	1:5000	#T9026	Merck (New Jersey, USA)
Cas9	1:1000	#14697	Cell Signalling Technology (Massachusetts, USA)
Mink1	1:700	#HPA056296	Human Protein Atlas (Stockholm, Sweden)
Immune profiling			

CD11b	1:300		BioLegend (California, USA)
Cd11c	1:200		BioLegend (California, USA)
Ly6C	1:700		BioLegend (California, USA)
LY6G	1:300		BioLegend (California, USA)
CD4	1:300		BioLegend (California, USA)
CD8	1:100		BioLegend (California, USA)
Live/dead	1:200		BioLegend (California, USA)
MHCII	1:500		BioLegend (California, USA)
CD45	1:500		BioLegend (California, USA)
CD3	1;100		BioLegend (California, USA)
CD16/32	1;100		BioLegend (California, USA)
F4/80	1:50		BioLegend (California, USA)
CD44	1:200		BioLegend (California, USA)
FOXP3	1;100		BioLegend (California, USA)
CDLA4	1:100		BioLegend (California, USA)
RORgt	1:40		BioLegend (California, USA)
TCR-beta	1:100		BioLegend (California, USA)
CD49b	1:100		BioLegend (California, USA)
CD19	1:100		BioLegend (California, USA)
IHC			
Mink1	1:50, pH6	#HPA056296	Human Protein Atlas (Stockholm, Sweden)
PCNA	1:50, pH6	#13110	Cell Signaling Technology (Massachusetts, USA)
CD8	1:50, pH6	#CST98941	Cell Signaling Technology (Massachusetts, USA)

Table 2.5. Reagents used in this study.

Reagents	Vendor
Mouse Kinome CRISPR Knockout Library (Brie) #75316	A gift from John Doench & David Root (Addgene) (Massachusetts, USA)
Matrigel™ Matrix	Corning (New York, USA)
Roswell Park Memorial Institute (RPMI) 1640 Medium	Thermo Fisher Scientific (Massachusetts, USA)
Fetal bovine serum	Thermo Fisher Scientific (Massachusetts, USA)
Penicillin – Streptomycin	Thermo Fisher Scientific

	(Massachusetts, USA)
TRIzol® Reagent	Invitrogen™, Thermo Fisher Scientific (Massachusetts, USA)
Polybrene	MilliporeSigma (Massachusetts, USA)
Puromycin	MilliporeSigma (Massachusetts, USA)
Lipofectamine™ 2000 transfection reagent	Invitrogen™, Thermo Fisher Scientific (Massachusetts, USA)
Dimethyl sulfoxide (DMSO)	MilliporeSigma (Massachusetts, USA)
PhosSTOP™	Roche (Basel, Switzerland)
cOmplete™ EDTA-free protease inhibitor cocktail	Roche (Basel, Switzerland)
BrightGreen 2X qPCR MasterMix-ROX	Applied Biological Materials (Vancouver, Canada)
PrimeScript™ RT Reagent Kit	Takara (Shiga, Japan)
WesternBright ECL HRP substrate	Advansta (California, USA)
PrimeSTAR GXL DNA Polymerase	Takara (Shiga, Japan)
QIAquick PCR Purification Kit	Qiagen (Maryland, USA)
QIAquick Gel Extraction Kit	Qiagen (Maryland, USA)
DNeasy Blood & Tissue Kit	Qiagen (Maryland, USA)
QIAprep Spin Miniprep Kit	Qiagen (Maryland, USA)
Plasmid Midi Kit	Qiagen (Maryland, USA)
Opal 4-Color Manual IHC Kit	Akoya Biosciences (Massachusetts, USA)
AR9 Tris-EDTA buffer	Perkin Elmer (Massachusetts, USA)

2.2.1 Cell lines and cell culture

The cell lines used in this study are listed in Table 2.1. Cells were grown in RPMI or DMEM supplemented with 10% fetal bovine serum (Thermo Fisher Scientific) and 1% penicillin – streptomycin (Thermo Fisher Scientific), and incubated at 37°C with 5% CO2. Cells were sub-cultured by washing with PBS and adding 1-2 mL Trypsin (Sigma-Aldrich) to de-attach the cells. The cells were centrifuged at 1200rpm for 4 min and reseeded in fresh dishes at an appropriate dilution.

The RIL-175 cell line stably expressing Cas9 was maintained in cell culture medium containing 5 μg/mL blasticidin. Lentivirus-infected cells were selected and maintained in medium containing 5 μg/mL blasticidin and 2 μg/mL puromycin. Single-cell-derived clones were generated by dilution cloning. The cells were limited to growth within 20 subculture passages.

2.2.2. Molecular cloning and plasmid amplification

To generate knockout cell lines, sgRNAs were cloned into the target vector plentiGuide-Puro (Addgene #52963), and lentiviral sgRNAs were generated by WeiZhen Biosciences (ShanDong, China) (Fig. 2.1). To generate Mink1 overexpression mouse model, four plasmids were prepared. The plasmids encoding mouse C-Myc with luciferase expression (pT3-EF1a-MYC-luc), CRISPR/Cas9 vector expressing sgTP53 (px330-sgp53), and vector expressing SB13 transposase (CMV-SB13) were kindly provided by Dr. Scott Lowe (MSKCC, New York, USA). To construct the pT3-EF1a-Mink1 plasmid, the protein-coding sequence of mMink1 (AAH52474.1) was first composed in the donor vector pDONR-221 (Hitrobio Biotechnology, Beijing, China), followed by insertion of the Mink1 fragment into the transposon-expressing vector pT3-EF1a-GW by Gateway cloning using LR Clonase (Thermo Fisher Scientific, Massachusetts, USA) (Fig. 2.2).

Cloned plasmid DNA (2-4 µl) was then transformed into E. coli DH5α competent cells, incubated on ice for 20 min, followed by heat shock at 42°C for 1.5 min and incubated on ice again for 1.5 min. Next, tubes with LB broth were incubated at 37°C for 1 hr and cultured in ampicillin-containing agar plates overnight. Single colonies were then selected and expanded in 400mL LB broth containing ampicillin overnight at 37°C, and plasmid DNA was extracted using a commercial Miniprep or Midiprep kit (Qiagen, Maryland, USA). Plasmids were Sanger Sequenced by Techdragon at Hong Kong, using primers targeting promoter sites.

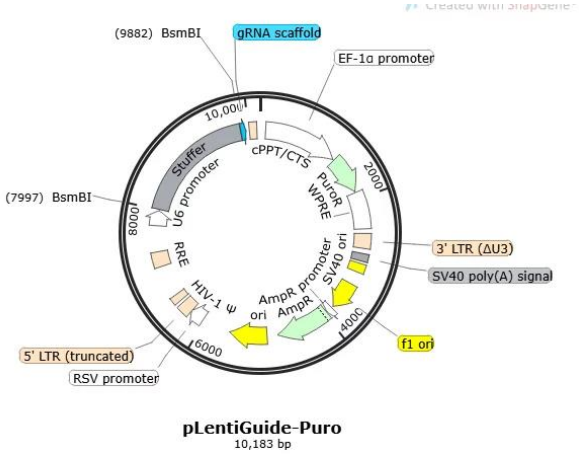

Figure 2.1 Map of pLentiGuide-Puro vector
Generated by SnapGeneâ software (GSL Biotech LLC, California, USA).

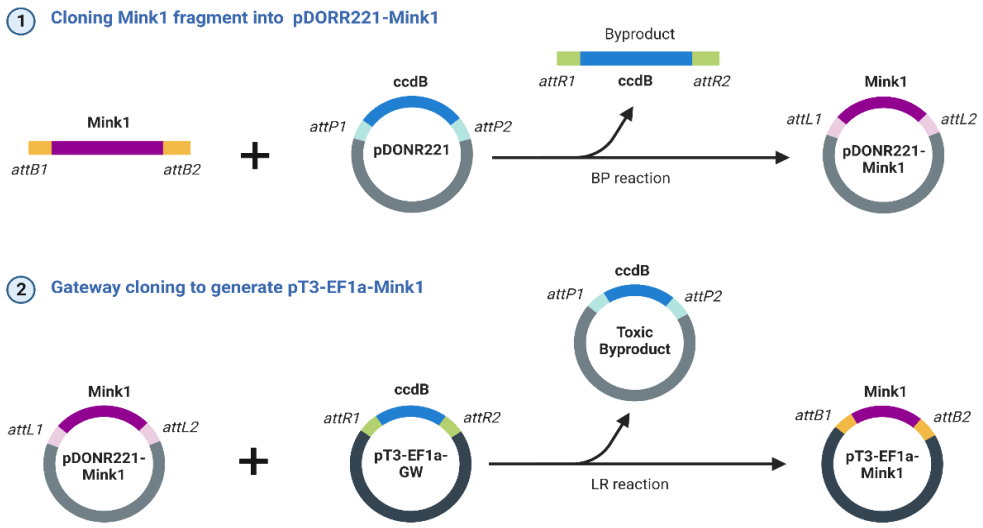

Figure 2.2 Workflow of cloning the pT3-EF1a-Mink1 plasmid

2.2.3 Cell viability assay

Knockout cell lines were seeded in 96-well plates (500 cells/well) and cultured for 4 or 6 days before cell counting. CellTiter-Glo® luminescent cell viability assay (Promega, Wisconsin, USA) was used in Mink1 knockout cells according to the manufacturer's instruction. Optical density (OD) values were read at 570 nm using a CLARIOstar Plus Microplate Reader (BMG LABTECH, Ortenberg, Germany). The experiments were performed in triplicate.

2.2.4 RNA extraction

Total RNA from cells or mouse tumor samples was extracted with TRIzol® reagent (Invitrogen, Massachusetts, USA). The cells or tumors were lysed using a homogenizer for 40s, followed by a 5 min pause on ice. Chloroform (Merck, New Jersey, USA) was added to TRIzol® Reagent at a 1:5 ratio, mixed by inversion, and incubated on ice for 3 min. After centrifuged at 13000 rpm for 30 min at 4°C, the top aqueous layer containing RNA was collected and transferred to a new tube. Isopropanol (Invitrogen, Massachusetts, USA) was added at a ratio of 1:1 to the collected aqueous RNA for precipitation, followed by centrifugation at 4°C for 10 min to obtain the RNA pellet. The pellet was washed with 75% ethanol, air-dried, re-dissolved in UltraPureTM distilled water (Invitrogen, Maryland, USA), and stored at -80°C. RNA concentration was determined using a NanoDrop™ One/OneC Microvolume UV-Vis Spectrophotometer (Thermo Scientific, Massachusetts, USA), and RNA quality was confirmed by obtaining an OD260/280 between 1.8-2.0.

2.2.5 cDNA synthesis and qPCR analysis

The PrimeScript™ RT Reagent Kit (Takara, Shiga, Japan) was used to generate cDNA following the manufacturer's protocol. Briefly, 500μg of RNA was incubated with 5X

PrimeScript Buffer containing a dNTP mixture, Oligo dT Primer, random hexamers, and PrimeScript RT Enzyme Mix. qPCR analysis was performed using the qPCR SYBR Green PCR kit (Applied Biological Materials, Canada). 2µl of cDNA, 6µl of 2X qPCR master-mix, 3.4µl of UltraPureTM distilled water, 0.3µl of both forward- and reverse-specific primers listed Table 2.2 were used per reaction. qPCR was performed in a 96-well or 384-well QuantStudio 7 Flex Real-time PCR system (Thermo Fisher Scientific, Massachusetts, USA). Relative expression differences were calculated using the $2^{-\Delta\Delta CT}$ method, with reference to GAPDH.

2.2.6 Western blot analysis

Proteins were extracted with RIPA lysis buffer mixed with protease and phosphatase inhibitors. The lysates were mixed with 6× SDS loading buffer and boiled at 95°C for 5 min. Gel electrophoresis was performed at 90 volts for 15 min, followed by 120 volts after 40-100µg of lysates onto an SDS polyacrylamide gel. Following electrophoresis, proteins were transferred from the gel to a methanol-activated polyvinylidene difluoride membrane at a constant voltage of 90 volts for 1.5 hours. Primary antibodies were applied and incubated overnight at 4°C, followed by the application of secondary antibodies (anti-mouse or anti-rabbit). Table 2.3 listed the primary antibodies used along with the working dilutions. Protein signals were visualized using an ECL system and exposed to an X-ray film.

2.2.7 Illumina sequencing for kinome-wide CRISRP library

A Mouse Kinome CRISPR knockout library (Brie) of 2852 optimized sgRNAs targeting 713 kinase genes and 100 non-targeting sgRNAs were obtained from Addgene. Lentiviral sgRNA libraries were synthesized by WZ Biosciences, and the multiplicity of infection (MOI) was calculated using serial dilutions of the virus. For pooled library

transduction, a total of $3.75x10^7$ RIL-175-Cas9 cells (>500-fold change library coverage) were transduced at a multiplicity of infection (MOI) of ~0.3 to ensure whole library representation. Only one sgRNA was transduced into each cell, and 12ug/mL polybrene was added to enhance transduction efficiency. After three days of 2 % puromycin selection, a pellet of 1.5×10^6 cells was used for evaluating the initial sgRNA distribution.

The genomic DNA of the transduced cells and tumors was extracted using DNeasy Blood & Tissue Kits (Qiagen), following the manufacturer's protocol, and quantified using a Nanodrop ND-1000 (Thermo Fischer Scientific). PCR was used to amplify the sgRNA cassette in 10 reactions per sample to ensure sufficient coverage. A mix of P5 primers with stagger regions of different lengths and P7 primers with different barcode sequences are listed in Table 2.2, followed by PCR thermocycling (Table 2.6). The four PCR products were pooled, cleaned using a QIAquick PCR Purification Kit (Qiagen), and gel-purified from a 2% agarose gel using a QIAquick Gel Extraction Kit (Qiagen). Library quality control and paired-end 150 base sequencing (1G read depth/sample to ensure a sequencing depth of >100 reads per sgRNA) were performed using NovaSeq (Novogene, Cambridge, UK).

Table 2.6 PCR cycling parameters

Cycle number	Denature	Anneal	Extend
1	98°C, 3 min		
2-36	98°C, 10s	63°C, 20s	72°C, 25s
37			72°C, 4 min

2.2.8 Bulk RNA sequencing

Before sequencing, a quality check was conducted by Agilent Technologies (OD260/280 1.8-2.0 and RNA integrity number (RIN)> 6). RNA extracted from the tumors of the HTVI models was sequenced to reach 100M reads per sample at the Center for PanorOmic Sciences at the University of Hong Kong using an Illumina NovaSeq 6000 sequencer. The average throughput is 190M reads and 94% of bases achieved a high-quality score (reads < 5% unknown bases and reads <50% of bases with a quality value < 11). Mouse Genome GRCm38 was used as reference genome for alignment. Expression estimation and tests for differential expression were performed using STAR 2.5.2, RSEM 1.2.31, and EBSeq 1.18.0. The results are presented as transcripts per million (TPM) and fold-changes in the OE group relative to the GW group.

2.2.9 Immune profiling

HTVI mouse model tumor samples were finely minced into small fragments in a 10 cm dish containing T cell medium and transferred to gentleMACS™ C Tubes with dissociation buffer containing 0.1 g/ml Collagenase IV and 10 mg/ml DNaseI. Tumor samples were dissociated with a gentleMACS™ dissociator using the m-Liver program and incubated at 37°C. The cell suspensions were filtered through a 70μm cell strainer and centrifuged at 600 × g for 10 min. The supernatant was subjected to Percoll purification by resuspending the cell pellet in a 40% Percoll solution. Next, 40% Percoll solution containing cells was gently transferred to a tube containing 80% Percoll solution and centrifuged at 1200 × g for 25 min with no brake. The middle colorless layer containing immune cells was transferred to a new falcon tube, topped with T cell medium, and centrifuged at 600 × g for 5 min. The cells were then resuspended in ACK lysis buffer for red blood cell lysis. After discarding the supernatant and resuspending

the pellet in 1mL mL FACS buffer, cell suspensions were used for immunostaining. One million cells were seeded in each well of a V-shaped 96 plates. Surface staining was performed by incubating cells for 20 min at 4°C. The cells were then fixed with the eBioscience™ Foxp3 / Transcription Factor Staining Buffer Set (Invitrogen) for 30 min, centrifuged at 1000 × g for 5 min, and stained intracellularly for 20 min at 4°C. Finally, the stained cells were washed with FACS buffer, resuspended in FACS buffer, and analyzed using a BD LSRFortessa™ Cell Analyzer (BD Biosciences). The antibodies used for immune profiling are listed in Table 2.1. Data acquisition and quantification were performed using FlowJo software (BD Biosciences).

2.2.10 Single cell analysis

Figure 2.3 presents the workflow of single-cell RNA seq preparation. Mouse HCC tumor samples were dissociated as described previously in sample preparation for immune profiling analysis. After dissociation, the cells were counted, stained with Live/Dead Fixable Near-IR Dead Cell dye (Invitrogen) for 30 min, and washed with FACS buffer. The stained cells were sorted into live cells using a FACSAria III cell sorter (BD Sciences) and sent for single-cell RNA sequencing analysis at BGI Genomics in Hong Kong.

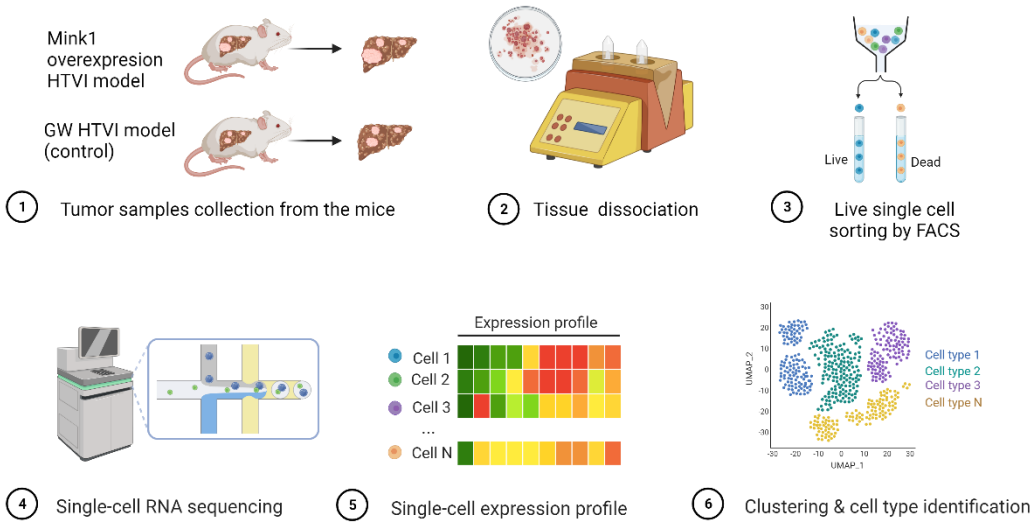

Figure 2.3 Workflow of single cell RNA sequencing analysis

2.2.11 Immunohistochemistry staining and immunofluorescence staining

Xylene was used for deparaffinizing formalin-fixed and paraffin-embedded (FFPE) tissue sections. Next, the sections were rehydrated with graded alcohol and distilled water. Antigen retrieval was done by microwave heating. To quench the endogenous peroxidase activity, 3% hydrogen peroxide was used. The sections were then treated with serum-free protein block solution (DAKO, Agilent Technologies) to prevent non-specific antibody binding and incubated with primary antibodies, as specified in Table 2.1, to target specific antigens of interest. After primary antibody incubation, the sections were washed with TBST and shaken to remove the unbound antibodies. For signal detection, anti-rabbit Envision^{TM} HRP-conjugated secondary antibody (DAKO) was applied to the sections. Positive signals from the antigen-antibody complexes were visualized using Liquid DAB and Substrate-Chromogen System (DAKO), resulting in a brown coloration at the site of antigen expression. Mayer's hematoxylin and Scott's tap water were used for counterstain. Finally, the immunohistochemical staining patterns were examined using a light microscope, and the stained regions were

quantified using the ImageJ software.

Multiplexed immunohistochemistry was performed using an Opal 4-Color Manual IHC Kit (Akoya Biosciences, Massachusetts, USA). Sections were deparaffinized in xylene and rehydrated in decreasing concentrations of alcohol and distilled water. Antigen retrieval was performed in 1X AR9 Tris-EDTA buffer (Perkin Elmer, Massachusetts, USA) for 15 min. Endogenous peroxidase activity was quenched using 3% hydrogen peroxide for 10 min at room temperature. The sections were then immersed in a blocking antibody diluent for 30 min at room temperature. The specimens were subsequently incubated with the antibodies listed in Table 2.1. The sections were washed thoroughly and incubated with Opal Polymer HRP Ms+Rb for 30 min at room temperature. Following a brief wash with 1xTBST, fluorophore was added to the tissue sections and incubated for 15 min. Staining steps were repeated for the remaining antibodies with different fluorophores. Finally, stripping was performed in 1x AR6 sodium citrate buffer in a microwave oven for 15 min. DAPI staining was performed after cooling the sections. Slides were mounted, and stained patterns were examined using a Leica TCS SPE confocal microscope and quantified using Nikon NIS-Elements Software (New York, USA).

2.2.12 *In vivo* mouse models

C57BL/6 wild-type mice and C57BL/6-Rag1-KO immunodeficient mice were obtained from The University of Hong Kong and The Chinese University of Hong Kong.

2.2.12.1 *In vivo* kinome-wide CRISPR screening

A Mouse Kinome CRISPR knockout library (Brie) of 2852 optimized sgRNAs targeting 713 kinase genes and 100 non-targeting sgRNAs were obtained from Addgene.

Lentiviral sgRNA libraries were synthesized by WeiZhen Biosciences (ShanDong, China), and the multiplicity of infection (MOI) was calculated by serial dilutions of the virus. For pooled library transduction, a total of $3.75x10^7$ RIL-175-Cas9 cells (>500-fold change library coverage) were transduced at a multiplicity of infection (MOI) of ~0.3 to ensure whole library representation. Only one sgRNA was transduced into one cell, and 12ug/mL polybrene was added to enhance transduction efficiency. After 3 days of 2 μg/mL puromycin selection, a pellet of 1.5 x 106 cells was used to evaluate the initial sgRNA distribution, and the remainder was injected subcutaneously into 8-week-old male Rag1-KO and WT mice (n=2) with Matrigel (1:1 dilution) (7.5×10^5 cells/mouse). Tumor volume was measured using the following formula: $(L \times W^2)/2$. Mice were sacrificed when Rag1-KO tumors grew to 500 mm^3, and tumors were excised for NGS analysis to evaluate the final library distribution, as described in Section 2.2.7.

2.2.12.2 Mink1 knockout subcutaneous mouse model

KO cells and cells transfected with sgNTC as a control were subcutaneously injected into four–five 10-week-old Rag1-KO and WT mice with Matrigel (1:1 dilution) (5000 or 50000 cells/mouse), and the tumor volume was measured using the formula described above.

2.2.12.3 Hydrodynamic tail vein $Trp53^{KO}$/C-Myc^{OE} HCC mouse model

To deliver the Sleeping Beauty transposon system to the livers of mice, we first generated a Sleeping-mediated exogenous expression of murine Mink1, as described in section 2.2.2. Afterwards, 15μg of pT3-EF1a-MYC-luc and px330-sgp53 together with 2.5μg of CMV-SB13 and 12.5μg of pT3-EF1a-Mink1 in a ratio of 1:25 dilutions with 2 mL 0.9% NaCl saline were filtered through a 0.22μm filter and injected into the lateral

tail vein of 8 weeks old C57BL/6 mice for 7s. As a control, 12.5µg of the empty vector pT3-EF1a-GW was added instead of Mink1 expressing plasmid.

2.2.13 Bioinformatics and statistical analysis

2.2.13.1 CRISPR screen data analysis

CRISPR data were analyzed using MAGeCK and MAGeCK-VISPR, as described by Wang et al. (2019). Briefly, raw sequencing data were processed using MAGeCK to obtain read counts for each sgRNA, with non-target (control) sgRNAs used to normalize the data. The statistical significance of each sgRNA was calculated using the learned mean-variance model. Essential genes (both positively and negatively selected) were identified by searching for genes whose sgRNAs were ranked consistently higher (by fold change and *p*-value) using robust rank aggregation (RRA). The MAGeCK TEST algorithm was used to compare treatments with the control samples to identify significantly enriched and depleted sgRNAs and genes. Genes with *p*-values less than 0.05 are candidate hits.

2.2.13.2 Survival analyses

Survival analyses based on the expression status of MINK1 were performed using the OSlihc, Cutoff-High (%):25; Cutoff-Low (%):25. Survival analyses for MINK1 correlation with cytotoxic T lymphocyte (CTL) levels on patient outcomes were performed using the Tumor Immune Dysfunction and Exclusion (TIDE) algorithm.

2.2.13.3 Gene set enrichment analysis for gene expression data

We performed Gene Set Enrichment Analysis (GSEA) by separating samples to low and high Mink1 TPM levels in the TCGA-LIHC cohort and used the Molecular Signatures Database to rank the pathways enriched in the Mink1-high group. For bulk

RNA data analysis, the R package DESeq2 was used, and the top 25% of differentiated genes (up or downregulated) with enrichment/depletion scores calculated using the formula "-log(*P*-value) x log_2FC" was applied to GSEA "preranked" algorithm.

2.2.13.4 Single cell RNA sequencing data analysis

Upon confirming cDNA integrity, library quality, number of sequenced cells, and average reads per cell as part of quality control, we utilized the Cell Ranger package to map the reads and generate gene-cell matrices. Subsequently, quality control was conducted by calculating the number of genes, unique molecular identifiers (UMIs), and proportion of mitochondrial genes for each cell using the Seurat R package. Cells with a low gene count (< 500) and high mitochondrial gene count (> 0.1) were removed from the analysis. We then performed comprehensive statistical analysis to calculate gene dispersion and cell coverage to construct a gene model for principal component analysis (PCA). Uniform Manifold Approximation and Projection (UMAP) was also performed using SingleR, and well-established cell type markers were visualized on dot plots.

2.2.13.5 Statistical analysis

The statistical significance of the data in this thesis was determined by Student's *t* test. The results are shown as means and standard deviations, and those with p values less than 0.05 were considered statistically significant (* $p<0.05$, ** $p<0.01$, *** $p<0.001$, and **** $p<0.0001$). Kaplan–Meier survival analysis was used to analyze overall survival, and a log-rank test was used to determine statistical significance.

Chapter 3 Identification of protein kinases critically involved in HCC immune regulation by *in vivo* kinome-wide CRISPR sgRNA knockout screen

3.1 Introduction

TKIs, including sorafenib and lenvatinib, are widely used worldwide for the treatment of advanced HCC. However, recent developments in immunotherapies, especially ICIs, have shown higher survival rates and mild side effects than TKIs, and are therefore recognized as the new standard of care for advanced HCC in the future (Finn, Qin, et al., 2020; Sangro et al., 2021). Nevertheless, the low objective response to ICIs urges researchers to modify treatment strategies to increase their clinical efficacy (Yau et al., 2020). Considering the difficulty of therapeutically targeting anti-tumor immune-related pathways compared to inhibiting kinases and the recent reports of kinase involvement in cancer immune evasion, a better understanding of the role of protein kinases in immune modulation in HCC may potentiate cancer immunotherapy.

CRISPR/Cas9 screening, an adaptive immune regulation mechanism in bacteria, has revolutionized our ability to uncover genes involved in cancer regulation (Fig 3.1). Significant progress has been made in cancer studies by using pooled *in vitro CRISPR* screening tools to identify and validate novel cancer drug targets. Wu et al. successfully identified glutaminyl-peptide cyclotransferase-like protein (QPCTL) as a key regulator of CD47 by employing a genome-scale CRISPR screen in human colon cancer cells (Wu et al., 2019). However, recent studies have highlighted the importance of the tumor microenvironment in cancer immunology studies and indicated the limitations of *in vitro* CRISPR screening in recapitulating the cancer environment (F. Li et al., 2020). Therefore, we applied a kinome-wide i*n vivo* CRISPR screen in an HCC mouse model.

Upon the successful establishment of an *in vitro* kinome-wide mouse CRISPR sgRNA knockout (KO) library, CRISPR library-transduced RIL-175-Cas9 cells were subcutaneously injected into C57BL/6 wild-type and C57BL/6-Rag1-KO

immunodeficient mice. Following tumor dissection and genomic DNA extraction, samples were sent for deep sequencing analysis to confirm whether sgRNAs were enriched or depleted using the normal immune environment in WT mice as a negative selection criterion.

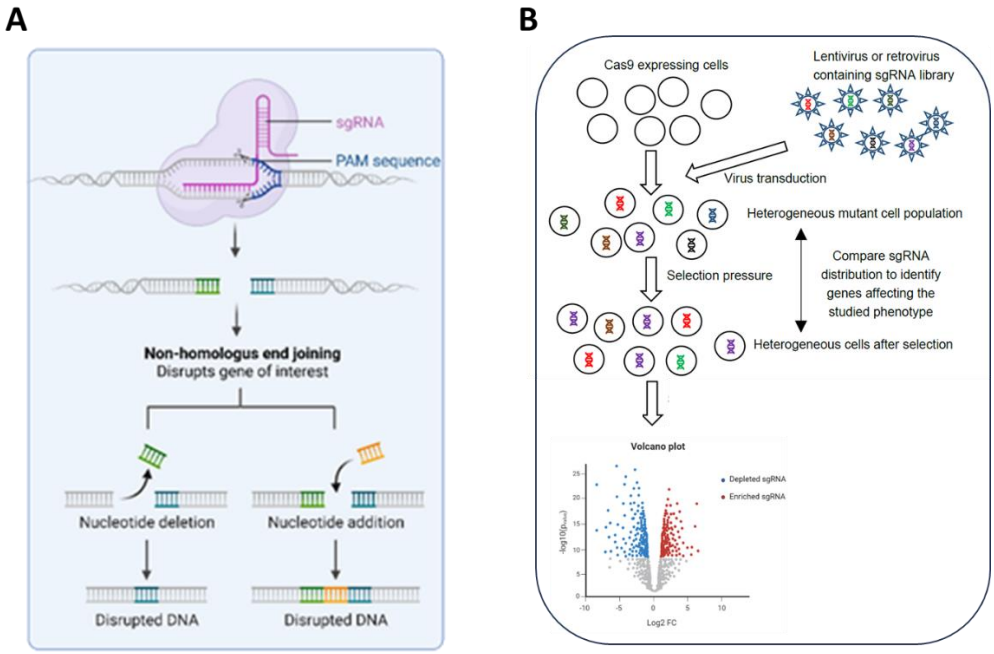

Figure 3.1 The principle of CRISPR/Cas9 Knockout pooled screening

(A) Originally, the CRISPR/Cas system served as a defense mechanism against infecting bacteriophages or viruses by selectively targeting specific genetic regions of the invading phages (Jansen et al., 2002). Currently, researchers use this technology for various genome-based studies, and one of the most powerful approaches is knockout pool screening. The CRISPR/Cas9 knockout system involves two key components: a guide RNA (sgRNA) and Cas9 endonuclease. sgRNA guides the Cas9 protein to a specific target site in the genome near the PAM sequence (Dang et al., 2015; Liu et al., 2019). Upon binding to the target site, Cas9 creates a double-strand break (DSB) in DNA, which is then repaired by the non-homologous end-joining pathway, creating indels that introduce loss-of-function mutations within the gene. **(B)** Customized sgRNA pooled libraries targeting different research interests have been designed, including epigenetic, kinome, and whole genome libraries. Briefly, sgRNAs with sequences proven to effectively knockout genes were integrated into viral vectors and delivered into a large pool of Cas9-expressing cells. Low titers and high cell coverage are required to ensure that each cell receives a single sgRNA, while each gRNA is represented by statistically sufficient cells (Joung et al., 2017). Upon different selection criteria, such as drug treatment or immune cell coculture, the composition of the sgRNAs in the pool changes, so that if cells carry gRNA that suppresses viability upon KO, cell populations with that gRNA will be depleted. Conversely, if cells carry gRNA that provide a growth advantage, enrichment in the cell populations will be observed.

3.2 Experimental outline

Figure 3.2 A summary of the workflow of *in vivo* kinome-wide CRISPR screening to identify potential kinase targets for immune evasion

(1) Construction of an *in vitro* kinome-wide CRISPR gRNA knockout library. (2) Establishment of an *in vivo* kinome-wide mouse CRISPR gRNA-knockout library. (3) Tumors of wild-type mice and immunodeficient mice injected with CRISPR library were collected for deep sequencing, followed by data analysis using Model-based Analysis of Genome-wide CRISPR/Cas9 Knockout (MAGeCK).

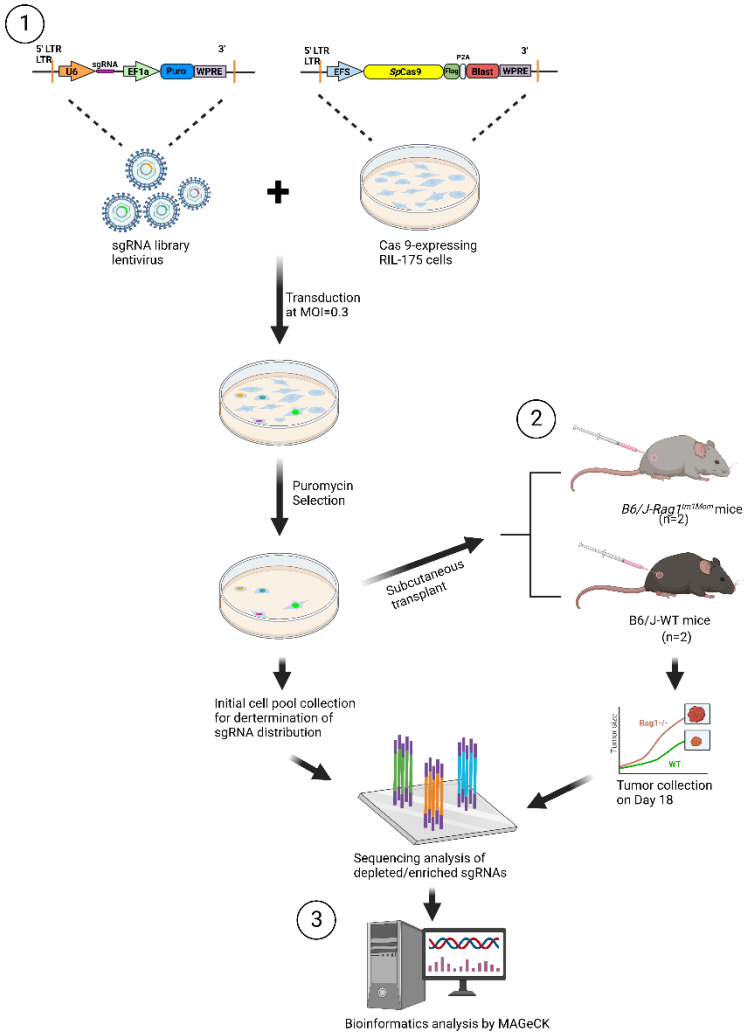

3.3 Result

3.3.1 Construction of an *in vitro* kinome-wide CRISPR sgRNA knockout library

To identify protein kinases that regulate anti-tumor immunity in the HCC mouse model, we first generated a mouse lentiviral CRISPR gRNA knockout library. We utilized the RIL-175 mouse HCC cell line, a p53-null/Hras mutant line syngeneic to the C57BL/6 mouse strain background, which is widely grown as a subcutaneous and orthotopic tumor for our screening experiment. The RIL-175 cell line stably transduced with a lentivirus encoding Cas9 was kindly provided by Prof. Stephanie Ma's lab (HKU), and Cas9 expression was confirmed by western blotting (Fig. 3.3A). Next, by performing the Rule Set 2 score algorithm developed by Doench et al., which prioritizes sgRNAs (i) targeting functional domains of protein structures; (ii) with minimal potential off-target sites; (iii) with target sites of each gene based on protein-coding sites at least 5% away from a previously selected sgRNA, we obtained a satisfactory average score of 0.678 for the mBrie library (Fig. 3.3B) (Doench et al., 2016). As a result, the mBrie mouse kinome library of lentiviral vectors encoding 2,852 unique sgRNAs targeting 713 mouse kinase genes with 100 non-targeting controls constructed by Addgene was chosen as our screening library because of the excellent efficiency of sgRNAs. After lentiviral packaging, the sgRNA library was transduced into the mouse HCC cell line RIL-175 expressing Cas9 *in vitro* and genomic DNA from the cell pellet was extracted to validate the quality of the sgRNA library. Using the MAGeCK algorithm after deep sequencing analysis, a 0.05% zero count of sgRNAs and a Gini Index of the read count distribution of approximately 0.05 were obtained, indicating a significantly low missed number of sgRNAs and high evenness of sgRNA distribution (Fig. 3.3C). Moreover, as expected, sgRNAs targeting essential genes to support cellular life and liver development were depleted in the initial cell pool after seven days of mBrie library transduction (Fig. 3D-E). These results confirmed the efficiency of the mBrie library in

addition to bioinformatics sgRNA prediction analysis.

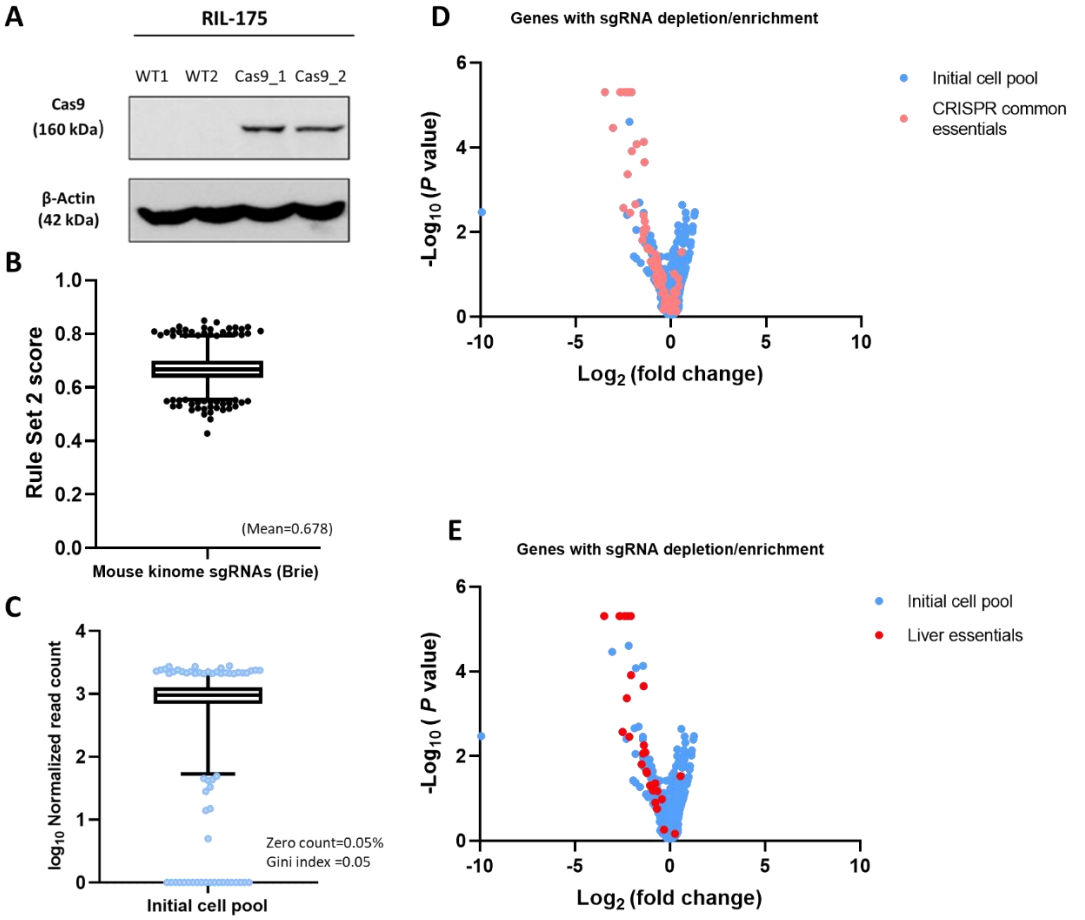

Figure 3.3 Quality controls performed to validate the kinome-wide mouse CRISPR gRNA knockout library before *in vivo* study

(A) Western blot demonstrating Cas9 expression in the RIL-175 cell line transduced with a lentivirus encoding Cas9; mouse β-actin was used as a control. **(B)** Box plot showing Rule set 2 scores of sgRNAs in the mBrie library (average score = 0.678). **(C)** Box plot showing sgRNA distribution in mBrie-transduced RIL-175-Cas9 cells by median-normalized log2 read counts of sgRNAs, zero count sgRNAs=0.05%, Gini index=0.05. (D-E) Volcano plot illustrating the comparison of kinase genes whose knockout can enhance or inhibit tumor cell growth, (D) depletion of essential genes (pink) compared to genes included in the initial library cell pool (blue); (E) depletion of liver development essential genes (red) compared to genes included in the initial library cell pool (blue).

3.3.2 Successful establishment of an *in vivo* kinome-wide mouse CRISPR sgRNA knockout library

To provide a native tumor microenvironment for cell–cell interactions that cannot be mimicked outside the organism for probing kinase-driven pathways involved in HCC immune regulation, we performed an *in vivo* CRISPR screen after the validation of the mBrie library. A total of $7.5x10^5$ mBrie-transduced RIL-175-Cas9 cells (over 500x library coverage) were subcutaneously injected into four C57BL/6 wild-type mice and four C57BL/6-Rag1-KO immunodeficient mice without mature B and T lymphocytes (n=2; half library/mice). Two weeks after transplantation, the tumors were dissected and genomic DNA was extracted for sequencing analysis. Significant differences in tumor growth were observed between immunocompetent wild-type and Rag1-KO immunodeficient mice. Larger tumors in Rag1-KO immunodeficient hosts were observed because of deficiencies in the immune system (Fig. 3.4 A, B).

Before sending the samples for deep sequencing to measure the sgRNA abundance distribution in the eight tumors and pre-transplantation cells, the extracted tumor genomic DNA harvested from the screen was amplified by PCR. The correct size of the purified PCR products (350 bp) was confirmed using agarose gel electrophoresis (Fig. 3.4C). After gel extraction, the samples were quantified using Qubit assay kits and sequenced by Novogene. Quality control measurements of the raw data confirmed the A/T/C/G content distribution for all sequenced samples at the target sgRNA region (25-50 bp position from read 1 of pair-end sequencing), indicating the successful extraction of sgRNA fragments from the tumors (Fig. 3.4D).

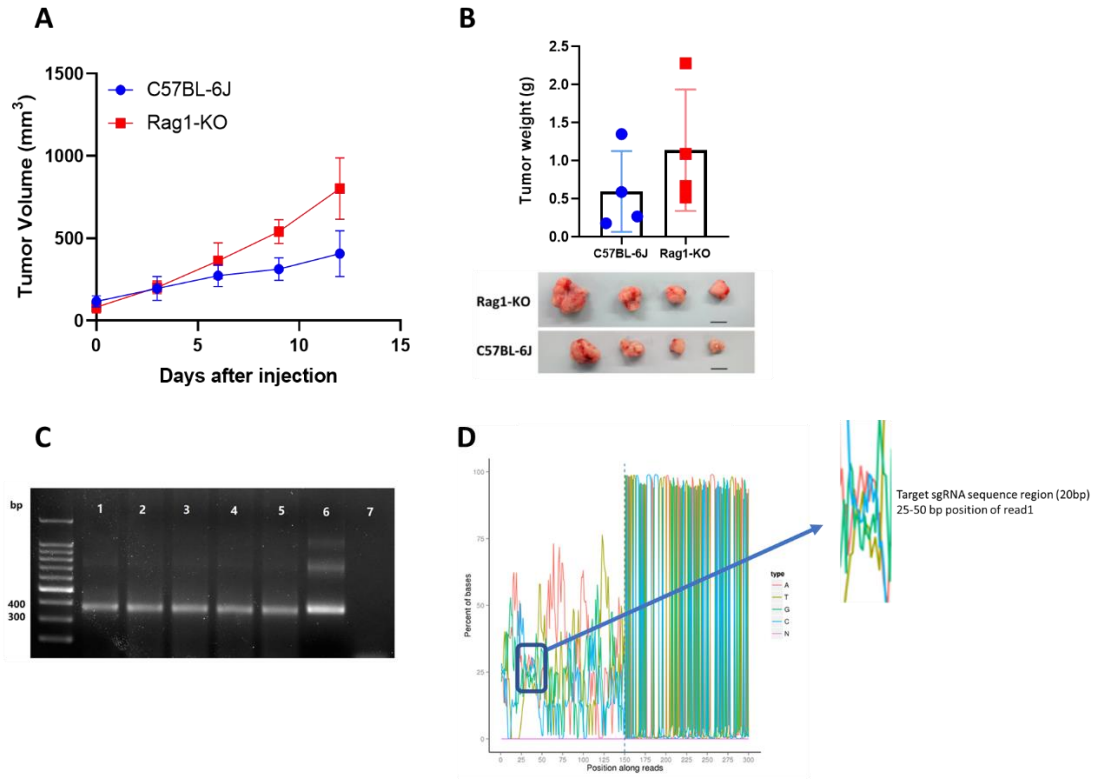

Figure 3.4. Visualization of tumor trend in *in vivo* CRISPR gRNA knockout screen with QC measurements

A, B Tumor growth curve **(A)** and tumor weight **(B)** of sgRNA library transduced with RIL-175-Cas9 subcutaneously injected into six WT mice and Rag1-KO mice; data are shown as mean ± SEM; n = 2 mice per group; scale bar = 1 cm. **(C)** Gel electrophoresis of the purified PCR products (left). Lane 1: Marker; lane 2: DNA extracted from RIL-175-Cas9 cells transduced with sgRNA library; lane 3-6: DNA samples from tumors of mice with library transplantation (1st) Rag1-KO mice1, (2nd) Rag1-KO mice2, (3rd) WT mice1, (4th) WT mice2, and lane 7: negative control. **(D)** Distribution of A/T/G/C base in raw data of sequenced sample sgRNA region ranged between position 25-50bp from read 1 of pair-end sequencing.

3.3.3 Kinome-wide *in vivo* CRISPR screen identifies MINK1 and other protein kinases as potential regulators of immune evasion in HCC

Inspection of sgRNAs enriched or depleted from tumors in WT immunocompetent hosts compared to Rag1-KO immunodeficient mice identified protein kinase targets that modulate the anti-tumor immune response in immunocompetent mice (Fig. 3.5 A). The most enriched sgRNAs included the key components of the interferon (IFN) γ pathway, *Jak1*, and *Jak2*, whereas sgRNAs targeting *Pak3, Sik2, Mink1, Raf1*, and *Pip5k1c* were significantly depleted in WT hosts (Fig. 3.5 B). Importantly, among the groups of sgRNAs that were significantly depleted in WT mice, only Mink1 (Misshapen-Like Kinase 1) sgRNAs were completely depleted in immunocompetent WT mice (Fig. 3.5 C-D). Therefore, we hypothesized that depletion of Mink1 promotes the suppression of tumor immunity, which will be investigated in the following sections.

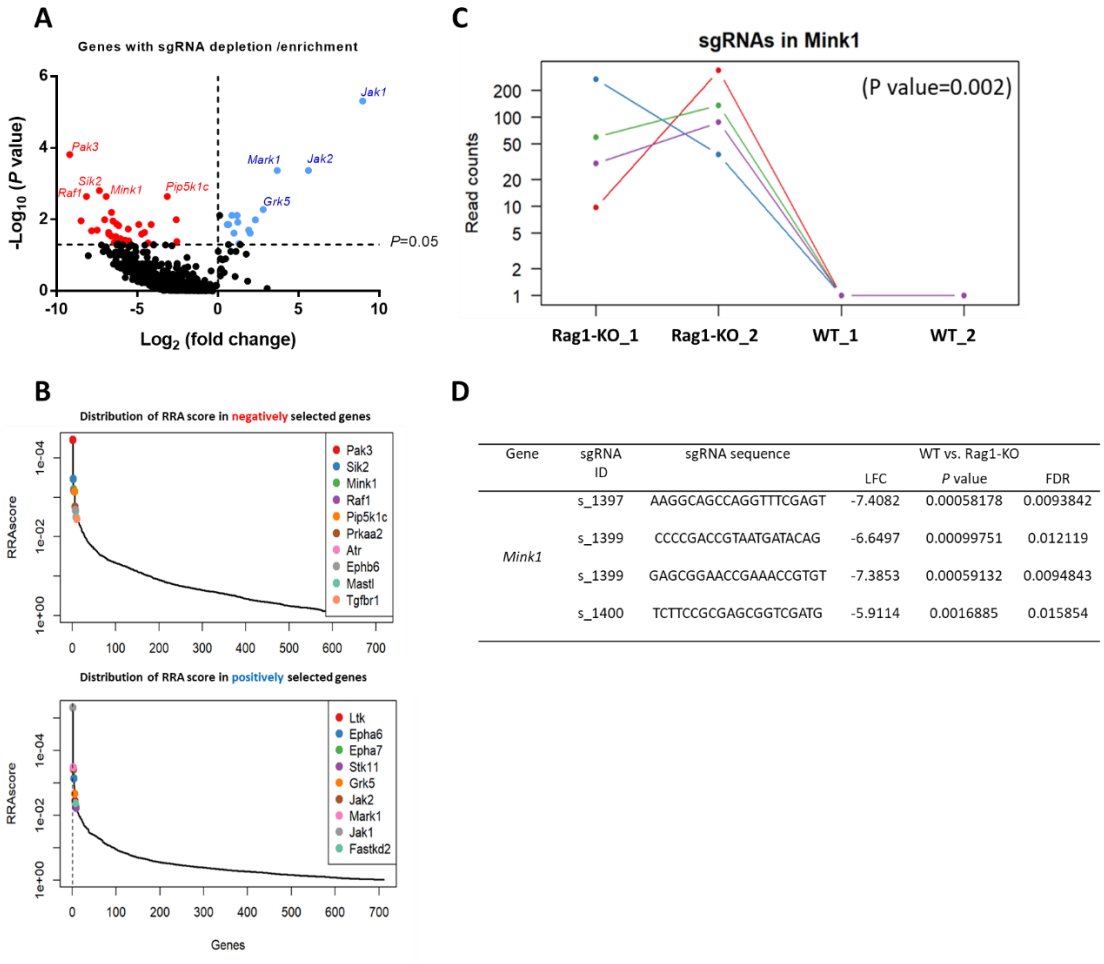

Gene	sgRNA ID	sgRNA sequence	WT vs. Rag1-KO		
			LFC	*P* value	FDR
Mink1	s_1397	AAGGCAGCCAGGTTTCGAGT	-7.4082	0.00058178	0.0093842
	s_1399	CCCCGACCGTAATGATACAG	-6.6497	0.00099751	0.012119
	s_1399	GAGCGGAACCGAAACCGTGT	-7.3853	0.00059132	0.0094843
	s_1400	TCTTCCGCGAGCGGTCGATG	-5.9114	0.0016885	0.015854

Figure 3.5 *In vivo* kinome-wide CRISPR screen identifies *Mink1* as a regulator of immune evasion

(A) Volcano plot illustrating the comparison of kinase genes whose knockout can enhance (blue) or inhibit (red) tumor cell growth in immunocompetent WT mice compared to Rag1-KO mice. **(B)** Illustration of the top 10 depleted genes and enriched genes in immunocompetent versus immunodeficient mice on the screen; genes ranked by Robust Rank Aggregation (RRA). **(C)** Plot showing the distribution of sgRNA read counts (normalized) in *Mink1* Rag1-KO and WT samples. **(D)** Detailed information on the performance of the four Mink1 sgRNAs in comparing Rag1-KO and WT samples.

3.4 Discussion

Many clinical trials of HCC have evaluated immunotherapeutic efficacy in patients with HCC, showing some promising results (Finn, Qin, et al., 2020; Sangro et al., 2021). However, HCC develops in a highly immunosuppressive environment, which prevents an effective response to ICI therapy. Therefore, there is an urgent need to elucidate the immune environment and molecular mechanisms of immune evasion in HCC to improve the efficacy of immunotherapy.

In recent years, the use of *in vivo* CRISPR screens with small, focused libraries has become a popular strategy for studying the regulators of cancer immunology (F. Li et al., 2020). Several studies have successfully identified potential targets for cancer immunotherapy using *in vivo* CRISPR screens (F. Li et al., 2020; Manguso et al., 2017; Wang et al., 2021). In addition, to determine whether a tumor with specific knockout genes can be recognized by the immune system, a comparison of tumor growth in immunocompetent and immunodeficient mice is a widely adopted approach. In this study, we adopted a library screening strategy using the mBrie kinome-wide library to identify protein kinases that sensitize HCC to anti-tumor immunity in wild-type and immunodeficient mice that differ in microenvironmental competency. We first confirmed the efficiency of sgRNAs from the mBrie library using Rule 2 set score, which removes sgRNAs with high off-target scores. RIL-175 cells were then infected with the mBrie CRISPR library at an MOI of 0.3 and selected with puromycin. Satisfactory sgRNA read counts (> 500 counts per sgRNA) and even distribution of sgRNAs were confirmed. Moreover, we found significant depletion of kinases (*Wee1, Cdc7*, and *Pkcι*), which have been reported to be developmentally lethal (Forteza et al., 2016; Kim et al., 2002; Mahajan & Mahajan, 2013). These results indicated that our CRISPR library can be used for *in vivo* CRISPR screening of WT immunocompetent

hosts and Rag1-KO immunodeficient mice. mBrie-transduced RIL-175-Cas9 cells were subcutaneously injected into wild type mice and Rag1-KO immunodeficient mice. As expected, tumors developed more rapidly in immunodeficient mice than in WT mice due to the presence of T and B cells. Thereafter, the tumors were dissected and genomic DNA was extracted for sequencing analysis. Our knockout library screening results are consistent with those of previous screening studies. For instance, *Pip5k1c* KO tumor cells in WT mice, compared to immunodeficient mice, are consistent with their role in enhancing tumor-associated macrophage recruitment (Xue et al., 2019). ATR kinase inhibitor has been proven to reverse T cell exhaustion, and this property was also confirmed in our screening results with depletion of *Atr* in WT mice (Vendetti et al., 2018). Moreover, tumor cells with knockout of *Jak1* and *Jak2* were significantly enriched in WT mice, consistent with findings showing that inhibition of JAK1/STAT1 signaling suppressed anti-tumor immunity (Owen et al., 2019). Similar *Jak*-null cell enrichment findings have been reported in previous *in vivo* CRISPR screening studies in melanoma models (Manguso et al., 2017). These results indicate that our *in vivo* screening was successful.

Functionally, our *in vivo* kinome CRISPR screen identified *Mink1* and other protein kinases as potential regulators of immune evasion in HCC. However, only HCC cells with *Mink1* knockout were completely eliminated in WT mice, suggesting a strong correlation between this gene with HCC immune regulation. In addition, Zhu and Lu (2020) stated that *Mink1* deficiency improved anti-tumor immunity and suppressed tumor growth in mice, which is consistent with our *in vivo* screening analysis (Zhu, 2020). Therefore, *Mink1* was chosen as the prime target for further experiments.

The studies in this chapter served as original evidence for our hypothesis that

modulation of tumor cell-intrinsic protein kinase activity may regulate HCC immune evasion pathways. Aberrant protein kinase pathways are important for shaping the immune TME, encouraging escape from anti-tumor immune responses to promote tumor progression (Spranger & Gajewski, 2018). Therefore, elucidating the molecular mechanisms by which tumor cell intrinsic kinase signaling drives immune evasion is critical to improve the design of rational immunotherapies with increased patient response rates. However, before we attempted to elucidate the novel effects of MINK1 on the tumor immune microenvironment, we first explored the role of Mink1 in HCC development and immune evasion with a Mink1 deficient mouse model and clinical sample analysis in the next chapter.

Chapter 4 Functional characterization and clinical relevance of MINK1 in HCC

4.1 Introduction

In vivo CRISPR screens are powerful tools for studying complex processes in cancer cell-intrinsic immune evasion. Considering the potential of targeting protein kinases involved in cancer immune surveillance to improve ICI efficiency, we constructed a kinome-wide mouse CRISPR knockout library and employed this library for *in vivo* CRISPR screening of WT and Rag1-KO mice (Chapter 3). We successfully identified kinases that were critically involved in HCC immunity. Importantly, one of the kinases in the library, Mink1, stands out from the library group, as deep sequencing analysis confirmed complete depletion of HCC cells infected with either of the four sgRNAs targeting Mink1 in WT mice, but not in immunodeficient Rag1KO mice. As a result, we hypothesized *that* Mink1 promotes cancer immune evasion and selected MINK1 as the focus of our study.

Misshapen-like kinase 1 (MINK1), also known as mitogen-activated protein kinase kinase kinase kinase 6 (MAP4K6), is a serine–threonine kinase belonging to the Ste20 family and the germinal center kinase (GCK) IV subfamily (Dan et al., 2000). It consists of 1312 amino acids and has a predicted mass of 149.8 kDa (Fig. 4.1) (Qu et al., 2004). However, the crystal structure of MINK1 is still unknown. MINK1 has three homologs: TRAF2 and NCK-interacting protein kinase (TNIK/MAP4K7), HPK/GCK-like kinase (HGK/MAP4K4), and Nik-related protein kinase (NRK), with TNIK being the most closely related (Dan et al., 2001; Larhammar et al., 2017; Mikryukov & Moss, 2012). The regulation of MINK1 involves self-interactions, which can occur through the formation of intermolecular dimers or intramolecular folding (Qu et al., 2004). This interaction allows the kinase domain to interact with the CNH domain, leading to activation of MINK1 kinase activity (Hu et al., 2004). Additionally, phosphorylation of the linker domain induces a conformational change that disrupts the interaction between

the kinase and CNH domains, resulting in activation of the MINK1 kinase (Qu et al., 2004).

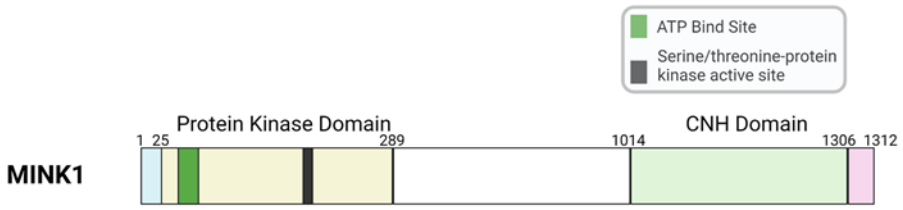

Figure 4.1 MINK1 domain structure

Structural studies have confirmed the conserved structural composition of GCK-IV family protein kinases, including an N-terminal protein kinase domain, a large intermediate linker domain, a citron homology domain (CNH), and a conserved C-terminal extension. The N-terminal protein kinase domain of MINK1 stretches from aa to 25-289 and is responsible for kinase activity, while the citron homology (CNH)-domain from aa 1014-1306 is predicted to interact with GTP-bound forms of Rac and Rho or to bind to docking proteins and lipids (Qu et al., 2004).

MINK1 is involved in various signaling pathways and cellular processes, including cytokinesis, neurodegeneration, and Ras-induced senescence. Several groups have described the function of MINK1 in upregulating kinase p38 through the Raf/MEK/ERK pathway upon activation by RAS (Wong et al., 2014; Yue et al., 2016). In colorectal cancer, it is negatively regulated by Adenomatous Polyposis Coli (Popow et al., 2019). MINK1 also activates the JNK pathway by phosphorylating JNK1 or JNK2 (Zhang et al., 2021). Moreover, MINK1 interacts with the core planar cell polarity (PCP) protein Prickle1, contributing to dendritic branching (Daulat et al., 2012). However, only a few studies have reported its function in cancer and immune regulation.

Recent studies have reported the functional role of MINK1 in the regulation of macrophage and Th17 cell differentiation. Mink1 suppresses the induction of Th17 cells and inhibits SMAD2 activation through direct phosphorylation (Fu et al., 2017). Further

research on the immune regulatory role of MINK1 suggests the promotion of MDSC migration and T cell suppression through MINK1 interaction with the NLRP3 LRR domain, in which blockage of the NLRP3 inflammasome improves anti-tumor immune responses (K. Zhu et al., 2021). MINK1 has also been reported to be a regulator of the Hippo pathway, activating LATS1/2 in parallel with MST1/2 by direct phosphorylation of the LATS-HM motif (Meng et al., 2015). LATS is a well-known tumor suppressor gene, but different studies have shown that LATS is a negative regulator of cancer immunity. Moroishi et al. (2016) demonstrated that LATS1/2 deletion in melanoma and breast cancer cells induced IFN response and stimulate cellular immune response (Moroishi et al., 2016). Thus, MINK1-meidated LATS phosphorylation may contribute to anti-tumor immune regulation. Studies have also shown that MINK1 facilitates binding of the glucocorticoid receptor (GR) to 14-3-3, whereas GR and 14-3-3 downregulate IFNγ production, leading to impairment of the immune response and promotion of immunotherapy resistance in different cancer types (Aida et al., 2014; Han et al., 2015; Munier et al., 2021). In 2020, Zhu and Lu reported that MINK1 deficiency improved anti-tumor immunity and suppressed tumor growth. Importantly, this is the first report demonstrating the efficacy of MINK1 in a murine cancer model (Zhu, 2020). However, instead of focusing on tumor cell-intrinsic immune regulation, they hypothesized that MINK1, expressed in $CD8^+$ T cells, regulates tumor growth. Overall, these publications provide a hint of MINK1's involvement in immune regulation (Fig 4.2).

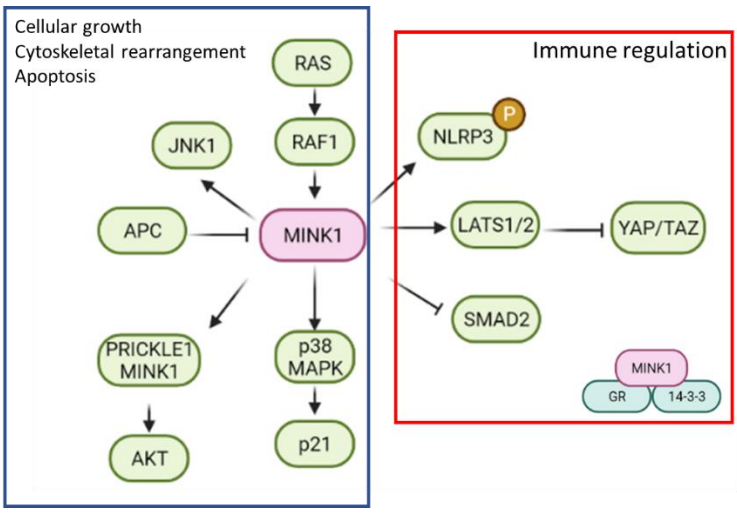

Figure 4.2 Summary of reported role of MINK1

Since the clinical relevance and significance of MINK1 in HCC have yet to be determined and the role of MINK1 in HCC immune regulation has not been reported, prior to conducting mouse experiments, we performed MINK1 gene expression analyses using a dataset available from the Gene Expression Omnibus (GEO) database and The Cancer Genome Atlas (TCGA) dataset. We also performed immunohistochemical (IHC) staining of HCC samples with paired non-tumor liver tissue samples. Furthermore, to assess the clinical relevance of MINK1 in cancer immunity, we used Tumor Immune Dysfunction and Exclusion (TIDE) analysis to examine whether the interaction between MINK1 and T cells is linked to HCC cancer outcomes.

Based on previous screening results, we hypothesized that MINK1 depletion could reverse the immune evasion mechanisms in an HCC mouse model. To functionally characterize the role of MINK1 in HCC regulation, we generated MINK1 KO derivatives of RIL-175 and Hep55.1c cell lines using CRISPR-Cas9 technology. We designed two different guide RNAs (sgRNAs) targeting Mink1 and cloned the sgRNAs

separately into a mammalian vector. After confirming the knockout efficiency of the Mink1 knockout clones, KO cells were subcutaneously injected into both immunocompetent WT mice and immunodeficient Rag1-KO mice.

4.2 Experimental outline

Figure 4.3 A summary of the workflow to examine the clinical relevance and functional role of MINK1 in HCC regulation

(1) Gene and protein expression analyses using IHC staining validation. (2) T cell dysfunction analysis of MINK1 in patients with HCC. (3) Design of Mink1 knockout RIL-175 cell lines. (4) Comparison of tumor growth in WT and Rag1-KO mice subcutaneously injected with Mink1 knockout cells.

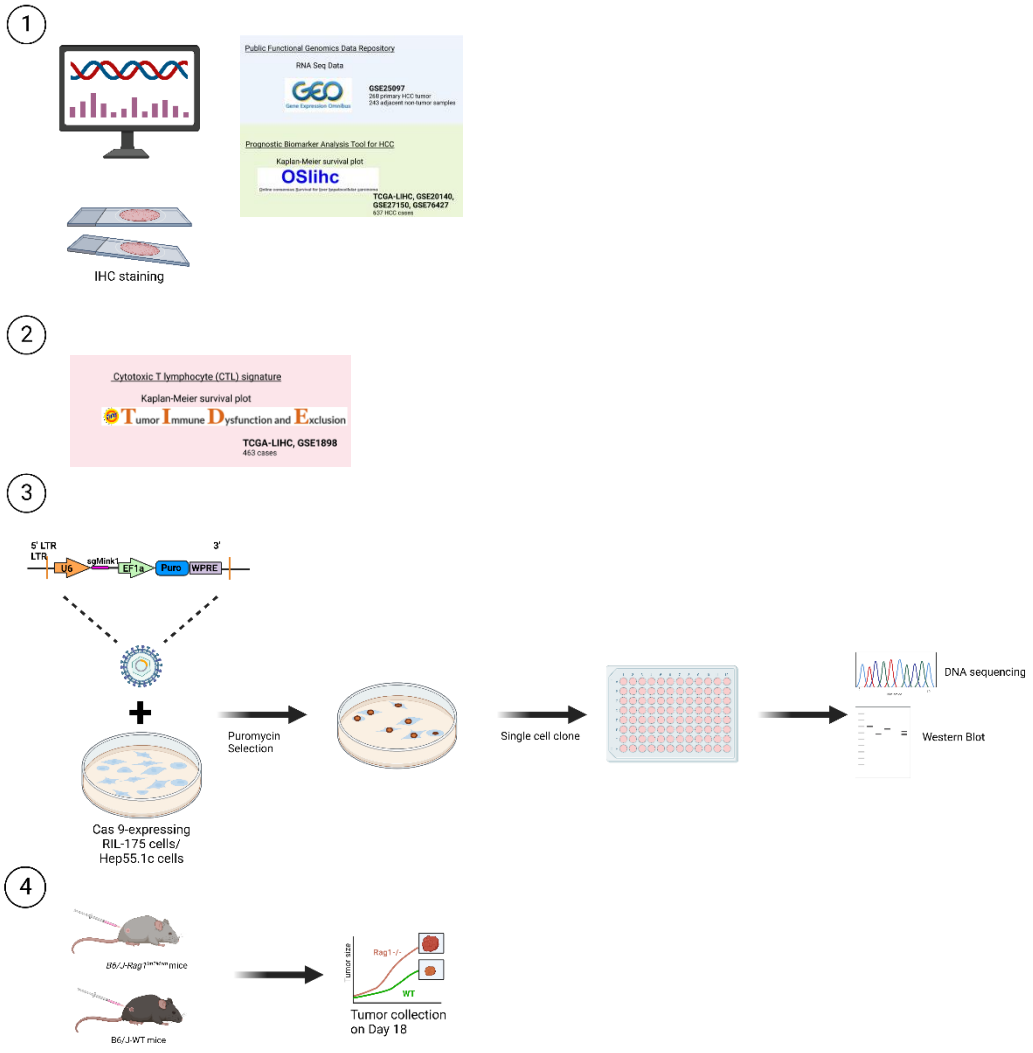

4.3 Results

4.3.1 Overexpression of MINK1 promotes poor prognosis in HCC patients

Our *in vivo* kinome-wide CRISPR knockout screen suggests the potential role of MINK1 in promoting HCC immune evasion. Next, we performed MINK1 gene expression analyses using two online available databases, the Gene Expression Omnibus (GEO) database and The Cancer Genome Atlas (TCGA) dataset, and measured MINK1 protein expression using IHC in an in-house clinical patient sample to examine its clinical relevance. Based on the gene expression profile GSE25097, which contained 268 primary HCC tumors and 243 adjacent non-tumor samples, MINK1 mRNA expression was significantly upregulated in primary HCC tumors compared to non-tumor samples (Fig. 4.4A). Kaplan–Meier survival plot to study the correlation between MINK1 expression and survival in HCC patients was generated using OSlihc, an analysis tool collecting data from TCGA-LIHC and GEO datasets (GSE76427, GSE20140, and GSE27150). The analysis showed that overall survival rates of HCC patients with high MINK1 expression were significantly lower than those of patients with low MINK1 expression ($p=0.045$; log-rank test) (Fig. 4.4B). Moreover, representative IHC staining images of paired sample case 53 showed that MINK1 protein expression was strongly upregulated in liver cancer tissues compared to paired normal tissues, exhibiting minimal MINK1 expression in the non-tumor sample but strong cytoplasmic staining in the corresponding tumor slide (Fig. 4.4C). These results suggest that MINK1 expression is enhanced in HCC and is correlated with poor prognosis and survival.

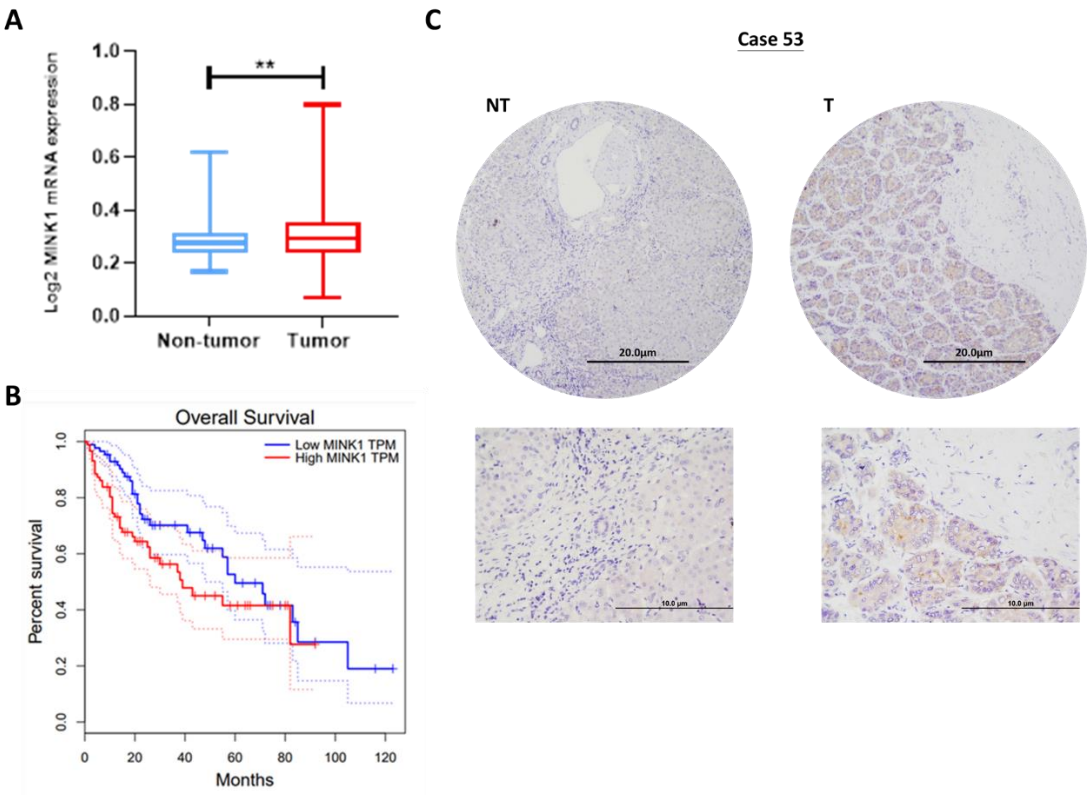

Figure 4.4 MINK1 overexpression was upregulated in HCC samples and correlated with poor prognosis.

(A) Analysis of the dataset GSE25097 showed upregulation of MINK1 mRNA in a cohort of 268 primary HCC tumors and 243 adjacent non-tumor samples (**$p < 0.01$, t-test). **(B)** Kaplan-Meier plots of the overall survival rates of HCC patients with high MINK1 overexpression are significantly lower than those of patients with low MINK1 expression ($p = 0.045$; log-rank test). **(C)** Immunohistochemical staining analysis comparing MINK1 protein expression in HCC tumor patient samples and paired normal tissues; upper scale bar = 20μm; Lower scale bar = 10μm.

4.3.2 MINK1 overexpression is positively correlated with T-cell dysfunction in HCC patients

To assess the clinical relevance of MINK1 in cancer immunity, we used Tumor Immune Dysfunction and Exclusion (TIDE) analysis to examine whether the interaction between MINK1 and T cells is linked to HCC cancer outcomes. Including gene expression profiles from over 189 human cancer studies, the TIDE algorithm is a computational method that employs Cox proportional hazards models to provide gene signatures of T cell dysfunction and predict how genes interact with cytotoxic T lymphocyte (CTL) function to influence survival (Jiang et al., 2018). Several recent studies have demonstrated the accuracy and utility of TIDE in predicting or evaluating the function of genes involved in immune evasion in various cancer types (Song et al., 2022). Briefly, we used this algorithm to estimate CTL levels in each sample within the TCGA-LIHC cohort using the average expression of CTL-specific genes, followed by separating samples into high and low CTL groups based on the mean CTL level to evaluate whether MINK1 influences the beneficial effect of CTL levels on patient prognosis. The MINK1-low patient group demonstrated increased CTL-associated overall survival benefit, whereas high levels of MINK1 weakened the overall survival benefit of CTL-high patients (Fig. 4.5A). Moreover, although the results were not significant, the survival risk score calculated by TIDE suggested that MINK1 was associated with HCC death risk owing to high correlations with CTL infiltration based on the TCGA-LIHC and GSE1898 cohorts (Fig. 4.5B-C). As high CTL levels are associated with an overall survival benefit and the T-cell dysfunction score of MINK1 is significantly high, these results suggest that MINK1 expression in HCC patients is positively correlated with T-cell dysfunction, and HCC patients with MINK1 deficiency may have a higher chance of anti-tumor immune escape.

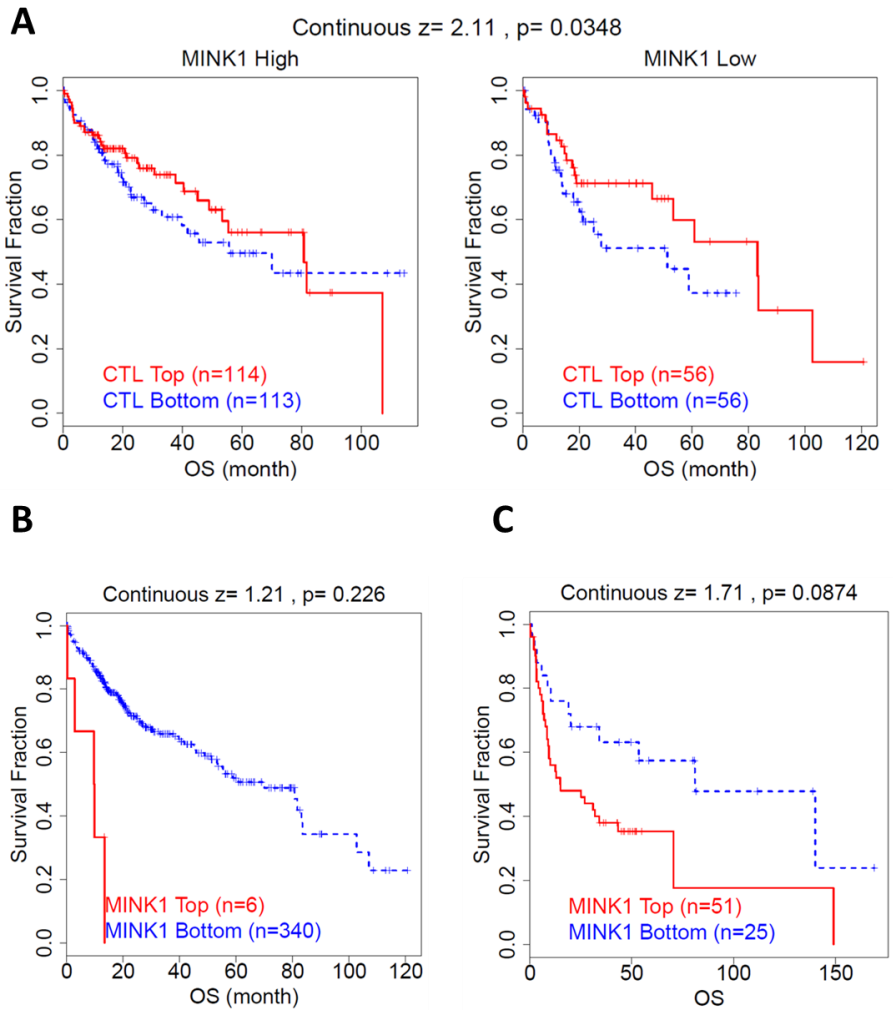

Figure 4.5 MINK1 overexpression was positively correlated with T-cell dysfunction in HCC patients

(A) Kaplan-Meier plots showing the association between the CTL level and overall patient survival for HCC patients from TCGA-LIHC with high (left) and low (right) MINK1 levels; z score= T-cell dysfunction score; CTL infiltration level was estimated as the average expression level of CD8A, CD8B, GZMA, GZMB, and PRF1; B, C Kaplan-Meier plots of the death risk of HCC patients from **(B)** TCGA-LIHC and **(C)** GSE1898 with different MINK1 levels; z score= survival risk score correlated with CTL infiltration; association between the CTL level and overall survival or survival risk factor was computed using the two-sided Wald test in the Cox-PH regression.

4.3.3 Successful generation of the Mink1 knockout HCC cell line with no effect on HCC cell proliferation

After determining the clinical relevance of MINK1 in HCC development, we evaluated its functional role of MINK1 in immune modulation in a mouse model of HCC by generating Mink1 KO HCC cell lines using CRISPR-Cas9 technology. In the previous chapters, we utilized the RIL-175 cell line for our CRISPR screening study. To confirm that the tumor-suppressing role of Mink1 in WT mice is not a cell type-specific observation, we included an additional HCC cell line, Hep55.1c, which is syngeneic to the C57BL/6 mouse strain background in the following studies. Two Mink1 sgRNA sequences were selected based on the MAGeCK analysis. After mouse *Mink1* was cloned into pLentiGuide-Puro and lentiviral packaging, we transfected cells that stably expressed Cas9 with the sgRNA-containing vector. Following single-cell clone generation, the knockout efficiency of Mink1 was confirmed by DNA sequencing of the growing clones, and western blotting was performed with protein extracted from clones. DNA sequencing confirmed that the indels were identified by KO sequencing. On the other hand, western blotting confirmed that Mink1 protein was absent in a subset of clones. Although Mink1 was depleted in Hep55.1c clones H1 and H2, only clones developed from one of the two sgRNA sequences in the RIL-175 cell line showed satisfactory results. Therefore, we selected clones 15 and 16 for the RIL-175 cell line, which showed the highest KO efficiency (Fig. 4.6 A-B). These cell lines can be used as models of HCC *in vivo*.

We used these cell lines to study the immune regulatory role of Mink1 in HCC. However, considering that sustained proliferation is a hallmark of cancer and MINK1 kinase activity has been linked to cell proliferation in other studies (Hu et al., 2004), we first confirmed that the tumor suppression effect of Mink1 KO cells is not mediated by

the regulation of cancer proliferation. We performed an *in vitro* cell proliferation assay in RIL-175 cells, which showed no significant effect of the Mink1 KO cell line on tumor cell proliferation compared with the parental cell line (Fig. 4.6 C). In addition, we evaluated HCC proliferation properties *in vivo* by IHC staining of tumor samples collected after subcutaneous injection of the parental cells and Mink1 KO cells into WT mice. IHC staining further confirmed that the tumor-suppressive effect of Mink1 in CRISPR screening was not due to cell proliferation, as the PCNA expression levels were similar in both samples (Fig 4.6 D-E).

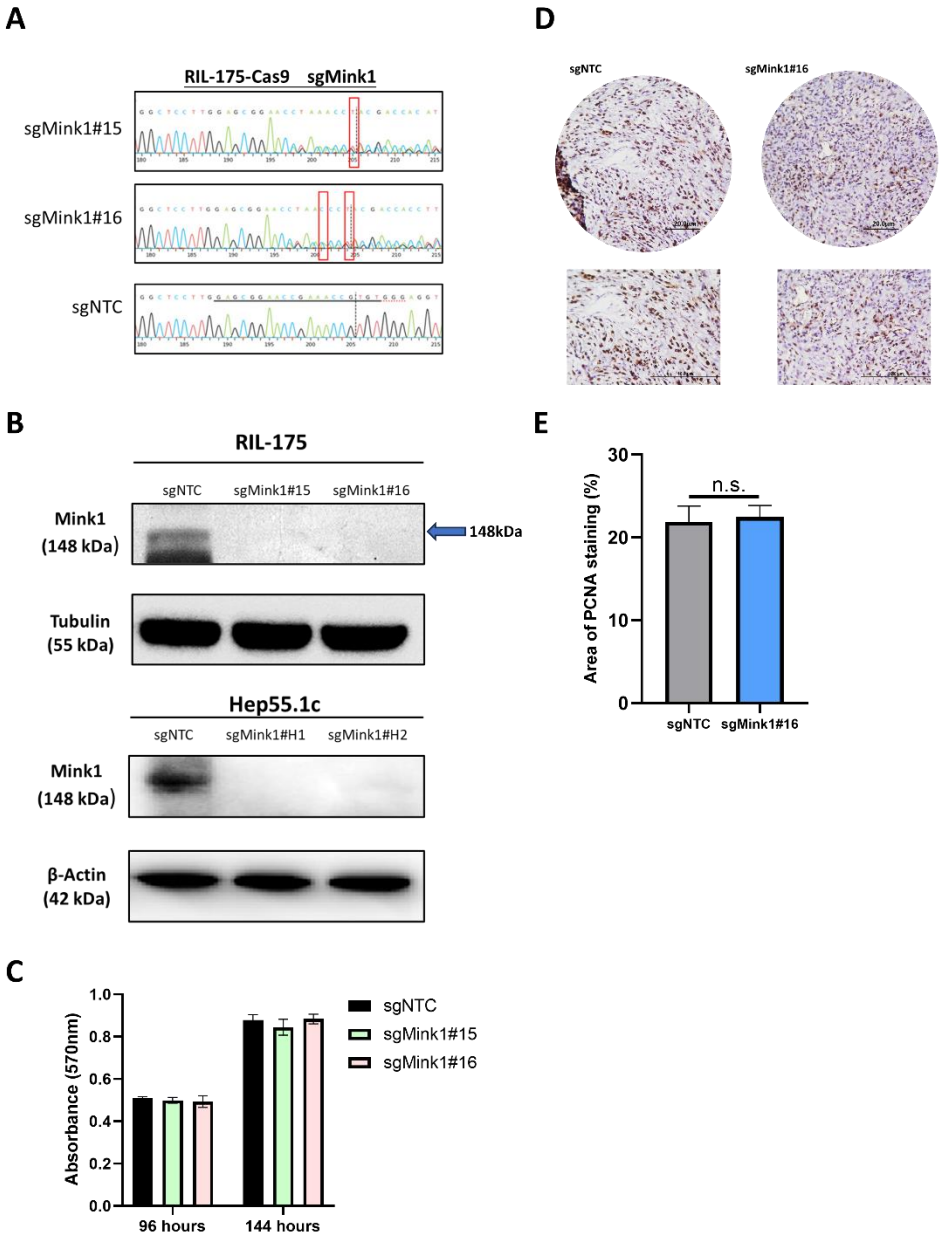

Figure 4.6 Mink1 knockout HCC cell lines are not involved in HCC cell proliferation

Knockout efficiency of Mink1 (sgMink1) in RIL-175-Cas9 validated by **(A)** Sanger sequencing, red squares indicate indels in each clone; **(B)** western blot demonstrating Mink1 expression in RIL-175 cell line and Hep55.1c cell line transduced with a lentivirus encoding sgMink1, mouse Tubulin, and β-actin were used as controls.**((C)** MTT assay results for cell proliferation in sgNTC, sgMink1#15, and sgMink1#16 after 96 and 144 h. **(D)** Immunohistochemical staining analysis of PCNA protein expression in sgNTC tumor samples and sgMink1#16 tumor samples from WT mice; upper scale bar = 20μm; Lower scale bar = 10μm; **(E)** Bar chart showing the percentage of areas stained with PCNA. ($p>0.05$ indicating no statistically significant differences between groups); Data are presented as mean ± standard error of the mean (SEM).

4.3.4 Mink1 knockout impairs tumor growth in immunocompetent mice, but not in immunodeficient mice

To confirm the successful generation of the Mink1 KO HCC cell lines by western blotting, we performed an *in vivo* study by subcutaneously injecting the two Mink1 KO cell lines into immunocompetent and immunodeficient mice to examine the role of Mink1 in HCC immunity. The cell injection number suggested by other HCC immune studies was used as the reference for our experimental design. In addition, we chose the minimal accepted cell number to be injected because a high cancer cell density may mask the tumor-suppressive role of Mink1 KO. As a result, 5000 cells per site (for RIL-175) or 50000 cells per site (for Hep55.1c) were injected into the flanks of mice at a cell: Matrigel ratio of 1:1. As shown in Fig. 4.7A-B, tumor growth was only observed in WT mice injected with control cells, but not in Mink1 KO cells, confirming the strong suppressive ability of the Mink1 KO cell lines. More importantly, tumors were observed in all control and KO cell lines injected into T- and B-cell-deficient mice, and the tumor weights were similar, confirming that the tumor suppression property of Mink1 KO cells was attained by the regulation of HCC immunity instead of HCC proliferation. This result further strengthens our hypothesis that Mink1 promotes HCC development via immune evasion-related pathways.

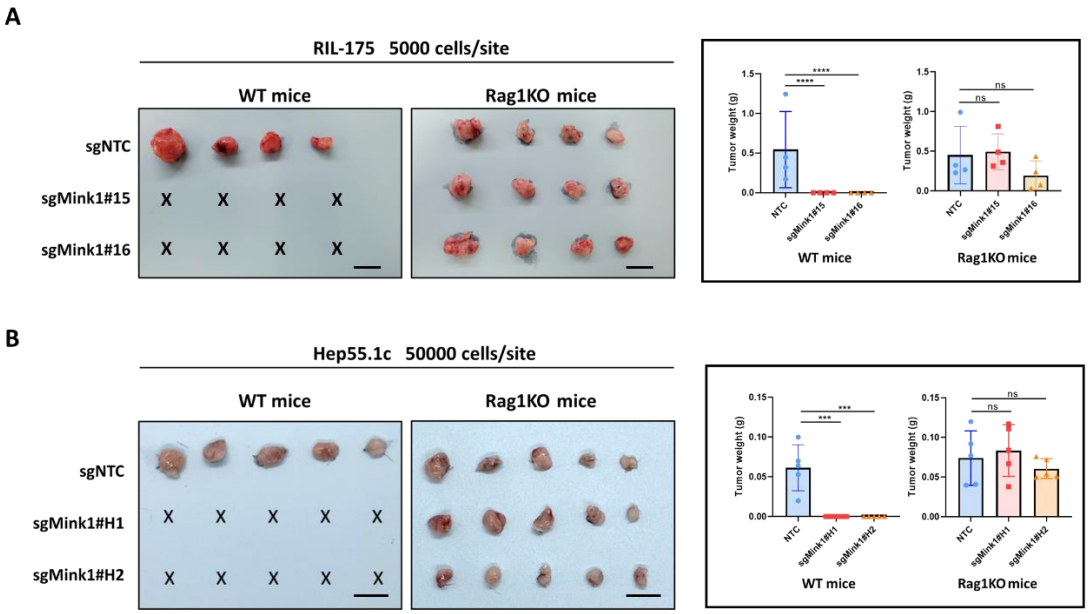

Figure 4.7 Mink1 KO model confirmed Mink1 promote HCC growth through HCC immune regulation

A-B Photograph of tumors and tumor weight of sgNTC, sgMink1(s) transduced **(A)** RIL-175-Cas9 or **(B)** Hep55.1-Cas9 was subcutaneously injected into WT and Rag1-KO mice. Representative images of tumor with injection of 5000 cells and 50000 cells for RIL-175 and Hep55.1c cell lines, respectively, scale bar = 1 cm. (***p < 0.001, ****p<0.0001 *t* test)

4.4 Discussion

In Chapter 3, our deep sequencing results of CRISPR KO screening suggested that Mink1 plays a role in HCC immune regulation, as evidenced by the significant depletion of tumor cells with Mink1 KO in immunocompetent WT mice but not in Rag1-KO mice. We further confirmed the potential role of MINK1 in modulating cancer immunity. For this purpose, we first determined the clinical relevance of MINK1 in HCC and T cell function in this chapter, followed by the generation of Mink1 KO HCC cell lines for *in vivo* studies.

By accessing HCC patient data retrieved from GEO25097 and TCGA-LIHC, our analysis indicated that MINK1 expression was enhanced in HCC and correlated with poor prognosis. Survival analyses of MINK1 correlation with cytotoxic T lymphocyte (CTL) levels on patient outcomes performed using the Tumor Immune Dysfunction and Exclusion (TIDE) algorithm further supported our hypothesis that MINK1 is negatively correlated with HCC immunity. To effectively assess whether Mink1 deletion improves anti-tumor immunity, we generated Mink1 KO clones in two different HCC cell lines, RIL-175 and Hep55.1c, and examined the effects of Mink1 deletion on HCC proliferation and immune regulation. After confirming the KO efficiency of the Mink1 KO clones, we subcutaneously injected the cells into Rag1-KO and WT mice. We predicted that the differences in the immune background of the two groups of mice would contribute to the variation in tumor growth rates, with tumors developing more rapidly under immunodeficient conditions. As expected, the tumor growth rate was similar in Rag1-KO mice injected with the control or KO clones. In WT mice, tumors were observed only in control cell lines, with no tumor growth occurring after KO cell injections, in line with our previous CRISPR screening findings that HCC cells with Mink1 KO were completely depleted in WT mice. This result further confirmed that

the tumor-promoting role of Mink1 may be through the regulation of T and B cells. Furthermore, by generating KO mouse models using two HCC cell lines, we confirmed that Mink1 is not cell line-specific. In conclusion, the latest publications demonstrating the role of MINK1 in various diseases and immune regulation, in addition to clinical sample analysis, support our findings that MINK1 modulates immune evasion in HCC and indicates MINK1 as a possible intervention target in tumor immunotherapy (Zhu, 2020). Inhibition of MINK improved the anti-tumor response in tumor mouse models, further supporting our findings.

To identify and characterize additional tumor cell-intrinsic mechanisms by which MINK1 affects the immune environment in HCC, it is critical to develop a new mouse model that resembles a human-like heterogeneous tumor microenvironment. As a result, we established a hydrodynamic tail vein injection (HTVI) delivery immunocompetent HCC mouse model to examine the effect of Mink1 overexpression in the immune microenvironment in the next chapter. Immune profiling and single-cell RNA sequencing were conducted to provide a detailed view of the changes in immune cell composition and gene expression in OE and GW models.

Chapter 5 Elucidation of molecular mechanisms by which MINK1 promotes tumor growth in $Trp53^{KO}$/$C\text{-}Myc^{OE}$ /Mink1 HCC mouse model

5.1 Introduction

In the previous chapters, we confirmed the role of Mink1 in the modulation of HCC anti-tumor immune responses, as evidenced by HCC clinical data analysis and functional analysis of Mink1 KO mouse models. We utilized a subcutaneous tumor model that is easy to trace for tumor growth, which is widely used in cancer studies in Chapter 3. However, this tumor model has great limitations for further exploration of the molecular mechanisms involving Mink1 in shaping the HCC immune microenvironment. The subcutaneous tumor model cannot fully capture the intricate dynamics and characteristics of cancer because it does not provide the conditions to replicate the complex tissue structure and malignant phenotype found in HCC tumors. Compared with spontaneously developed tumors, rapid tumor growth, which was originally considered an advantage of the subcutaneous model, further hinders immune selection and tumor heterogeneity (Olson et al., 2018). Moreover, although the observation of complete suppression of tumor growth in the *in vivo* Mink1 KO experiment is encouraging, this makes the next steps of the study to collect tumors for downstream analysis impossible. Therefore, in this chapter, we describe the development of an overexpression model using the hydrodynamic tail vein injection (HTVI) method.

HTVI is a well-established method in liver cancer research that generates an HCC model by the rapid injection of a large volume of DNA plasmids encoding the gene of interest into the mouse tail vein, leading to direct gene delivery to the liver (Fig. 5.1) (Bonamassa et al., 2011). To maintain long-term gene expression in hepatocytes, the sleeping beauty (SB) transposon system and CRISPR-Cas9 system were employed to perform gene knock-in and knockout, respectively (Bell et al., 2010). Different combinations of HTVI models have been proven to pathologically resemble human

HCC (DuPage et al., 2009). Therefore, we adopted a combination of the HTVI technique with the SB transposon system and the CRISPR Cas9 KO system that efficiently targets multiple genes in one injection to generate a liver-specific overexpression (OE) model.

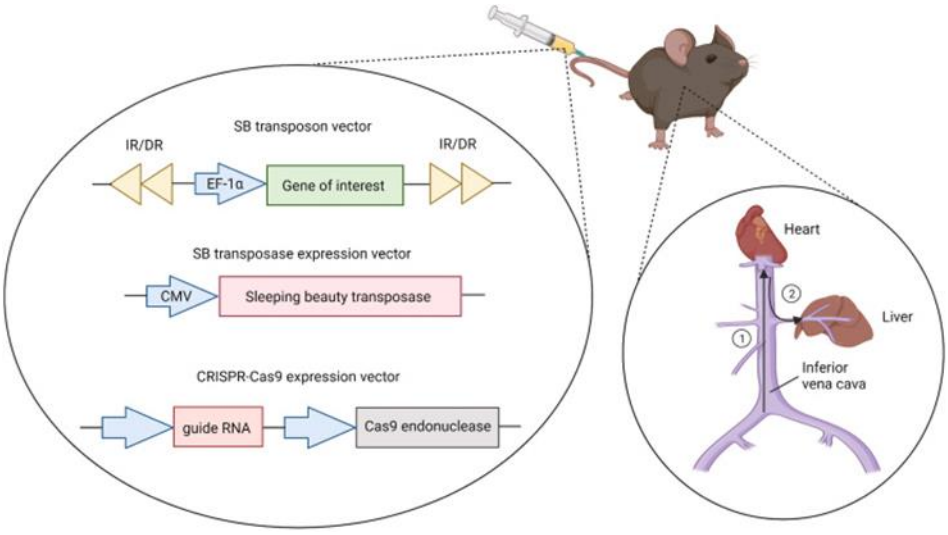

Figure 5.1 Schematic presentation of hydrodynamic tail vein injection with construction of plasmid DNAs

Note. The figure is modified from [Preclinical mouse models of hepatocellular carcinoma: An overview and update] (Gu & Lee, 2022)

HTVI involves rapid delivery of a large volume of DNA plasmids encoding the gene of interest into the mouse lateral tail vein within 7s. Following transient heart dysfunction and retrograde flow, pressurized injection enhances the permeability of the capillary endothelium, facilitating the entry of DNA plasmids into hepatocytes (Ju et al., 2016). The structure and delivery logistics of the SB transposon system and the CRISPR Cas9 system employed in the HTVI model are well established. The SB transposon system utilizes two plasmids, one harboring the SB transposase gene and the other serving as the transposon, which contains the target gene flanked by inverted/direct repeat sequences (IR/DRs) (Hackett et al., 2005). As for the CRISPR system, in contrast to the CRISPR vector construction introduced in Chapter 4.1, gRNA and Cas9 endonuclease were included in the same vector in the HTVI model.

The models developed in our laboratory are driven by oncogenic c-Myc, overexpression of Mink1 (or control vector), and deletion of p53. To elucidate the molecular mechanisms by which MINK1 evades immune responses in HCC, tumors

harvested from the HTVI models were collected for multiple experiments. First, we identified which gene expression pathways were upregulated or downregulated in the OE model by bulk RNA sequencing of Mink1 OE tumors and control tumors, followed by GSEA, Kyoto Encyclopedia of Genes and Genomes (KEGG) pathway analysis, and Gene Ontology (GO) enrichment analysis. Next, we compared the immune landscape of the Mink1 OE tumor and control groups. Tumors were dissociated and HCC immune cells were isolated for immunophenotyping using different flow cytometry panels. Finally, we performed single-cell RNA analysis of the TME established by tumors to study the interaction between Mink1 overexpressed HCC cells and immune cells. By combining the analyses of these approaches, we were able to offer a preliminary interpretation of the mechanisms by which Mink1 is involved in HCC immune evasion.

5.2 Experimental outline

Figure 5.2 A summary of the workflow to study the molecular mechanisms by which MINK1 promotes tumor growth in Trp53^{KO}/C-Myc^{OE} /Mink1 HCC mouse model (1) Establishment of a Trp53^{KO}/C-Myc^{OE} /Mink1 HTVI HCC mouse model. Tumors of Mink1 OE and GW mice after HTVI were collected for (2) bulk RNA sequencing, followed by data analysis using GSEA, KEGG, and GO enrichment analysis; (3) immune profile after tumor infiltration of immune cells to compare the immune cell composition between Mink1 OE and GW mice; and (4) single-cell RNA sequencing after dissociation of tumor samples, followed by data analysis using Rstudio and SingleR.

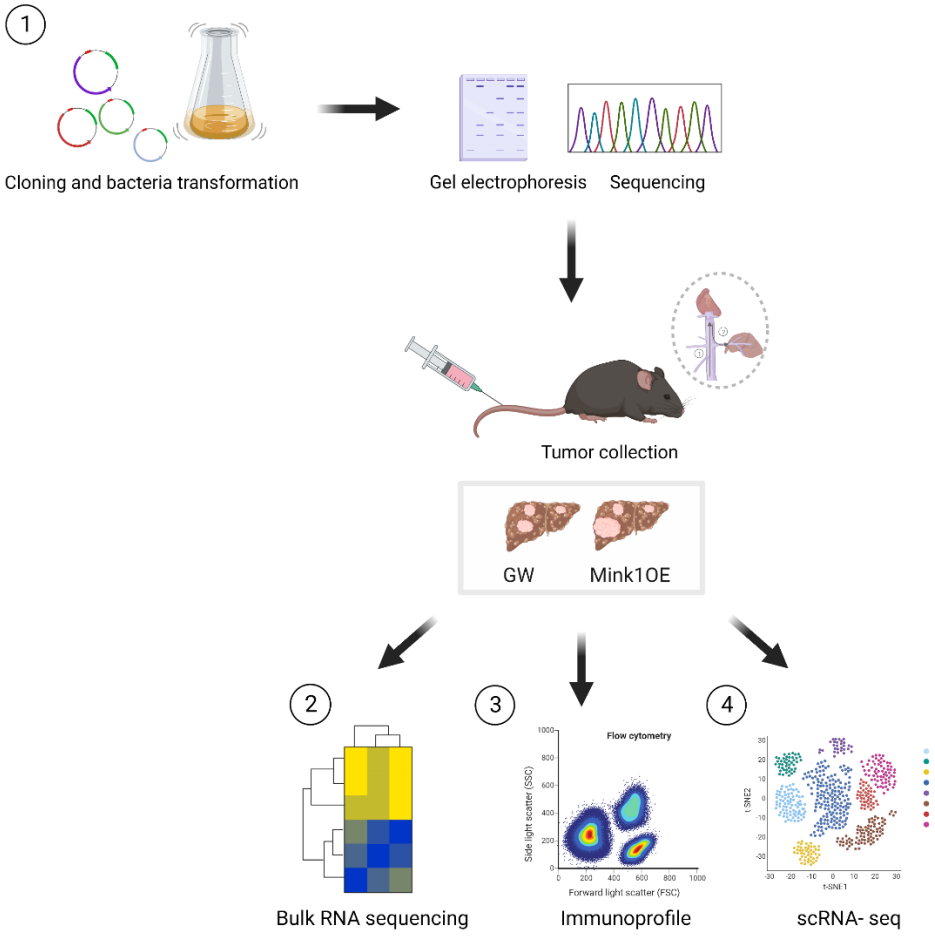

5.3 Result

5.3.1 Successful establishment of a Trp53^{KO}/C-Myc^{OE} /Mink1 HCC mouse model

In Chapter 4, the subcutaneous Mink1 KO model has proven the role of Mink1 in evading the actions of HCC anti-tumor immunity. Unfortunately, the strong tumor suppression effect of the KO model makes further tumor analysis difficult. In order to validate the MINK1-dependent pathways and MINK1 altered TME and immune cell composition that has not yet been revealed in the previous chapter by subcutaneous model, it is important to shift to a suitable Mink1 overexpression mouse model where we could examine the interplay between HCC tumor cells and the immune system *in vivo*.

We utilized the widely employed HTVI technique, which allows customizable genetic alterations to be introduced into the model to create an autochthonous mouse model for HCC. We selected genetic modifications in this model to replicate the HCC background, based on gene relevance and mutation occurrence frequency in human HCC cases. Given the high prevalence of MYC amplification (17%) and TP53 mutation or deletion (33%) in HCC patients, we induced HCC tumors in our model by knocking out Tp53 and overexpressing Myc (Llovet et al., 2021). Either Mink1 overexpression or GW control was also delivered to the mouse models. Another reason for selecting the HTVI model with Tp53 KO and Myc overexpression modification is that we have confirmed that this model has a functional immune response and is sensitive to immune therapies based on our in-house unpublished data, and another study reported by Chiu et al. showed tumor resistance to PD1 inhibitors. In their study, PD1 treatment boosted the anti-tumor immune responses in this HTVI model.

As described in Chapter 5.1, we constructed plasmids for the Sb transposon system and

CRISPR system prior to HTVI. The detailed flow for generating the four plasmids, SB 13 transposase expressing vector (CMV-SB13), transposon-expressing MINK1/ GW control, and MYC (pT3-EF1a-Mink1/ pT3-EF1a-GW and pT3-EF1a-MYC-luc) and CRISPR/Cas9 vector expressing sgTP53 (px330-sgp53) for HTVI is explained in section 2.2. Briefly, the protein-coding sequence of mMink (AAH52474.1) was cloned into donor vector pDONR-221. Subsequently, the Mink1 coding region was inserted into the transposon-expressing vector pT3-EF1a-GW using the Gateway^{TM} cloning method facilitated by the LR Clonase. Before sending the plasmid for sequencing to check whether this sleeping beauty system indeed mediated the exogenous expression of mMink1, the correct size of the extracted plasmid DNA was confirmed by agarose gel electrophoresis. As shown in Fig. 5.3 A, a clear band was observed at the calculated size of pT3-EF1a-Mink1 (8kb). We then confirmed the insertion of the Mink1 fragment by sequencing using both the EF1a forward primer and the BGH reverse primer (Fig. 5.3 B).

Since pT3-EF1a-MYC-luc is a luciferase-containing plasmid, *in vivo* tracking of transfection and injection efficiency, in addition to tumor growth, can be performed by bioluminescence imaging. Tumor growth was monitored weekly using bioluminescence imaging (BLI). As shown in Fig. 5.3 C, on day 14 after HTVI, luciferase signals were detected in the livers of both the control Trp53^{KO}/CMyc^{OE}/GW (GW) and Trp53^{KO}/C-Myc^{OE}/Mink1 (Mink1) groups, confirming c-Myc oncogene transfection efficiency and successful delivery of plasmids. Subsequent tumor growth until day 28 showed that Mink1 mice had faster tumor development than GW mice, supported by significantly increased luciferase expression and larger liver tumors in Mink1 mice, with higher tumor weights and liver-to-tumor ratios compared to GW mice (Fig 5.3 D). Upon liver harvesting from both GW and Mink1 OE groups, tumor tissues

were collected to evaluate Mink1 expression in the tumors. Western blot analysis demonstrated an increase in Mink1 protein expression in Mink1 OE mice compared to GW tumors (Fig.e 5.3 E). qPCR analysis further confirmed the upregulation of Mink1 mRNA (Fig. 5.3 F). Moreover, immunohistochemical staining (IHC) revealed higher Mink1 expression in Mink1 OE tumor tissues than in GW (Fig. 5.3 G). These results not only confirmed the successful generation of the Mink1 OE model, but also substantiated the role of Mink1 in promoting HCC development in this study. Throughout this chapter, we used the same model to further explore the potential mechanism of Mink1-regulated HCC immunity.

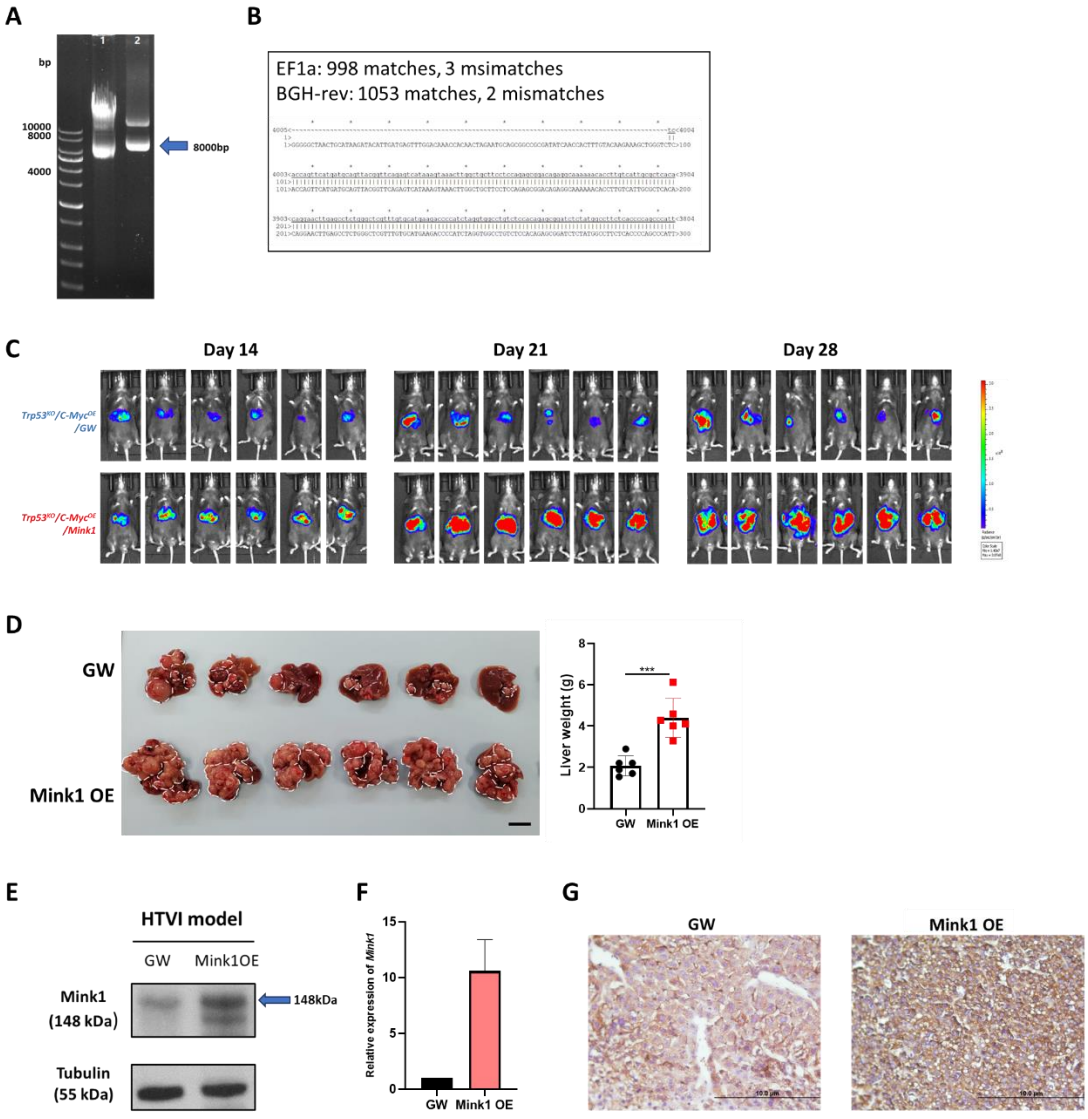

Figure 5.3 Visualization of tumor trend in Trp53^{KO}/C-Myc^{OE} /Mink1 HCC mouse model with QC measurements

(A) Gel electrophoresis of pT3-EF1a-Mink1 plasmid. Lane 1: Marker; Lane 2-3: Plasmid DNA extracted from the pT3-EF1a-Mink1 plasmid (400ng, 200ng). **(B)** Representative sequencing alignment result of the pT3-EF1a-Mink1 plasmid with Mink1 cds using EF1a and BGH primers. **(C)** Bioluminescence images of Trp53^{KO}/C-Myc^{OE} /Mink1 and Trp53^{KO}/C-Myc^{OE} /GW mice at days 14, 21, and 28 subjected to HTVI; n=6 per group. **(D)** Tumor weight of Mink1 OE and GW mice; data are shown as mean ± SEM; n=6 per group; scale bar = 1 cm. **(E)** Western blot demonstrating Mink1 expression in the tumors of Mink1 OE and GW mice; mouse tubulin was used as a control. **(F)** qPCR analysis comparing Mink1 mRNA expression in Mink1 OE and GW mice. **(G)** Immunohistochemical staining analysis comparing MINK1 protein expression in Mink1 OE and GW tumors; scale bar = 10μm. (***$p < 0.001$, *t* test).

5.3.2 Bulk RNA sequencing data reveals significantly enrichment of inflammatory-related pathways and suppression of immune-related pathways in Mink1 OE mice

To elucidate the molecular mechanism by which Mink1 drives immunosuppression in HCC, bulk RNA sequencing was performed. Tumor samples were prepared for sequencing after confirming higher Mink1 protein expression in Mink1 OE tumors than in GW tumors and verifying the RNA quality. DEG analysis was performed to normalize raw RNA expression and to identify differentially expressed genes in the Mink1 OE and GW groups. GSEA using 50 mouse hallmark gene sets from the Molecular Signatures Database revealed upregulation of 64% of gene sets in Mink1 OE, in which 11 gene sets, including pathways related to inflammatory response and TNFα signaling via NFκB, were significant at a false discovery rate (FDR) < 25% (Fig 5.4 A). In parallel, we compared MINK1-low HCC samples with MINK1-high HCC samples using TCGA-LIHC and found significant enrichment of these two pathways in Mink1-high HCC samples. Notably, the inflammatory cytokine *Il6*, which is involved in both gene sets mentioned above, and the granulocyte colony stimulating factor *Csf3* were highly expressed in Mink1 OE samples (Fig. 5.4 B). Heatmaps demonstrated the top-ranked upregulated genes in both Mink1 OE and GW groups (Fig. 5.4 C). To explore the potential downstream pathways related to T cell activation in Mink1 OE, we performed KEGG and GO analyses. KEGG analysis revealed upregulation of the inflammatory mediator regulation pathway and downregulation of the antigen processing and presentation and cytokine-cytokine interaction pathways (Fig. 5.4 D). GO analysis showed downregulated genes related to immune cell function, such as regulation of T cell proliferation, NK cell chemotaxis, and Th1 cell cytokine production (Fig. 5.4 E). These findings suggest that Mink1 overexpression may induce changes in gene networks associated with immune microenvironment remodeling and a robust

inflammatory response. Further exploration of the immune profile is important for understanding the effects of Mink1 OE on the immune microenvironment.

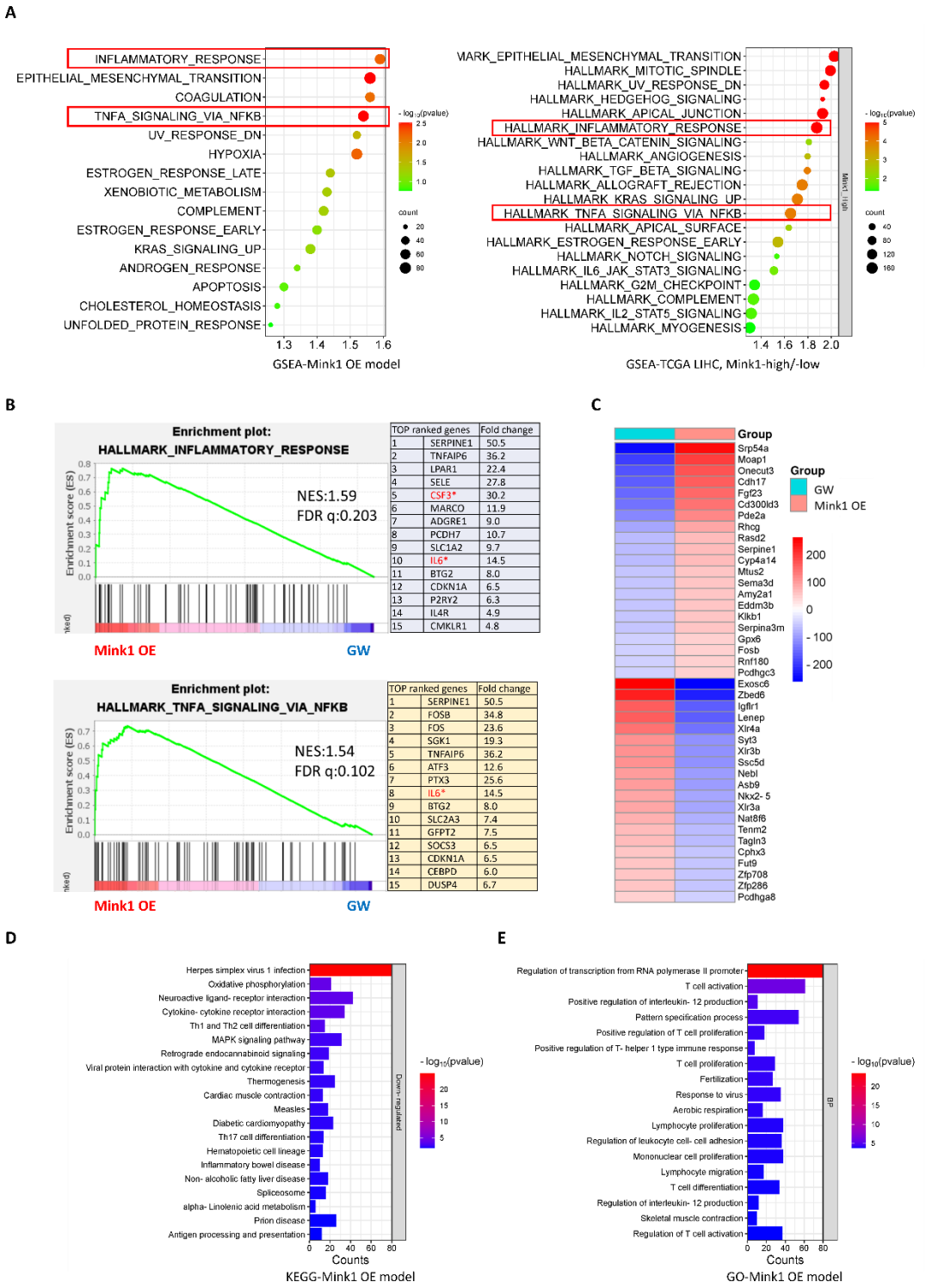

TOP ranked genes		Fold change
1	SERPINE1	50.5
2	TNFAIP6	36.2
3	LPAR1	22.4
4	SELE	27.8
5	CSF3*	30.2
6	MARCO	11.9
7	ADGRE1	9.0
8	PCDH7	10.7
9	SLC1A2	9.7
10	IL6*	14.5
11	BTG2	8.0
12	CDKN1A	6.5
13	P2RY2	6.3
14	IL4R	4.9
15	CMKLR1	4.8

TOP ranked genes		Fold change
1	SERPINE1	50.5
2	FOSB	34.8
3	FOS	23.6
4	SGK1	19.3
5	TNFAIP6	36.2
6	ATF3	12.6
7	PTX3	25.6
8	IL6*	14.5
9	BTG2	8.0
10	SLC2A3	7.4
11	GFPT2	7.5
12	SOCS3	6.5
13	CDKN1A	6.5
14	CEBPD	6.0
15	DUSP4	6.7

Figure 5.4 Bulk RNA sequencing data reveals significant enrichment of inflammatory-related pathways and suppression of immune-related pathways in Mink1 OE mice

(A) Scatter plot illustrating significantly enriched pathways in the Mink1 OE group (left) and TCGA-LIHG Mink1 high or low groups (right). The vertical axis represents enriched pathways, and the horizontal axis represents the normalized enrichment score. The area of the circle in the graph shows the gene set size, and the depth of color represents log10 of the *p* value. **(B)** GSEA-based hallmark enrichment plot of representative gene sets from enriched pathway Inflammatory response (left) and TNFA signaling via NFκB (right), red stars mark the *Il6* and *Csf3* genes. (normalized enrichment score: 1.59, FDR q-value: 0.203; normalized enrichment score: 1.54, FDR q-value: 0.102 respectively). **(C)** Heatmap showing the top enriched and downregulated genes in the GW and OE groups; upregulated genes are in red and downregulated genes are in blue. D-E Bar charts represent the classification of significantly differentially expressed genes in **(D)** KEGG analysis with downregulation and **(E)** gene ontology (GO) biological processes (BP) with downregulation. The vertical axis represents the enriched pathways, the horizontal axis represents the number of genes present in each category, and the depth of color represents the log10 of the *p* value.

5.3.3 Tumor cell–intrinsic Mink1 overexpression promotes neutrophil recruitment and suppresses $CD8^+$ T cell infiltration

To determine which immune cell population is affected by Mink1-drived HCC immune regulation, we performed immune profiling using our HTVI models. This analysis allowed us to immunophenotype and compare the immune infiltration of Mink1 OE and GW tumors to assess the contribution of tumor-intrinsic Mink1 in shaping the TME of HCC tumors. Tumor-infiltrating $CD45^+$ immune cells from the Mink1 and GW groups were first isolated, followed by flow cytometric analysis using the two different antibody panels with antibodies listed in the Methods Chapter 2.1 which covers the major immune cell populations commonly present in the TME. Previous studies have emphasized the role of Mink1 in suppressing Th17 differentiation (Fu et al., 2017). Therefore, we designed a panel including Treg and Th17 cells to confirm whether Mink1 disrupts Th17/Treg balance in HCC. Moreover, two antibody panels were used to prevent spectral overlap between the fluorochromes. The myeloid cell panel includes B cells, monocytes, macrophages, natural killer (NK) cells, dendritic cells (DCs), and neutrophils. The Treg panel includes $CD4^+$ T helper cells, $CD8^+$ cytotoxic T cells, Th17 cells, and Tregs. A gating strategy for identifying different populations is shown in Fig. 5.5 A-B. The frequency of all the immune cell populations was determined as the percentage of $CD45^+$ immune cells.

Our analysis showed that while the overall T cell composition decreased in Mink1 OE samples, most T cell subsets did not change significantly compared to GW samples, except for the $CD8^+$ subset, which decreased from 25% in GW to 18% in Mink1 OE samples (Fig. 5.5 C). To confirm the suppressive effect of Mink1 on $CD8^+$ T cells, we conducted multiplex fluorescent immunohistochemical staining using CD8 and Mink1 antibodies in paraffin-embedded tissue sections. The fluorescent signal of Mink1

expression (red) was specifically detected within the tumor nodule of the Mink1 OE model but was absent in the nearby tumor microenvironment and the majority region in the GW sample (Fig. 5.5 D). Additionally, a significantly higher percentage of tumor-infiltrating $CD8^+$ T cells (green) was observed in GW tumor tissue slides than in Mink1 OE. Whereas GW tumors were heavily infiltrated by $CD8^+$ T cells, even in the tumor core, Mink1 OE tumors showed much lower CD8 expression in the tumor nodules, and a proportion of $CD8^+$ cells accumulated in the tumor rim of Mink1 OE tumors, suggesting that Mink1 overexpression possibly suppressed $CD8^+$ T cell infiltration rather than cell proliferation (Fig. 5.5 D). Immune profile analysis showed that the DC subset that has been reported to activate $CD8^+$ T cells also decreased slightly in Mink1 OE mice (Fig 5.5. B). Interestingly, there was a slight decrease in $Foxp3^+$ Treg cells in Mink1 OE tumors and the increase in $RORgt^+$ Th17 cells was not significant, which contradicts to previous reports that suggested Mink1 suppresses Th17 cells (Fig. 5.5 B). In the myeloid panel, there was a mild increase in $LY6C^+CD11b^+CD3^-CD19^-$ monocytes upon Mink1 overexpression. Conversely, we observed a significant increase in neutrophil infiltration, as demonstrated by Ly6G immunohistochemical staining (Fig. 5.5 B).

The upregulation of Mink1 leads to notable alterations in the TME, including a reduction in $CD8^+$ T cells and a substantial increase in neutrophil infiltration. Given the drastic increase in the neutrophil population in our Mink1 OE model and the well-known immunosuppressive role of TANs in cancer, we would like to investigate the specific mechanisms by which Mink1 overexpressed HCC cells contribute to neutrophil recruitment. However, immune profiling provides only a general overview of immune cell composition in the TME, prompting us to conduct single-cell RNA sequencing (scRNA-seq) analysis to gain comprehensive molecular insights into the intricate

interactions between tumors and neutrophils at the single-cell level.

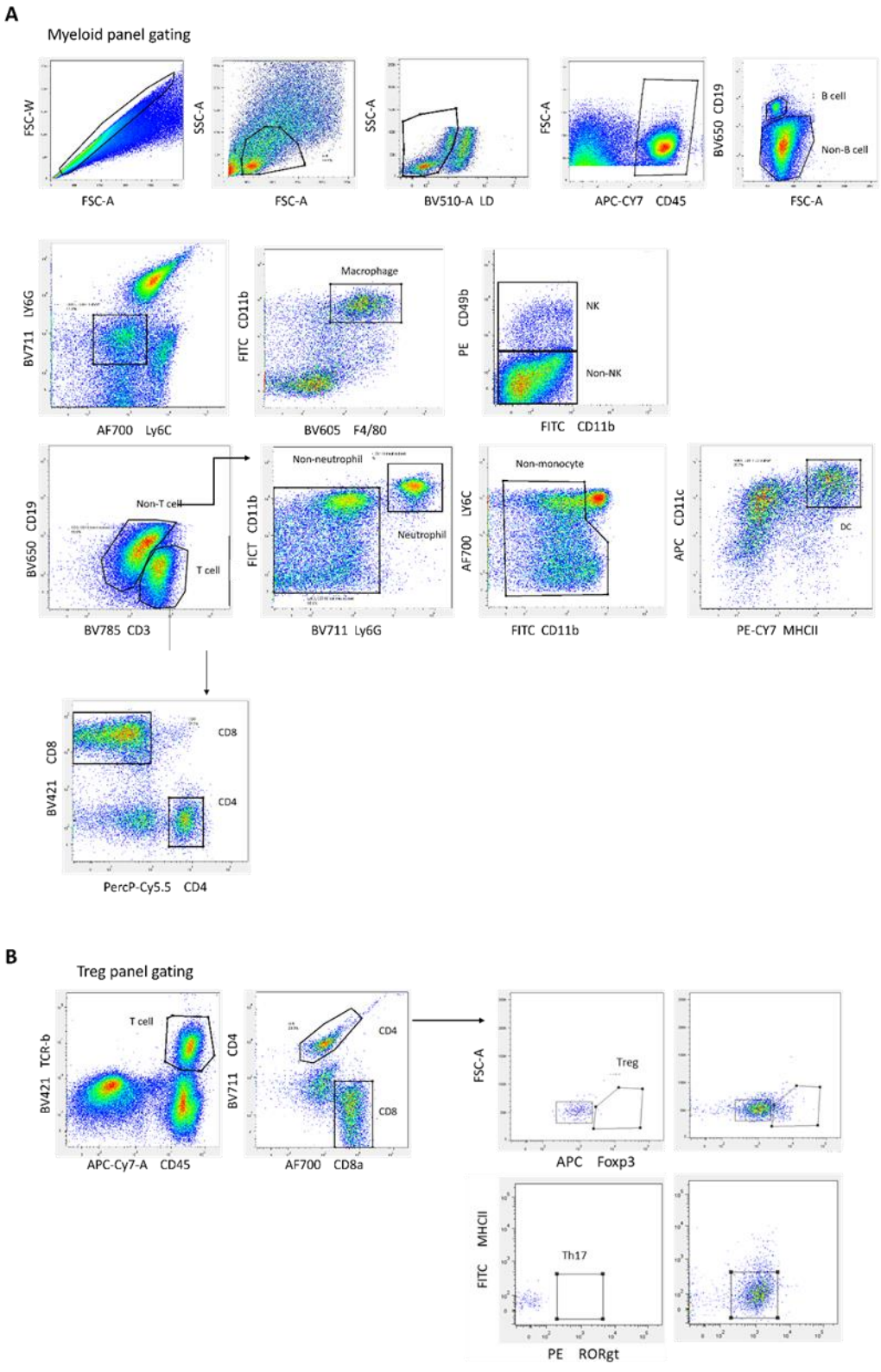

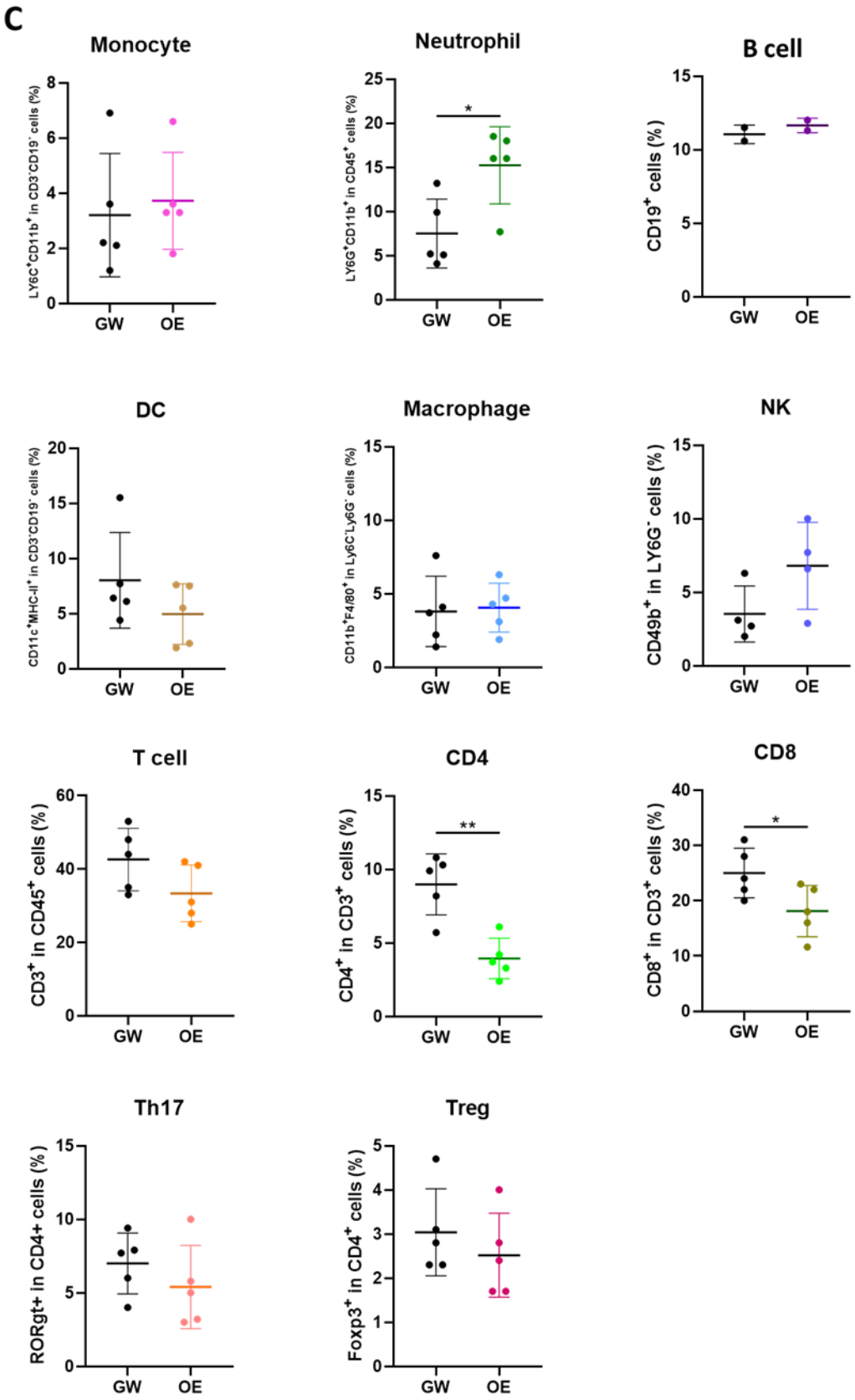
C
Monocyte
LY6C+CD11b+ in CD3-CD19- cells (%)
GW
OE
Neutrophil
LY6G+CD11b+ in CD45+ cells (%)
*
B cell
CD19+ cells (%)
DC
CD11c+MHC-II+ in CD3-CD19- cells (%)
Macrophage
CD11b+F4/80+ in Ly6C-Ly6G- cells (%)
NK
CD49b+ in LY6G- cells (%)
T cell
CD3+ in CD45+ cells (%)
CD4
CD4+ in CD3+ cells (%)
**
CD8
CD8+ in CD3+ cells (%)
Th17
RORgt+ in CD4+ cells (%)
Treg
Foxp3+ in CD4+ cells (%)

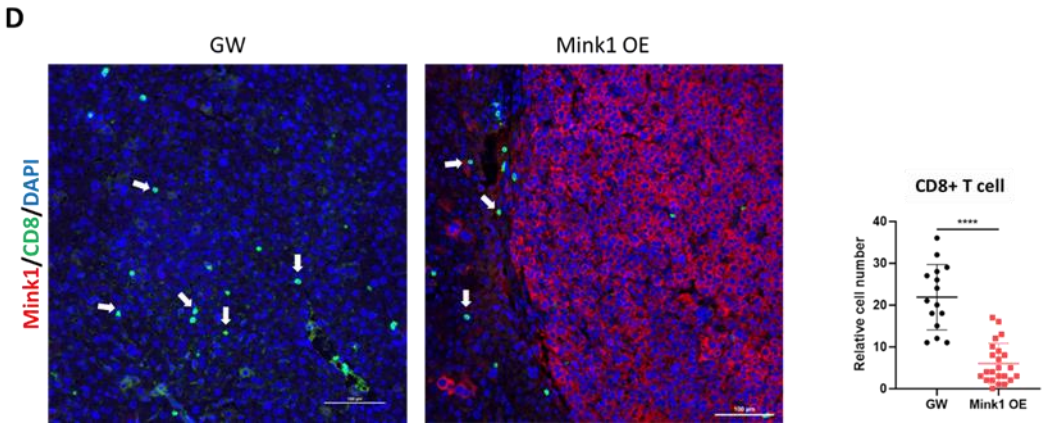

Figure 5.5 Immune profile reveals neutrophil recruitment and suppression of CD8$^+$ T cell infiltration in Mink1 OE mice

A-B Flow cytometry immunophenotyping gating strategy of **(A)** Myeloid panel, **(B)** Treg panel. **(C)** Representative flow cytometry plots of immune cells characterized by the immune profile; DC, dendritic cells, CD4=CD4$^+$ T cells, CD8=CD8$^+$ T cells; Treg, regulatory T cells, Th17=T helper 17 cells. **(D)** Representative images of CD8 (green) and Mink1 (red) co-immunofluorescence staining in GW and Mink1 OE, with arrows indicating CD8$^+$ T cells. Scale bar=100μm (left and middle). Quantification of tumor-infiltrating CD8$^+$ T cells in GW and Mink1 OE in 20 pairs of multiplex IHC images, regions for images taken are near tumor nodules but randomly selected (right). (****$p < 0.0001$, *t* test)

5.3.4 Single cell sequencing analysis revealed increased populations of immunosuppressive cells and suggested the pivotal role of PD-L1^{+} neutrophils to promote tumor development in Mink1 OE model

Immune profiling of our HTVI model revealed the overall immune milieu, highlighting the differences between GW and Mink1 OE immune cell compositions, further confirming the immunosuppressive role of Mink1 in HCC and its impact on the anti-tumor immune response. However, it is important to consider the limitations of fluorescent channels in this analysis, as this may lead to potential steric effects during cell staining, and subsequently, erroneous data interpretation (Gomes de Castro et al., 2017). To ensure the validity of our immune profiling findings, we conducted single-cell RNA sequencing analysis that not only assessed surface protein expression but also provided insights into the underlying genetic and transcriptional states of tumor cells and tumor-infiltrating immune cells. Single-cell RNA-seq analysis has emerged as a prominent tool for cancer immune studies because of its ability to dissect intricate TME at the cellular level. By characterizing individual cells, this technique surpasses the limitations of bulk RNA sequencing and reveals heterogeneity within samples by identifying distinct cell populations including rare immune subsets. It also provides insights into gene expression patterns and provides a comprehensive study of immune responses, cellular communication, and immune-related gene regulation (Chen et al., 2019). In this study, scRNA-seq analysis allowed us to explore the interplay between neutrophils and Mink1 in our HTVI model. These findings could offer clues to modulate the immune response and enhance outcomes in patients with HCCs.

Tumor cells were prepared for scRNA analysis by dissociating the tumor tissue into a single-cell suspension using dissociation buffer and sorting the cells with live/dead staining. After receiving normalized sequencing data, we followed a bioinformatics

pipeline, which is explained in Chapter 2.2, to classify the variation and genetic context of the TME components. Briefly, we removed cells with low sequencing depth, low gene counts, or high mitochondrial gene expression and excluded genes that were not expressed in a sufficient number of cells to reduce noise and computational burden through quality control and filtering steps (Fig. 5.6 A). Next, we employed SingleR to classify cells into phenotypic subpopulations. By comparing cell gene expression to a reference dataset, this computational method assigns cells to the most similar reference cell type, aiding the identification of distinct cell populations within the dataset (Fig. 5.6 B). Clusters that could not be defined by SingleR were separated based on widely adopted biomarkers that were not included in the SingleR database (Fig. 5.6 C). Since T cells are the focus of this study, we extracted the T cell cluster from the heterogeneous cell population and proceeded to further subcluster it into distinct T cell subsets, such as $CD8^+$ T cells and Tregs (Fig. 5.6 D). We also confirmed Mink1 overexpression in the HCC cell cluster in Mink1 OE samples. After splitting the defined cell type clusters into GW and Mink1 OE groups, we found that changes in immune cell composition corroborated our immunophenotyping data. The overall T-cell compartment, $CD8^+$ cells, and $CD4^+$ cells were slightly decreased in Mink1 OE tumors compared to GW tumors (Fig. 5.6 F). No changes in Th17 cell and Treg numbers confirmed that the ability of Mink1 to suppress Th17 differentiation was not applicable to our model. Using T cell exhaustion markers, including *Lag3*, *Pdcd1*, and *Havcr2*, which were not used in the immune profile, we found an increase in exhausted T cells in Mink1 OE tumors (Fig. 5.6. F). Moreover, consistent with the immune profile analysis, an increase in the neutrophil population and a decrease in the DC population were observed in Mink1 OE tumors (Fig. 5.6 F).

Using gene expression data, we were able to observe immunological features that could

not be obtained from the FACS data, such as additional markers of T cell exhaustion. We narrowed our immune cell population of interest to neutrophils, which were further clustered into four subtypes: Neu01_CCL5, Neu02_PD-L1, Neu03_MMP9, and Neu04_Cd170. Owing to the absence of definitive markers distinguishing N1 and N2 neutrophils, it remains uncertain whether the increased population of neutrophils in the OE sample is N2 pro-tumor neutrophils. Nevertheless, as the major neutrophil increase in the OE sample belongs to two specific populations, Neu03, which expressed high levels of the protumor marker matrix metalloproteinase-9 (Mmp9), and Pd-l1-expressing Neu04, we suggest that the increased neutrophil population observed in our scRNA-seq analysis is protumorigenic. We also found that the Pd-l1^{+} neutrophil population in OE sample is absent in the GW sample (Fig. 5.6 G). Moreover, in addition to the increased expression of *Pd-l1* (Cd274) in neutrophils, sequencing analysis showed increased *Pd-1* (Pdcd1) expression in T cells in the OE samples (Fig. 5.6 H). To further validate our pathway analysis results from bulk RNA sequencing, pathway enrichment in the neutrophil cluster was analyzed using GSEA. The GSEA results suggested that apart from the inflammatory and TNFα pathways indicated in bulk RNA-seq analysis, the IL6/JAK/STAT3 pathway was strongly upregulated in the neutrophil population in the Mink1 OE sample. The expression of *Il-6r* was upregulated in neutrophils, whereas that of *Il-6* was upregulated in HCC cells (Fig. 5.6 I).

In summary, our scRNA-seq analysis of Mink1 OE and GW tumors revealed significant remodelling in the TME, characterized by a drastic increase in neutrophil population, which aligns with the findings of our immune profiling. We inferred that these alterations collectively contribute to an immunosuppressive TME and robust inflammatory response, possibly due to the recruitment of neutrophils and subsequent immunosuppressive cell populations upon Mink1 overexpression. Moreover, we

established a connection between Mink1 and HCC immune evasion, suggesting the potential involvement of $Mmp9^{+}$ and $Pd\text{-}l1^{+}$ neutrophils in this process.

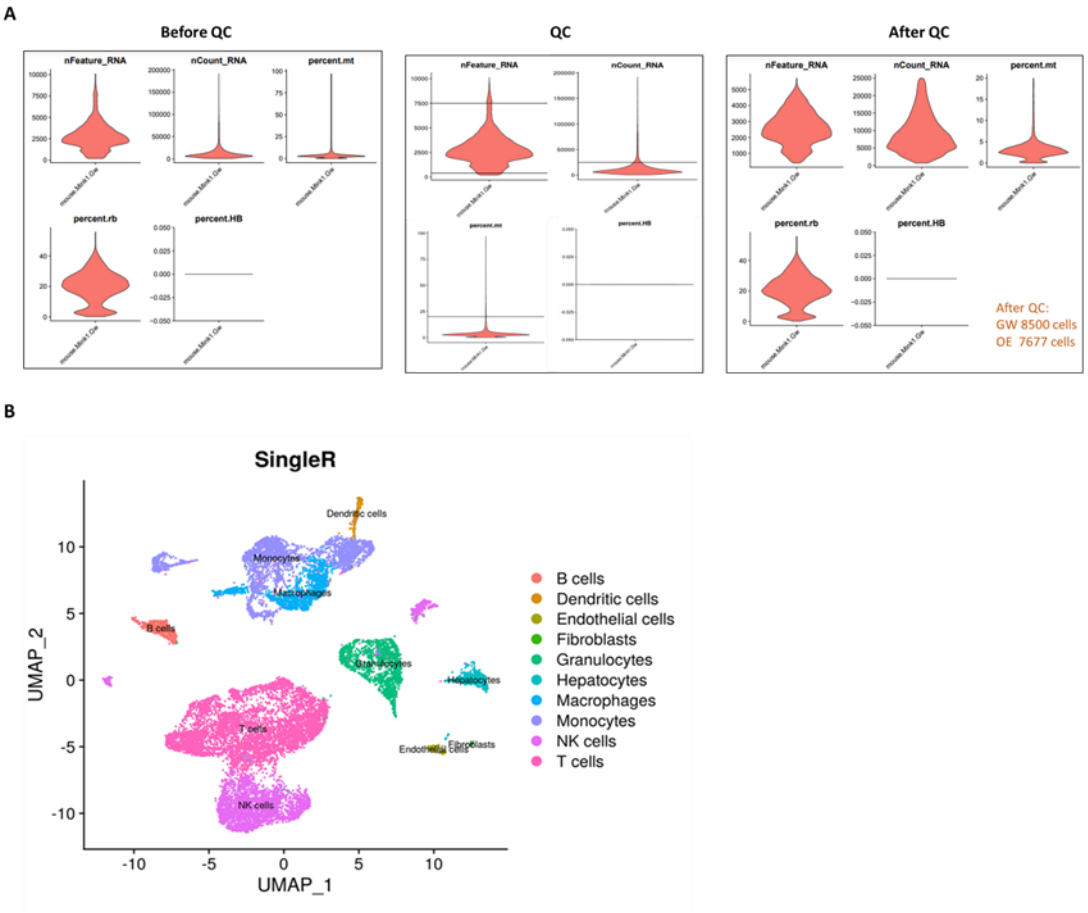

C

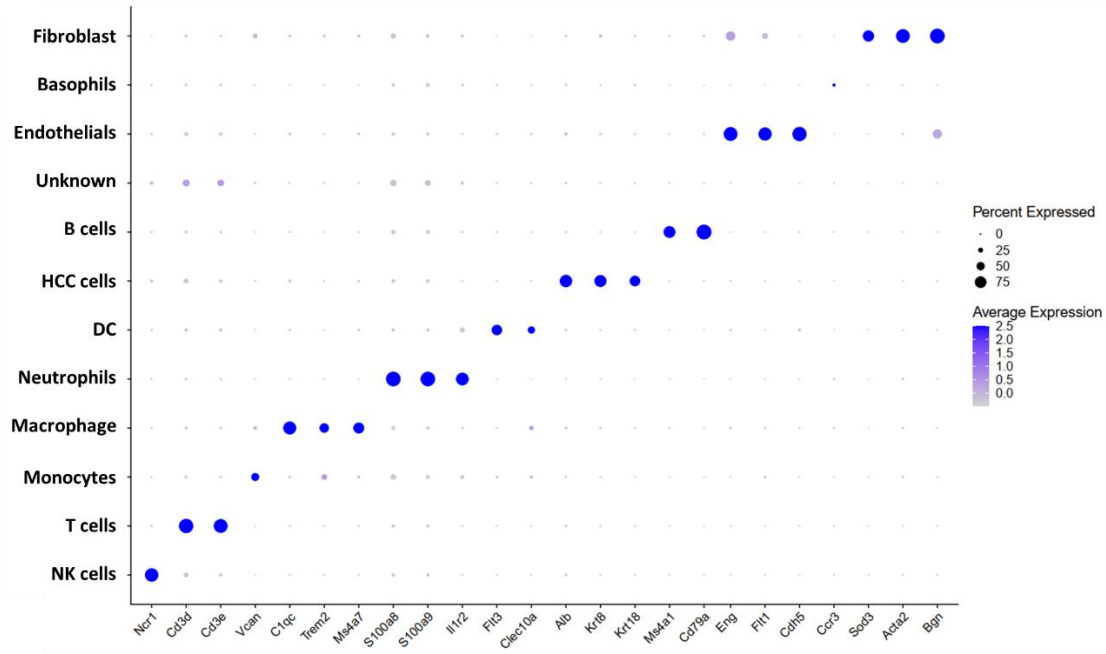
Fibroblast
Basophils
Endothelials
Unknown
B cells
HCC cells
DC
Neutrophils
Macrophage
Monocytes
T cells
NK cells
Ncr1
Cd3d
Cd3e
Vcan
C1qc
Trem2
Ms4a7
S100a8
S100a9
Il1r2
Flt3
Clec10a
Alb
Krt8
Krt18
Ms4a1
Cd79a
Eng
Flt1
Cdh5
Ccr3
Sod3
Acta2
Bgn
Percent Expressed
0
25
50
75
Average Expression
2.5
2.0
1.5
1.0
0.5
0.0

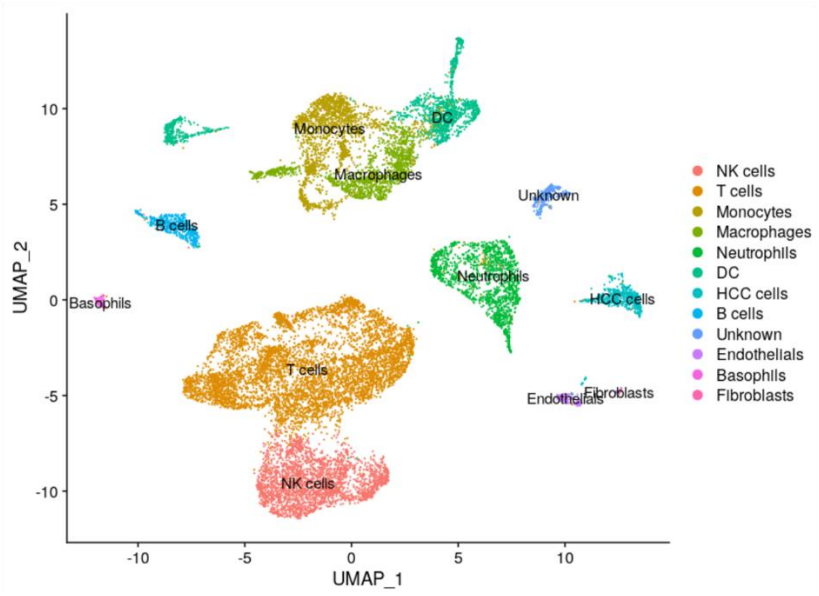
Monocytes
DC
Macrophages
Unknown
B cells
Neutrophils
Basophils
HCC cells
T cells
Endothelials
Fibroblasts
NK cells
UMAP_2
UMAP_1
10
5
0
-5
-10
-10
-5
0
5
10
NK cells
T cells
Monocytes
Macrophages
Neutrophils
DC
HCC cells
B cells
Unknown
Endothelials
Basophils
Fibroblasts

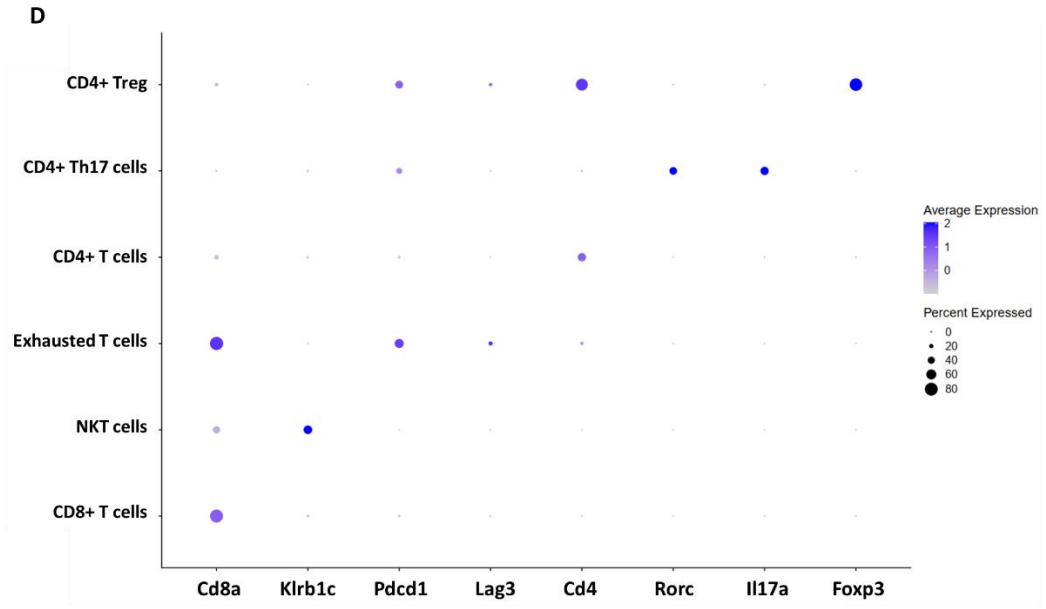
D
CD4+ Treg
CD4+ Th17 cells
CD4+ T cells
Exhausted T cells
NKT cells
CD8+ T cells
Cd8a
Klrb1c
Pdcd1
Lag3
Cd4
Rorc
Il17a
Foxp3
Average Expression
2
1
0
Percent Expressed
0
20
40
60
80

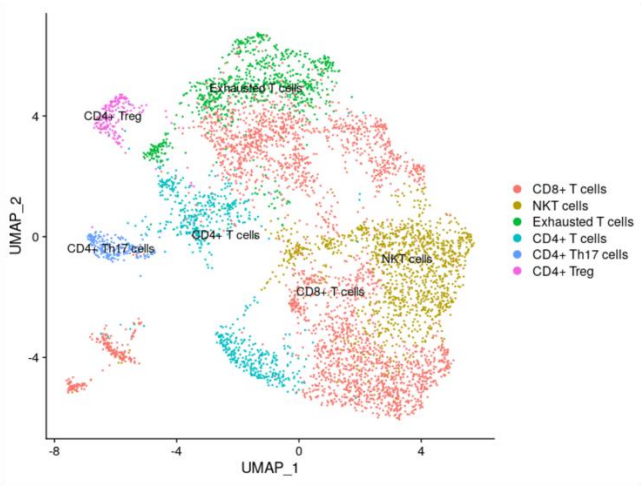
Exhausted T cells
CD4+ Treg
CD4+ T cells
CD4+ Th17 cells
NKT cells
CD8+ T cells
UMAP_2
UMAP_1
CD8+ T cells
NKT cells
Exhausted T cells
CD4+ T cells
CD4+ Th17 cells
CD4+ Treg

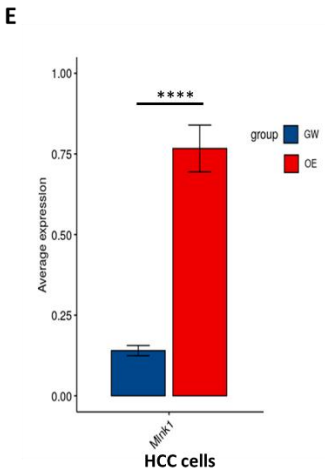
E
****
group
GW
OE
Average expression
Mrkl
HCC cells

F

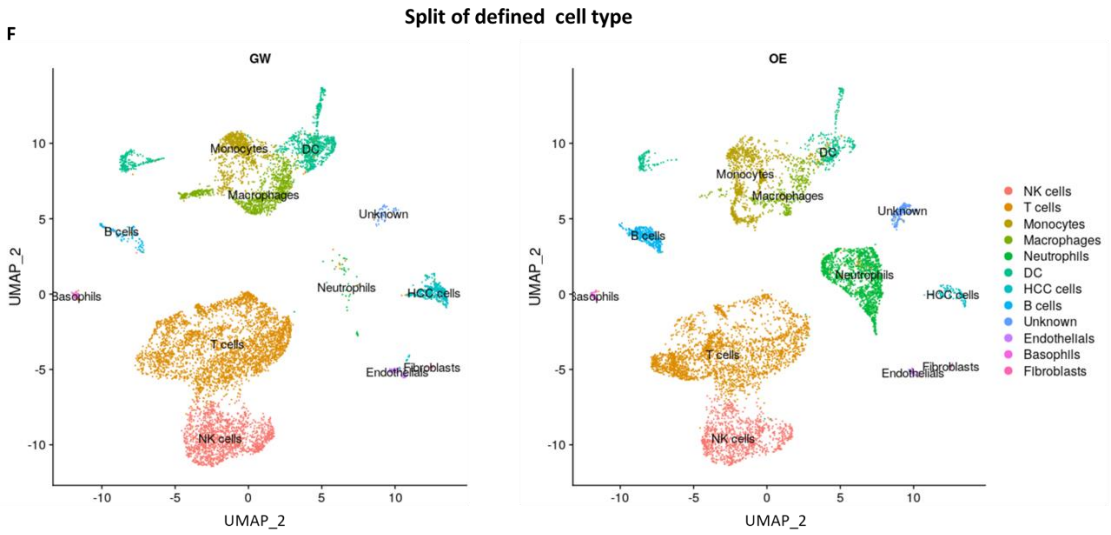

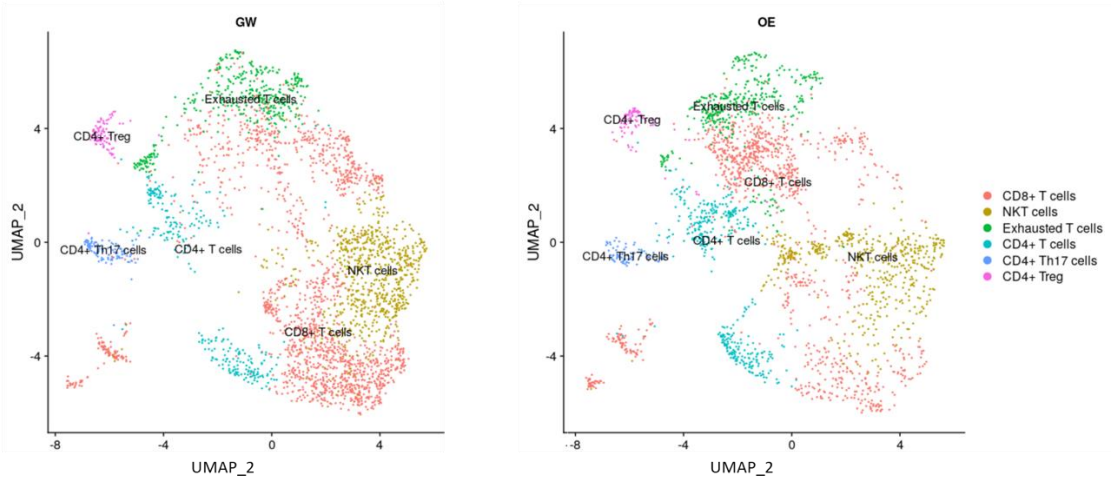

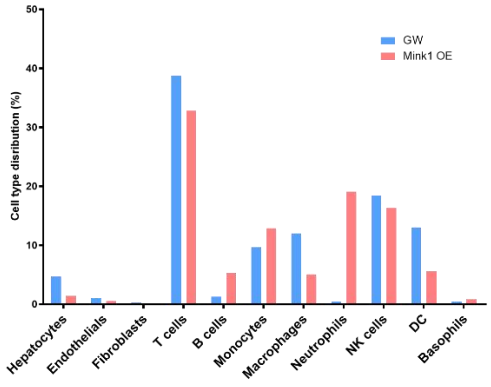

Cell type clustering

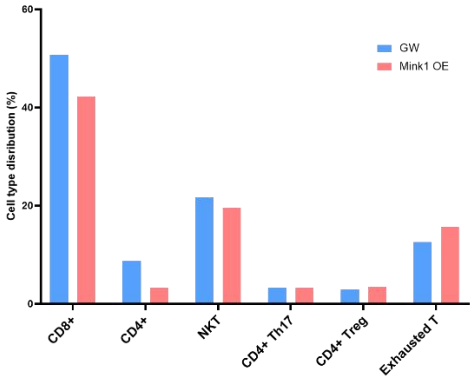

T cell type clustering

G

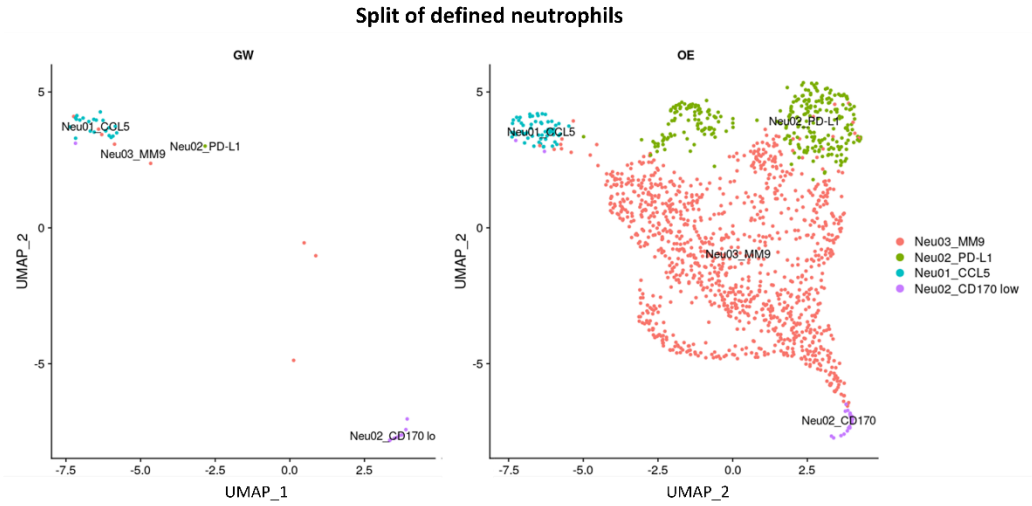
Split of defined neutrophils
GW
OE
Neu01_CCL5
Neu03_MM9
Neu02_PD-L1
Neu02_CD170 lo
Neu02_CD170
UMAP_1
UMAP_2
Neu03_MM9
Neu02_PD-L1
Neu01_CCL5
Neu02_CD170 low

H

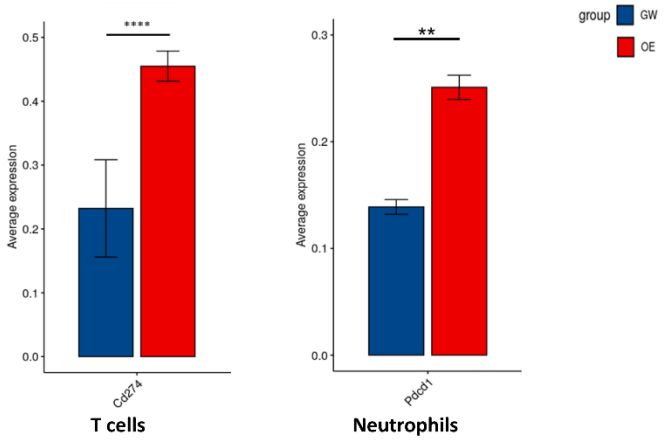
group
GW
OE
****
**
Average expression
Cd274
Pdcd1
T cells
Neutrophils

I

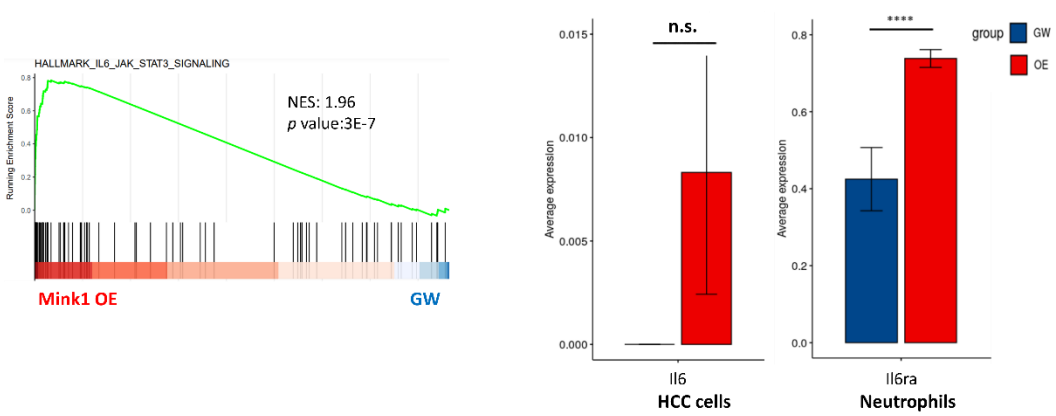
HALLMARK_IL6_JAK_STAT3_SIGNALING
NES: 1.96
p value:3E-7
Running Enrichment Score
Mink1 OE
GW
n.s.
****
group
GW
OE
Average expression
Il6
Il6ra
HCC cells
Neutrophils

Figure 5.6 Single-cell sequencing analysis revealed increased populations of immunosuppressive cells and suggested the pivotal role of PD-L1^{+} neutrophils to promote tumor development in Mink1 OE model

(A) Single-cell violin plots generated by an R package, Seurat, to present quality control (QC) and filtering of scRNA-seq data before QC (left), cut-off during QC (middle), and after QC (right); nFeature_RNA= the number of genes, nCount_RNA= the number of reads, percent.mt=percent of mitochondrial gene reads, percent.rb=percent of ribosomal genes reads, percent.Hb=percent of hemoglobin gene reads. **(B)** UMAP-presenting cell type identification generated by SingleR. **(C)** Dot plot showing regions of well-published gene markers for different cell types located on UMAP (right) and defined cell-type clusters (left). **(D)** Dot plot showing regions of well-published gene markers for different T cell types located on UMAP (right) and defined T cell-type clusters (left). **(E)** Dot plot (left) and bar chart (right) showing Mink1 expression in different cell clusters in GW and OE groups. **(F)** UMAP and bar charts presenting the landscape of the tumor microenvironment (upper) and tumor immunity (lower) in the GW and OE groups. **(G)** UMAP presenting the neutrophil landscape in the GW and OE groups. **(H)** Bar chart showing Pdcd1 expression in T cells and Cd274 expression in neutrophils. **(I)** GSEA-based hallmark enrichment plot of representative gene set from enriched pathway IL6/JAK/STAT3 (left) and bar chart showing Il-6 expression in HCC cells (middle) and Il-6ra expression (right) in neutrophils. (*p<0.05, **p < 0.01, ****p<0.0001 *t* test)

5.4 Discussion

In Chapter 4, we demonstrate the role of MINK1 in immune evasion in HCC using a subcutaneous Mink1 knockout model. To deepen our understanding of Mink1's impact on intratumoral immune composition and its therapeutic implications, it is crucial to establish a mouse model that better recapitulates the immune profiles of HCC patients. Thus, the primary objectives of this chapter encompass the development of clinically relevant mouse models exhibiting immune heterogeneity and the investigation of alterations in the TME following Mink1 overexpression. We used HTVI to induce HCC tumors in immunocompetent C57BL/6J mice with *Trp53* knockout and C-Myc overexpression background, together with Mink1 overexpression plasmids or control GW plasmid delivery. After confirming the successful establishment of the mouse model, we conducted bulk RNA sequencing, immune profiling, and single-cell RNA sequencing to identify Mink1-regulated genes and pathways that may influence the interplay between tumor cells and the immune system.

Our mouse model took advantage of the pT3-EF1a-MYC-luc plasmid expressing luciferase, which allowed us to monitor liver tumor growth *in vivo* per week. The growth of tumors in the Mink1 OE group continued until day 28, when the tumors were harvested. Moreover, a significantly higher tumor-to-liver ratio was observed in the Mink1 OE group than that in the GW group. Therefore, our Mink1 OE model served to validate the Mink1-mediated HCC development described in the previous chapter using an independent model. Next, we performed bulk RNA sequencing to identify the Mink1-regulated genes and pathways that play a role in immune evasion in HCC. Enrichment of inflammatory response and TNFA signaling via NFκB pathways in both the Mink1 OE model and Mink1-high group of TCGA-LIHC sequencing data based on GSEA analysis suggested that Mink1 promotes inflammation-driven HCC immune

evasion. This is consistent with a previous study that reported that Mink1 activates the NLRP3 inflammasome (K. Zhu et al., 2021). Another study also indicated that Mink1 contributes to proinflammatory cytokine production in rheumatoid arthritis by inhibiting the interaction of Mink1 with miR-17-5p via miRNA sponges (Zhang et al., 2021).

Tumor-elicited inflammation contributes to the establishment of an immunosuppressive TME. Research has indicated that the cytokine milieu environment within the TME not only initiates a tumor-promoting inflammatory response but also influences the formation of an immunosuppressive phenotype (L. Li et al., 2020; Zhao et al., 2021). Furthermore, TNFα-induced epithelial-mesenchymal transition (EMT) was previously reported to lead to the upregulation of immune suppressors, including PD-L1 and CD73, in HCC models (Ju et al., 2020; Watanabe et al., 2022). Additionally, increased TNF-α expression has been linked to unfavorable overall survival outcomes in patients with HCC (Tan et al., 2019). We also observed an increase in *Il-6* expression in Mink1 OE samples. *Il-6* was the top-ranked gene in both enriched pathways in our GSEA analysis and is known to act as a major factor in inhibiting the anti-cancer immune response by stimulating the production of immunosuppressive cells, such as MDSCs and tumor-associated neutrophils (Shang et al., 2019; Weber et al., 2021). In addition, we observed a significant increase in *Csf3* expression in OE samples. CSF3, also recognized as a granulocyte colony-stimulating factor, was found to play a pivotal role in fostering the proliferation and development of neutrophils by interacting with its receptor present on neutrophil precursor cells to trigger the downstream JAK-STAT3 pathway (Tian et al., 1996). Mice deficient in Csf3 have been reported to exhibit chronic neutropenia, a symptom associated with deficiencies in neutrophil production (Lieschke et al., 1994). Therefore, CSF3 therapy is used to treat severe congenital neutropenia. In contrast, anti-

Csf3 treatment repressed neutrophil populations while concurrently augmenting the responses of NK cells, macrophages, and T cells in cancer models (Morris et al., 2015). In addition to *Csf3*, upregulation of immunosuppressive genes, such as *Tgfb*, was also observed in bulk RNA sequencing. Dysregulated TGF-β signaling is known to induce cancer-associated fibroblasts, which mediate immune evasion of tumor cells (Chakravarthy et al., 2018). Moreover, TGF-β has been found to promote tumor progression by polarizing neutrophils to the pro-tumor N2 phenotype (Fridlender et al., 2009). Therefore, we hypothesized that Mink1-elicited inflammation in HCC would promote immune evasion.

Next, we assessed the effects of Mink1 OE on the remodeling of the tumor-infiltrating immune composition. To this end, we performed an immune profile analysis using two antibody panels. In general, we observed profound changes in the TME of Mink1 OE tumors, suggesting an important role for Mink1 in shaping the HCC TME. We showed that Mink1 overexpression has distinct effects on neutrophil recruitment and DC suppression. This may reflect the promotion of inflammation-related pathways in previous bulk RNA-sequencing sessions. In an inflamed tumor microenvironment, pro-inflammatory cytokines and chemokines secreted by cancer cells and stromal cells can act as potent chemoattractants for neutrophils and facilitate their migration from the bloodstream into the tumor tissue (Dumitru et al., 2013; Shaul & Fridlender, 2017). Subsequently, tumor-infiltrating neutrophils release additional inflammatory factors that favor tumor growth. We hypothesized that this crosstalk between neutrophils and cancer cells creates a positive feedback loop that sustains the pro-inflammatory TME in Mink1 OE models. Moreover, the quantification of tumor-infiltrating $CD8^+$ T cells showed a significant decrease in $CD8^+$ cells in Mink1 OE tumor nodules compared to GW tumors. In addition, Mink1 OE tumors showed a small presence of $CD8^+$ T cells,

albeit mostly found at the edges of the tumor, suggesting that intrinsic Mink1 suppresses $CD8^+$ T cell infiltration.

We were highly intrigued by the significant increase in the neutrophil population. Neutrophils are the most abundant leukocytes and play a crucial role in the initial defense of the host against invading microorganisms (Kobayashi & DeLeo, 2009). While less characterized than other immune cell types in the TME, tumor-infiltrating neutrophils (TAN) are now recognized as important players in the pathophysiology of cancer. Recent research has shed light on the role of neutrophils in cancer pathogenesis, leading to their emergence as key mediators of tumor progression and potential targets for cancer therapies (Deng et al., 2021; Xiao et al., 2021). A consensus has been reached to include increased levels of neutrophils in the peripheral blood and the neutrophil-to-lymphocyte ratio (NLR) as prognostic factors in cancer patients (Cupp et al., 2020). Studies have revealed that neutrophils in HCC promote disease progression via MMP9, which contributes to tissue remodeling (Geh et al., 2022). Moreover, neutrophil accumulation in HCC has been associated with an immunosuppressive microenvironment. Elevated expression of certain chemokines (CXCL1-5, CXCL12, CXCL16, and CCL5) in HCC tumor cells promotes the recruitment of neutrophils into the TME (Korbecki et al., 2020). Once recruited into the TME, neutrophils can polarize into a pro-tumor phenotype. They suppress anti-tumor immune responses by inhibiting the functions of both $CD4^+$ and $CD8^+$ T cells (Germann et al., 2020; Nielsen et al., 2021). Neutrophils express PD-L1 to inhibit T cell proliferation while also promoting the expansion of Tregs (Y. Shi et al., 2020; Wang et al., 2017). Furthermore, neutrophils employ arginase 1 to suppress T cells (Vonwirth et al., 2020). IL-10 and TGF-β production by $CD4^+$ is also encouraged by TAN (Geh et al., 2022). These actions of TANs contribute to an immunosuppressive TME and evasion of anti-tumor immune

responses.

The role of TANs in cancer has been previously underestimated, partly because of the perception that their short lifespan may limit their impact on tumor development. However, as research progresses, the significance of neutrophils in cancer pathogenesis and immune regulation has become increasingly apparent (Cupp et al., 2020; Geh et al., 2022). These findings have led to the exploration of neutrophil-directed therapies as potential strategies to modulate immune response and improve outcomes in patients with HCC and other cancers. Therefore, we aimed to understand the complex interactions between tumor-intrinsic Mink1, neutrophils, and other components in the HCC immune environment using scRNA-seq analysis.

Our findings not only validate the previously reported FACS data regarding alterations in the immune cell landscape in Mink1 OE tumors, but also reveal an increased population of exhausted T cells with high *Pd1*, *Tim-3*, and *Lag3* expression. Using the Mink1 OE model, we uncovered a potential mechanism for HCC immune evasion, involving the recruitment and development of $PDL1^{+}$ neutrophils and $MMP9^{+}$ neutrophils. The majority of studies have confirmed the pro-tumor effect of MMP9 and further suggest its role in supporting the pro-tumor TME by preventing T cell trafficking into tumor cells via inactivation of chemoattractants (Que et al., 2022). The induction of PD-L1 expression on immune cells is primarily driven by inflammation and the pro-tumor TME (Han et al., 2020). Our scRNA-seq results showed increased Pd-1 expression in T cells and amplified expression of its ligand in neutrophils. This observation aligns with previous research indicating that increased PD-L1 levels in neutrophils possess notable suppressive effects on T-cell proliferation through the PD-1/PD-L1 pathway (Zhang & Xu, 2017). A noteworthy study by Wang et al. revealed a

novel role of GM-CSF in upregulating PD-L1 expression on neutrophils to suppress T-cell immunity through interaction with PD-1 in T cells (Wang et al., 2017). As our bulk RNA analysis showed increased expression of CSF3, another member of the CSF family, in the inflammatory pathway, we further examined whether this inflammatory factor also induces the expression of PD-L1 on neutrophils. Our GSEA analysis of the neutrophil population implicated the involvement of the IL6/JAK/STAT3 pathway in Mink1 overexpression samples. Notably, phosphorylation of STAT3 is responsible for MMP9 production, suggesting a potential mechanism of enriched Mmp9 expression in the neutrophil population in our model (Jia et al., 2017). As IL6 has been associated with upregulation of PD-L1 expression in neutrophils, we conducted gene expression analysis and confirmed the upregulation of Il-6r in neutrophils and Il-6 in HCC cells of the Mink1 OE sample. This is consistent with the study by Wang et al. which proposed IL6 to induce the activation of $PDL1^{+}$ neutrophils within the TME through the IL6-STAT3 pathway, thereby fostering immune suppression in HCC (Cheng et al., 2018). The recruitment of neutrophils to the TME may involve the production of chemokines and cytokines by cancer cells, creating a chemotactic gradient that attracts neutrophils to the tumor site. Further identification of the key receptor-ligand interactions between neutrophils and HCC cells is imperative to explore the mechanism of neutrophil recruitment in our model. Nonetheless, our findings shed light on the potential modulation of the HCC immune microenvironment by Mink1 via $Mmp9^{+}$ and $Pd\text{-}l1^{+}$ neutrophils. The recruitment of TANs may contribute to establishing an immunosuppressive niche in HCC. This discovery holds significant therapeutic potential given the strong correlation between TANs and HCC.

Chapter 6 Conclusion and future perspective

6.1 Conclusion

HCC is the third most lethal cancer worldwide with an increasing incidence. Despite advances in therapeutic strategies, including first-line treatment with lenvatinib and a variety of ICIs, drug resistance in systematic therapy and the low response rate to ICIs remain major hurdles in HCC treatment. Tumor cells employ diverse immune evasion mechanisms to reduce the efficacy of immunotherapy. Therefore, there is an urgent need to study the detailed mechanisms of cancer–immune evasion.

Kinase inhibitors play a prominent role in cancer treatment by targeting pathways related to tumor growth and proliferation. Recent studies have shown that kinase oncogenes also contribute to immune escape and ICI resistance, suggesting the potential of kinase inhibitors to enhance anti-tumor immune responses. Therefore, the present study aimed to identify a subset of kinases that play critical roles in HCC immune regulation using an in vivo kinome-wide CRISPR screen and HCC mouse models. We further built upon our understanding of intercellular communication of the candidate kinases in the TME and elucidated the mechanisms of immune evasion triggered by the selected kinases, with the hope that such an understanding may contribute to improving the efficiency and response rate of immune therapies. We successfully established that a novel kinase, Mink1, is involved in HCC immune evasion through recruitment of pro-tumor neutrophils.

We constructed an in vitro kinome-wide CRISPR gRNA knockout library to identify potential kinase targets for immune evasion in HCC. The efficiency of the mBrie kinase library sgRNAs was validated using the Rule 2 set score, and the distribution of sgRNAs after RIL-175 cell transduction was confirmed by sequencing. An in vivo kinome-wide mouse CRISPR gRNA-knockout library was established by

subcutaneously injecting RIL-175 cells containing sgRNA pool. To confirm whether kinase-knockout HCC cells can be recognized by the immune system, we assessed the depletion of HCC cells with different gRNA knockouts in immunocompetent and B and T cell-deficient mice using the CRISPR screening approach. We focused on kinase gene-knockout HCC cells that were suppressed in immunocompetent mice compared with immunodeficient mice, indicating that the presence of an immune microenvironment can inhibit the growth of tumor cells upon inactivation of the kinase gene. In addition to the observation of rapid tumor growth in immunodeficient mice, depletion of HCC cells with immunosuppressive kinases were knocked out in WT mice, and enrichment of immune-supporting kinases provided strong evidence for the successful generation of our in vivo CRISPR screening model. Our screening results identified Mink1 as a possible candidate since Mink1 KO HCC cells were the only type of kinase-knockout cells within the sgRNA library that were completely eliminated in WT mice. TCGA-LIHC and GEO cohort analyses and IHC staining analysis demonstrated the clinical relevance of MINK1 by suggesting that MINK1 overexpression promotes poor prognosis in HCC patients. Web-based TIDE analysis also provided evidence of a correlation between MINK1 overexpression and T-cell dysfunction in patients with HCC. The role of Mink1 was further validated using Mink1 KO HCC mouse models after confirming the KO efficiency of Mink1 in RIL-175 and Hep55.1c cell lines. Tumor growth was only observed in WT mice injected with control cells, but not in Mink1 KO cells, whereas tumors were observed in all control and KO cell lines injected into immunodeficient mice, indicating that MINK inhibition improved the anti-tumor response. To our knowledge, this is the first study to reveal a significant role of MINK1 in modulating immune evasion in HCC.

Our next goal was to identify and characterize the intrinsic mechanisms through which

MINK1 affects the immune environment in HCC. For this purpose, we established a hydrodynamic tail vein injection (HTVI) delivery immunocompetent HCC mouse model that resembles a human-like heterogeneous TME to examine the effect of Mink1 overexpression in the HCC immune microenvironment. We conducted bulk RNA sequencing of $Trp53^{KO}$/$C\text{-}Myc^{OE}$ /Mink1 and $Trp53^{KO}$/$C\text{-}Myc^{OE}$ /GW HCC mouse models, with GSEA analysis found significant enrichment of pathways related to inflammatory response and TNFα signaling via NFκB in Mink1 OE samples. A number of inflammatory factors such as *Il-6* and *Csf3*, which are well known for neutrophil development and function, have been upregulated in OE model. The release of IL-6 and CSF3 may be regulated by inflammasomes such as NLRP3, which has been reported to be activated by MINK1 (K. Zhu et al., 2021). Furthermore, GO analysis showed that genes related to T cell function were downregulated in OE tumors. These results suggest some limited ideas that Mink1 may induce HCC immune evasion through a robust inflammatory response. To further explore the changes in gene networks associated with immune microenvironment remodeling by Mink1, we conducted immune profiling and scRNA-seq analyses. By assessing the effects of Mink1 OE on the immune microenvironment, we have demonstrated that overexpression of Mink1 results in dynamic changes in TME components, leading to a significant increase in neutrophil population and decrease in $CD4^+$ and $CD8^+$ T cell populations. Consistent with previous results, we showed that Mink1 overexpression contributed to an inflammatory and immunosuppressive TME in an HCC mouse model. Concurrently, scRNA-seq analysis confirmed that changes in the immune cell composition corroborated our immunophenotyping data. Mink1 OE enhances neutrophil recruitment and proliferation of exhausted T cells. We found that the increase in the neutrophil population belonged to clusters specifically expressing *Mmp9* and *Pd-l1*. PD-L1 expression on neutrophils has been reported to contributes to an impaired immune

response. Therefore, we hypothesized that the suppressive effects on T-cell in our Mink1 OE model may be mediated through the PD-1/PD-L1 pathway. Single-cell analysis confirmed increased *Pd-1* and *Pd-l1* expression in T cells and neutrophils, respectively. It has been proposed that the induction of PD-L1 expression on neutrophils is driven by inflammation and the pro-tumor TME. In a study performed using a gastric cancer model, Wang et al. demonstrated that members of the CSF family promote neutrophil activation by upregulating PD-L1 expression in neutrophils to suppress T-cell immunity through the IL6/STAT3 pathway. Considering that we observed upregulation of *Il-6* and *Csf3* in our bulk RNA-seq results, we suggest that upregulation of *Pd-l1* expressing neutrophils may be regulated by *Il6* and *Csf3*. In line with this hypothesis, our gene expression analysis indicated the enrichment of the IL6/STAT3 pathway together with the upregulation of *Il-6r* in neutrophils and *Il-6* in HCC cells of the Mink1 OE sample.

In summary, using different Mink1 HCC mouse models in this thesis, we have shown that Mink1 plays an important role in shaping the TME and evading anti-tumor immune responses in HCC by recruiting neutrophils that mostly express Pd-l1 and Mmp9 to the TME. We hypothesized that this immunosuppressive pro-tumor neutrophil activation is regulated by IL-6 and CSF3 and that neutrophils suppress T cell immunity by binding PD-L1 to PD-1 on exhausted T cells (Fig. 6). Such knowledge can be used to design rational treatment combinations of ICIs with inhibition of Mink1 to improve the response rate and effectiveness of immunotherapies for patients with HCC. Nonetheless, further experiments are required to understand the mechanism of neutrophil recruitment by Mink1 and delineate the immunosuppressive effects of neutrophils.

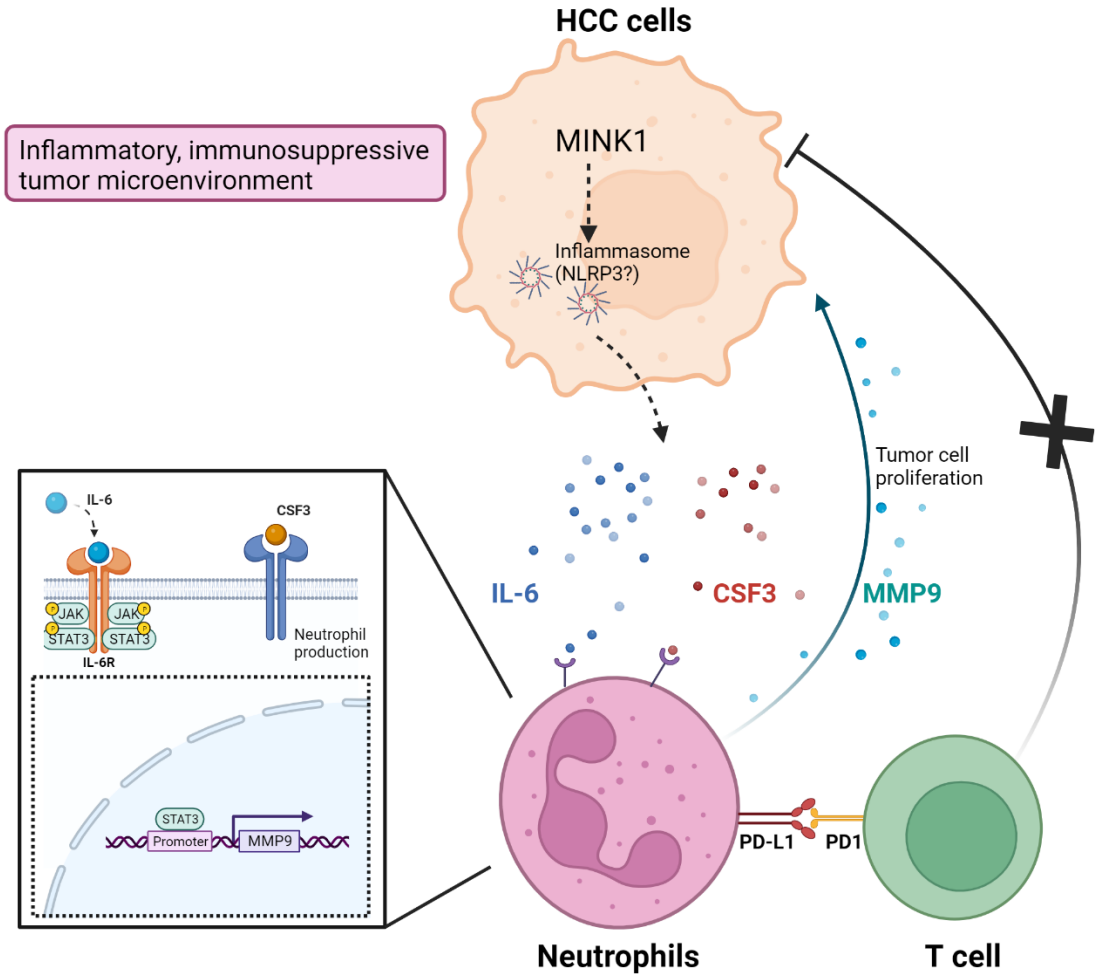

Figure 6 Summary of the study

The mechanism of tumor cell-intrinsic Mink1 regulated HCC immune evasion is driven by IL-6- and CSF3-induced neutrophil recruitment and suppression of T-cell function through PD-1 and PD-L1 interactions between neutrophils and T cells. MINK1 may activate inflammasomes including NLRP3 to release IL-6 and CSF3. Increased MMP9 expression may be regulated by the IL6/JAK/STAT3 pathway in neutrophils. MMP9 released by neutrophils may facilitate tumor cell proliferation, forming a positive loop between cancer cells and neutrophils. The dotted arrows and boxes indicate the mechanism with published research support. However, this remains to be confirmed in our model.

6.2 Future perspective

6.2.1 Inhibition of hepatic neutrophils in Mink1 OE-induced mouse HCC model

We observed an increase in neutrophil population upon Mink1 overexpression in our previous mouse model, suggesting that Mink1 facilitates neutrophil recruitment to promote HCC progression and immune evasion. Follow-up experiments will be performed to confirm whether Mink1 OE-induced mouse HCC is attenuated by antibody-mediated depletion of hepatic neutrophils. If neutrophil suppression reversed the tumor-promoting effect of Mink1, neutrophil recruitment would be the main factor leading to HCC development upon Mink1 overexpression. To further confirm that this effect is immune-specific and that neutrophil recruitment promotes HCC progression through an immune evasion mechanism, we performed antibody-mediated depletion of hepatic neutrophils in Rag1-KO mice.

6.2.2 Verification of neutrophil activation and migration by Mink1 OE HCC cells conditioned medium (CM)

Our previous results suggest an effect of Mink1 on pro-tumor neutrophil recruitment. However, we have not directly proven that recruitment is stimulated by inflammatory mediators in the TME of Mink OE tumors. Therefore, it is imperative to validate the activation and migration of neutrophils under the influence of Mink1 overexpressing HCC cell conditioned medium (CM) by (1) flow cytometry to measure CD11b upregulation and ROS production as an assessment of neutrophil activity and (2) chemotaxis assay to evaluate the migration of neutrophils. For this purpose, Mink1 OE HCC CM was collected by incubating Mink1 OE HCC cells in a medium supplemented with 10% FBS to facilitate cell migration, followed by co-culture with neutrophils.

6.2.3 Exploring the neutrophil recruitment mechanism

Although we and other researchers have proposed *Il-6* and *Csf3* as chemoattractants that regulate *Pd-l1* expressing neutrophil recruitment in tumor models, to confirm this result and to identify other potential key neutrophil attractants not explored in our previous study, we should conduct a comprehensive profiling of cytokines and chemokines in Mink1 OE HCC cells CM (Cheng et al., 2018). This helps to elucidate the interplay between tumor cells, neutrophils, and the Mink1 OE TME. Moreover, this enriches our understanding of the tumor cell-intrinsic molecular mechanism that remains unexplored regarding how Mink1 orchestrates neutrophil behavior. The levels of cytokines and chemokines secreted in response to Mink1 overexpressing HCC CM can be measured using flow cytometry and Luminex. After narrowing down the candidate cytokines or chemokines, cytokine production in the plasma was measured by ELISA.

6.2.4 Validation of neutrophil extracellular traps formation

In addition to chemokine and cytokine regulation, neutrophil extracellular trap (NETs)-related processes may also contribute to HCC progression and immune evasion. NET ejected by activated neutrophils exert immunosuppressive effects via PD-1/PD-L1 (Kaltenmeier et al., 2021). Moreover, CSF3 promotes NET formation by recruiting neutrophils (L. Liu et al., 2020; Park et al., 2016). Evaluating NET formation by NETosis quantification assays and visualization of NETs by fluorescence staining of H3cit can help determine whether the interaction of recruited neutrophils with cancer cells and other immune cells is accompanied by NET release.

6.2.5 Potential therapy of Mink1 inhibitor combined with immune checkpoint inhibitors

In recent years, the FDA has approved several ICI combination therapies with durable clinical responses and satisfied overall survival for HCC patients. However, the low response rate remains a major challenge. Therefore, future studies should focus on optimizing the immunotherapeutic approaches. Our results have proved Mink1 plays a critical role in HCC immune evasion by recruiting pro-tumor neutrophils. Moreover, we identified a *Pd-l1* expressing neutrophil population in tumor with Mink1 overexpression, suggesting Mink1 evades HCC immune by suppressing T cell through PD-1/PD-L1 pathway. Therefore, we believe Mink1 inhibition may improve immunotherapy response rate and efficiency. A combination of Mink1 inhibitors with other immune checkpoint inhibitors will be a rational design worth investigating. As virtual screening for Mink1 potential inhibitors using the Glide score (Schroedinger) was utilized, we will procced to *in vivo* approach to examine the efficiency of Mink1 inhibitors.

References

Agdashian, D., ElGindi, M., Xie, C., Sandhu, M., Pratt, D., Kleiner, D. E., Figg, W. D., Rytlewski, J. A., Sanders, C., Yusko, E. C., Wood, B., Venzon, D., Brar, G., Duffy, A. G., Greten, T. F., & Korangy, F. (2019). The effect of anti-CTLA4 treatment on peripheral and intra-tumoral T cells in patients with hepatocellular carcinoma. *Cancer Immunol Immunother*, *68*(4), 599-608. https://doi.org/10.1007/s00262-019-02299-8

Aida, K., Miyakawa, R., Suzuki, K., Narumi, K., Udagawa, T., Yamamoto, Y., Chikaraishi, T., Yoshida, T., & Aoki, K. (2014). Suppression of Tregs by anti-glucocorticoid induced TNF receptor antibody enhances the antitumor immunity of interferon-alpha gene therapy for pancreatic cancer. *Cancer Sci*, *105*(2), 159-167. https://doi.org/10.1111/cas.12332

Akiba, J., Yano, H., Ogasawara, S., Higaki, K., & Kojiro, M. (2001). Expression and function of interleukin-8 in human hepatocellular carcinoma. *Int J Oncol*, *18*(2), 257-264. https://doi.org/10.3892/ijo.18.2.257

Alqahtani, A., Khan, Z., Alloghbi, A., Said Ahmed, T. S., Ashraf, M., & Hammouda, D. M. (2019). Hepatocellular Carcinoma: Molecular Mechanisms and Targeted Therapies. *Medicina (Kaunas)*, *55*(9). https://doi.org/10.3390/medicina55090526

Anderson, K., Ryan, N., Alkhimovitch, A., Siddiqui, A., & Oghumu, S. (2021). Inhibition of PI3K Isoform p110gamma Increases Both Anti-Tumor and Immunosuppressive Responses to Aggressive Murine Head and Neck Squamous Cell Carcinoma with Low Immunogenicity. *Cancers (Basel)*, *13*(5). https://doi.org/10.3390/cancers13050953

Ardito, F., Giuliani, M., Perrone, D., Troiano, G., & Lo Muzio, L. (2017). The crucial role of protein phosphorylation in cell signaling and its use as targeted therapy (Review). *Int J Mol Med*, *40*(2), 271-280. https://doi.org/10.3892/ijmm.2017.3036

Arvanitakis, K., Mitroulis, I., & Germanidis, G. (2021). Tumor-Associated Neutrophils in Hepatocellular Carcinoma Pathogenesis, Prognosis, and Therapy. *Cancers (Basel)*, *13*(12). https://doi.org/10.3390/cancers13122899

Azab, M., Zaki, S., El-Shetey, A. G., Abdel-Moty, M. F., Alnoomani, N. M., Gomaa, A. A., Abdel-Fatah, S., Mohiy, S., & Atia, F. (2011). Radiofrequency ablation combined with percutaneous ethanol injection in patients with hepatocellular carcinoma. *Arab J Gastroenterol*, *12*(3), 113-118. https://doi.org/10.1016/j.ajg.2011.07.005

Bancerek, J., Poss, Z. C., Steinparzer, I., Sedlyarov, V., Pfaffenwimmer, T., Mikulic, I., Dolken, L., Strobl, B., Muller, M., Taatjes, D. J., & Kovarik, P. (2013). CDK8

kinase phosphorylates transcription factor STAT1 to selectively regulate the interferon response. *Immunity*, *38*(2), 250-262. https://doi.org/10.1016/j.immuni.2012.10.017

Beckebaum, S., Zhang, X., Chen, X., Yu, Z., Frilling, A., Dworacki, G., Grosse-Wilde, H., Broelsch, C. E., Gerken, G., & Cicinnati, V. R. (2004). Increased levels of interleukin-10 in serum from patients with hepatocellular carcinoma correlate with profound numerical deficiencies and immature phenotype of circulating dendritic cell subsets. *Clin Cancer Res*, *10*(21), 7260-7269. https://doi.org/10.1158/1078-0432.CCR-04-0872

Bell, J. B., Aronovich, E. L., Schreifels, J. M., Beadnell, T. C., & Hackett, P. B. (2010). Duration of expression and activity of Sleeping Beauty transposase in mouse liver following hydrodynamic DNA delivery. *Mol Ther*, *18*(10), 1796-1802. https://doi.org/10.1038/mt.2010.152

Berzofsky, J. A., & Terabe, M. (2009). The contrasting roles of NKT cells in tumor immunity. *Curr Mol Med*, *9*(6), 667-672. https://doi.org/10.2174/156652409788970706

Bonamassa, B., Hai, L., & Liu, D. (2011). Hydrodynamic gene delivery and its applications in pharmaceutical research. *Pharm Res*, *28*(4), 694-701. https://doi.org/10.1007/s11095-010-0338-9

Bottcher, J. P., Knolle, P. A., & Stabenow, D. (2011). Mechanisms balancing tolerance and immunity in the liver. *Dig Dis*, *29*(4), 384-390. https://doi.org/10.1159/000329801

Bronte, V., Serafini, P., Mazzoni, A., Segal, D. M., & Zanovello, P. (2003). L-arginine metabolism in myeloid cells controls T-lymphocyte functions. *Trends Immunol*, *24*(6), 302-306. https://doi.org/10.1016/s1471-4906(03)00132-7

Bruix, J., Chan, S. L., Galle, P. R., Rimassa, L., & Sangro, B. (2021). Systemic treatment of hepatocellular carcinoma: An EASL position paper. *J Hepatol*, *75*(4), 960-974. https://doi.org/10.1016/j.jhep.2021.07.004

Bruix, J., Gores, G. J., & Mazzaferro, V. (2014). Hepatocellular carcinoma: clinical frontiers and perspectives. *Gut*, *63*(5), 844-855. https://doi.org/10.1136/gutjnl-2013-306627

Cabrera, R., Ararat, M., Xu, Y., Brusko, T., Wasserfall, C., Atkinson, M. A., Chang, L. J., Liu, C., & Nelson, D. R. (2013). Immune modulation of effector CD4+ and regulatory T cell function by sorafenib in patients with hepatocellular carcinoma. *Cancer Immunol Immunother*, *62*(4), 737-746. https://doi.org/10.1007/s00262-012-1380-8

Cai, L., Zhang, Z., Zhou, L., Wang, H., Fu, J., Zhang, S., Shi, M., Zhang, H., Yang, Y., Wu, H., Tien, P., & Wang, F. S. (2008). Functional impairment in circulating

and intrahepatic NK cells and relative mechanism in hepatocellular carcinoma patients. *Clin Immunol*, *129*(3), 428-437. https://doi.org/10.1016/j.clim.2008.08.012

Cao, M., Xu, Y., Youn, J. I., Cabrera, R., Zhang, X., Gabrilovich, D., Nelson, D. R., & Liu, C. (2011). Kinase inhibitor Sorafenib modulates immunosuppressive cell populations in a murine liver cancer model. *Lab Invest*, *91*(4), 598-608. https://doi.org/10.1038/labinvest.2010.205

Carambia, A., Frenzel, C., Bruns, O. T., Schwinge, D., Reimer, R., Hohenberg, H., Huber, S., Tiegs, G., Schramm, C., Lohse, A. W., & Herkel, J. (2013). Inhibition of inflammatory CD4 T cell activity by murine liver sinusoidal endothelial cells. *J Hepatol*, *58*(1), 112-118. https://doi.org/10.1016/j.jhep.2012.09.008

Caraux, A., Lu, Q., Fernandez, N., Riou, S., Di Santo, J. P., Raulet, D. H., Lemke, G., & Roth, C. (2006). Natural killer cell differentiation driven by Tyro3 receptor tyrosine kinases. *Nat Immunol*, *7*(7), 747-754. https://doi.org/10.1038/ni1353

Casadei-Gardini, A., Rimini, M., Kudo, M., Shimose, S., Tada, T., Suda, G., Goh, M. J., Jefremow, A., Scartozzi, M., Cabibbo, G., Campani, C., Tamburini, E., Tovoli, F., Ueshima, K., Aoki, T., Iwamoto, H., Torimura, T., Kumada, T., Hiraoka, A., . . . Cascinu, S. (2022). Real Life Study of Lenvatinib Therapy for Hepatocellular Carcinoma: RELEVANT Study. *Liver Cancer*, *11*(6), 527-539. https://doi.org/10.1159/000525145

Cast, A. E., Walter, T. J., & Huppert, S. S. (2015). Vascular patterning sets the stage for macro and micro hepatic architecture. *Dev Dyn*, *244*(3), 497-506. https://doi.org/10.1002/dvdy.24222

Chakravarthy, A., Khan, L., Bensler, N. P., Bose, P., & De Carvalho, D. D. (2018). TGF-beta-associated extracellular matrix genes link cancer-associated fibroblasts to immune evasion and immunotherapy failure. *Nat Commun*, *9*(1), 4692. https://doi.org/10.1038/s41467-018-06654-8

Chen, H., Ye, F., & Guo, G. (2019). Revolutionizing immunology with single-cell RNA sequencing. *Cell Mol Immunol*, *16*(3), 242-249. https://doi.org/10.1038/s41423-019-0214-4

Cheng, Y., Li, H., Deng, Y., Tai, Y., Zeng, K., Zhang, Y., Liu, W., Zhang, Q., & Yang, Y. (2018). Cancer-associated fibroblasts induce PDL1+ neutrophils through the IL6-STAT3 pathway that foster immune suppression in hepatocellular carcinoma. *Cell Death Dis*, *9*(4), 422. https://doi.org/10.1038/s41419-018-0458-4

Crispe, I. N. (2009). The liver as a lymphoid organ. *Annu Rev Immunol*, *27*, 147-163. https://doi.org/10.1146/annurev.immunol.021908.132629

Cupp, M. A., Cariolou, M., Tzoulaki, I., Aune, D., Evangelou, E., & Berlanga-Taylor,

A. J. (2020). Neutrophil to lymphocyte ratio and cancer prognosis: an umbrella review of systematic reviews and meta-analyses of observational studies. *BMC Med*, *18*(1), 360. https://doi.org/10.1186/s12916-020-01817-1

Dan, I., Watanabe, N. M., Kobayashi, T., Yamashita-Suzuki, K., Fukagaya, Y., Kajikawa, E., Kimura, W. K., Nakashima, T. M., Matsumoto, K., Ninomiya-Tsuji, J., & Kusumi, A. (2000). Molecular cloning of MINK, a novel member of mammalian GCK family kinases, which is up-regulated during postnatal mouse cerebral development. *FEBS Lett*, *469*(1), 19-23. https://doi.org/10.1016/s0014-5793(00)01247-3

Dan, I., Watanabe, N. M., & Kusumi, A. (2001). The Ste20 group kinases as regulators of MAP kinase cascades. *Trends Cell Biol*, *11*(5), 220-230. https://doi.org/10.1016/s0962-8924(01)01980-8

Dang, Y., Jia, G., Choi, J., Ma, H., Anaya, E., Ye, C., Shankar, P., & Wu, H. (2015). Optimizing sgRNA structure to improve CRISPR-Cas9 knockout efficiency. *Genome Biol*, *16*, 280. https://doi.org/10.1186/s13059-015-0846-3

Daulat, A. M., Luu, O., Sing, A., Zhang, L., Wrana, J. L., McNeill, H., Winklbauer, R., & Angers, S. (2012). Mink1 regulates beta-catenin-independent Wnt signaling via Prickle phosphorylation. *Mol Cell Biol*, *32*(1), 173-185. https://doi.org/10.1128/MCB.06320-11

de La Coste, A., Romagnolo, B., Billuart, P., Renard, C. A., Buendia, M. A., Soubrane, O., Fabre, M., Chelly, J., Beldjord, C., Kahn, A., & Perret, C. (1998). Somatic mutations of the beta-catenin gene are frequent in mouse and human hepatocellular carcinomas. *Proc Natl Acad Sci U S A*, *95*(15), 8847-8851. https://doi.org/10.1073/pnas.95.15.8847

Deng, G. L., Zeng, S., & Shen, H. (2015). Chemotherapy and target therapy for hepatocellular carcinoma: New advances and challenges. *World J Hepatol*, *7*(5), 787-798. https://doi.org/10.4254/wjh.v7.i5.787

Deng, H., Kan, A., Lyu, N., He, M., Huang, X., Qiao, S., Li, S., Lu, W., Xie, Q., Chen, H., Lai, J., Chen, Q., Jiang, X., Liu, S., Zhang, Z., & Zhao, M. (2021). Tumor-derived lactate inhibit the efficacy of lenvatinib through regulating PD-L1 expression on neutrophil in hepatocellular carcinoma. *J Immunother Cancer*, *9*(6). https://doi.org/10.1136/jitc-2020-002305

Doench, J. G., Fusi, N., Sullender, M., Hegde, M., Vaimberg, E. W., Donovan, K. F., Smith, I., Tothova, Z., Wilen, C., Orchard, R., Virgin, H. W., Listgarten, J., & Root, D. E. (2016). Optimized sgRNA design to maximize activity and minimize off-target effects of CRISPR-Cas9. *Nat Biotechnol*, *34*(2), 184-191. https://doi.org/10.1038/nbt.3437

Dumitru, C. A., Lang, S., & Brandau, S. (2013). Modulation of neutrophil granulocytes

in the tumor microenvironment: mechanisms and consequences for tumor progression. *Semin Cancer Biol*, *23*(3), 141-148. https://doi.org/10.1016/j.semcancer.2013.02.005

DuPage, M., Dooley, A. L., & Jacks, T. (2009). Conditional mouse lung cancer models using adenoviral or lentiviral delivery of Cre recombinase. *Nat Protoc*, *4*(7), 1064-1072. https://doi.org/10.1038/nprot.2009.95

El-Khoueiry, A. B., Sangro, B., Yau, T., Crocenzi, T. S., Kudo, M., Hsu, C., Kim, T. Y., Choo, S. P., Trojan, J., Welling, T. H. R., Meyer, T., Kang, Y. K., Yeo, W., Chopra, A., Anderson, J., Dela Cruz, C., Lang, L., Neely, J., Tang, H., . . . Melero, I. (2017). Nivolumab in patients with advanced hepatocellular carcinoma (CheckMate 040): an open-label, non-comparative, phase 1/2 dose escalation and expansion trial. *Lancet*, *389*(10088), 2492-2502. https://doi.org/10.1016/S0140-6736(17)31046-2

Esteban-Fabro, R., Willoughby, C. E., Pique-Gili, M., Montironi, C., Abril-Fornaguera, J., Peix, J., Torrens, L., Mesropian, A., Balaseviciute, U., Miro-Mur, F., Mazzaferro, V., Pinyol, R., & Llovet, J. M. (2022). Cabozantinib Enhances Anti-PD1 Activity and Elicits a Neutrophil-Based Immune Response in Hepatocellular Carcinoma. *Clin Cancer Res*, *28*(11), 2449-2460. https://doi.org/10.1158/1078-0432.CCR-21-2517

Fabregat, I., Moreno-Caceres, J., Sanchez, A., Dooley, S., Dewidar, B., Giannelli, G., Ten Dijke, P., & Consortium, I.-L. (2016). TGF-beta signalling and liver disease. *FEBS J*, *283*(12), 2219-2232. https://doi.org/10.1111/febs.13665

Feng, Y., Tang, X., Li, C., Su, Y., Wang, X., Li, N., Zhang, A., Jiang, F., & Wu, C. (2022). ARID1A Is a Prognostic Biomarker and Associated with Immune Infiltrates in Hepatocellular Carcinoma. *Can J Gastroenterol Hepatol*, *2022*, 3163955. https://doi.org/10.1155/2022/3163955

Finn, R. S., Ikeda, M., Zhu, A. X., Sung, M. W., Baron, A. D., Kudo, M., Okusaka, T., Kobayashi, M., Kumada, H., Kaneko, S., Pracht, M., Mamontov, K., Meyer, T., Kubota, T., Dutcus, C. E., Saito, K., Siegel, A. B., Dubrovsky, L., Mody, K., & Llovet, J. M. (2020). Phase Ib Study of Lenvatinib Plus Pembrolizumab in Patients With Unresectable Hepatocellular Carcinoma. *J Clin Oncol*, *38*(26), 2960-2970. https://doi.org/10.1200/JCO.20.00808

Finn, R. S., Qin, S., Ikeda, M., Galle, P. R., Ducreux, M., Kim, T. Y., Kudo, M., Breder, V., Merle, P., Kaseb, A. O., Li, D., Verret, W., Xu, D. Z., Hernandez, S., Liu, J., Huang, C., Mulla, S., Wang, Y., Lim, H. Y., . . . Investigators, I. M. (2020). Atezolizumab plus Bevacizumab in Unresectable Hepatocellular Carcinoma. *N Engl J Med*, *382*(20), 1894-1905. https://doi.org/10.1056/NEJMoa1915745

Fleuren, E. D., Zhang, L., Wu, J., & Daly, R. J. (2016). The kinome 'at large' in cancer.

Nat Rev Cancer, *16*(2), 83-98. https://doi.org/10.1038/nrc.2015.18

Forteza, R., Figueroa, Y., Mashukova, A., Dulam, V., & Salas, P. J. (2016). Conditional knockout of polarity complex (atypical) PKCiota reveals an anti-inflammatory function mediated by NF-kappaB. *Mol Biol Cell*, *27*(14), 2186-2197. https://doi.org/10.1091/mbc.E16-02-0086

Franssen, B., Jibara, G., Tabrizian, P., Schwartz, M. E., & Roayaie, S. (2014). Actual 10-year survival following hepatectomy for hepatocellular carcinoma. *HPB (Oxford)*, *16*(9), 830-835. https://doi.org/10.1111/hpb.12206

Fridlender, Z. G., Sun, J., Kim, S., Kapoor, V., Cheng, G., Ling, L., Worthen, G. S., & Albelda, S. M. (2009). Polarization of tumor-associated neutrophil phenotype by TGF-beta: "N1" versus "N2" TAN. *Cancer Cell*, *16*(3), 183-194. https://doi.org/10.1016/j.ccr.2009.06.017

Fu, G., Xu, Q., Qiu, Y., Jin, X., Xu, T., Dong, S., Wang, J., Ke, Y., Hu, H., Cao, X., Wang, D., Cantor, H., Gao, X., & Lu, L. (2017). Suppression of Th17 cell differentiation by misshapen/NIK-related kinase MINK1. *J Exp Med*, *214*(5), 1453-1469. https://doi.org/10.1084/jem.20161120

Fu, J., Xu, D., Liu, Z., Shi, M., Zhao, P., Fu, B., Zhang, Z., Yang, H., Zhang, H., Zhou, C., Yao, J., Jin, L., Wang, H., Yang, Y., Fu, Y. X., & Wang, F. S. (2007). Increased regulatory T cells correlate with CD8 T-cell impairment and poor survival in hepatocellular carcinoma patients. *Gastroenterology*, *132*(7), 2328-2339. https://doi.org/10.1053/j.gastro.2007.03.102

Fujimoto, A., Furuta, M., Shiraishi, Y., Gotoh, K., Kawakami, Y., Arihiro, K., Nakamura, T., Ueno, M., Ariizumi, S., Nguyen, H. H., Shigemizu, D., Abe, T., Boroevich, K. A., Nakano, K., Sasaki, A., Kitada, R., Maejima, K., Yamamoto, Y., Tanaka, H., . . . Nakagawa, H. (2015). Whole-genome mutational landscape of liver cancers displaying biliary phenotype reveals hepatitis impact and molecular diversity. *Nat Commun*, *6*, 6120. https://doi.org/10.1038/ncomms7120

Futreal, P. A., Coin, L., Marshall, M., Down, T., Hubbard, T., Wooster, R., Rahman, N., & Stratton, M. R. (2004). A census of human cancer genes. *Nat Rev Cancer*, *4*(3), 177-183. https://doi.org/10.1038/nrc1299

Gao, B., Radaeva, S., & Park, O. (2009). Liver natural killer and natural killer T cells: immunobiology and emerging roles in liver diseases. *J Leukoc Biol*, *86*(3), 513-528. https://doi.org/10.1189/JLB.0309135

Gao, Q., Wang, X. Y., Qiu, S. J., Yamato, I., Sho, M., Nakajima, Y., Zhou, J., Li, B. Z., Shi, Y. H., Xiao, Y. S., Xu, Y., & Fan, J. (2009). Overexpression of PD-L1 significantly associates with tumor aggressiveness and postoperative recurrence in human hepatocellular carcinoma. *Clin Cancer Res*, *15*(3), 971-979.

https://doi.org/10.1158/1078-0432.CCR-08-1608

Garon, E. B., Spira, A. I., Goldberg, S. B., Chaft, J. E., Papadimitrakopoulou, V., Cascone, T., Antonia, S. J., Brahmer, J. R., Camidge, D. R., Powderly, J. D., Wozniak, A. J., Felip, E., Wu, S., Ascierto, M. L., Elgeioushi, N., & Awad, M. M. (2023). Brief Report: Safety and Antitumor Activity of Durvalumab Plus Tremelimumab in Programmed Cell Death-(Ligand)1-Monotherapy Pretreated, Advanced NSCLC: Results From a Phase 1b Clinical Trial. *J Thorac Oncol*, *18*(8), 1094-1102. https://doi.org/10.1016/j.jtho.2023.04.020

Geh, D., Leslie, J., Rumney, R., Reeves, H. L., Bird, T. G., & Mann, D. A. (2022). Neutrophils as potential therapeutic targets in hepatocellular carcinoma. *Nat Rev Gastroenterol Hepatol*, *19*(4), 257-273. https://doi.org/10.1038/s41575-021-00568-5

Germann, M., Zangger, N., Sauvain, M. O., Sempoux, C., Bowler, A. D., Wirapati, P., Kandalaft, L. E., Delorenzi, M., Tejpar, S., Coukos, G., & Radtke, F. (2020). Neutrophils suppress tumor-infiltrating T cells in colon cancer via matrix metalloproteinase-mediated activation of TGFbeta. *EMBO Mol Med*, *12*(1), e10681. https://doi.org/10.15252/emmm.201910681

Gerner, M. Y., Casey, K. A., & Mescher, M. F. (2008). Defective MHC class II presentation by dendritic cells limits CD4 T cell help for antitumor CD8 T cell responses. *J Immunol*, *181*(1), 155-164. https://doi.org/10.4049/jimmunol.181.1.155

Giannitrapani, L., Cervello, M., Soresi, M., Notarbartolo, M., La Rosa, M., Virruso, L., D'Alessandro, N., & Montalto, G. (2002). Circulating IL-6 and sIL-6R in patients with hepatocellular carcinoma. *Ann N Y Acad Sci*, *963*, 46-52. https://doi.org/10.1111/j.1749-6632.2002.tb04093.x

Gomes de Castro, M. A., Hobartner, C., & Opazo, F. (2017). Staining of Membrane Receptors with Fluorescently-labeled DNA Aptamers for Super-resolution Imaging. *Bio Protoc*, *7*(17), e2541. https://doi.org/10.21769/BioProtoc.2541

Gomes, M. A., Priolli, D. G., Tralhao, J. G., & Botelho, M. F. (2013). Hepatocellular carcinoma: epidemiology, biology, diagnosis, and therapies. *Rev Assoc Med Bras (1992)*, *59*(5), 514-524. https://doi.org/10.1016/j.ramb.2013.03.005

Gross, S., Rahal, R., Stransky, N., Lengauer, C., & Hoeflich, K. P. (2015). Targeting cancer with kinase inhibitors. *J Clin Invest*, *125*(5), 1780-1789. https://doi.org/10.1172/JCI76094

Gu, C. Y., & Lee, T. K. W. (2022). Preclinical mouse models of hepatocellular carcinoma: An overview and update. *Exp Cell Res*, *412*(2), 113042. https://doi.org/10.1016/j.yexcr.2022.113042

Guichard, C., Amaddeo, G., Imbeaud, S., Ladeiro, Y., Pelletier, L., Maad, I. B.,

Calderaro, J., Bioulac-Sage, P., Letexier, M., Degos, F., Clement, B., Balabaud, C., Chevet, E., Laurent, A., Couchy, G., Letouze, E., Calvo, F., & Zucman-Rossi, J. (2012). Integrated analysis of somatic mutations and focal copy-number changes identifies key genes and pathways in hepatocellular carcinoma. *Nat Genet*, *44*(6), 694-698. https://doi.org/10.1038/ng.2256

Guo, X. Y., Zhang, J. Y., Shi, X. Z., Wang, Q., Shen, W. L., Zhu, W. W., & Liu, L. K. (2020). Upregulation of CSF-1 is correlated with elevated TAM infiltration and poor prognosis in oral squamous cell carcinoma. *Am J Transl Res*, *12*(10), 6235-6249. https://www.ncbi.nlm.nih.gov/pubmed/33194026

Hackett, P. B., Ekker, S. C., Largaespada, D. A., & McIvor, R. S. (2005). Sleeping beauty transposon-mediated gene therapy for prolonged expression. *Adv Genet*, *54*, 189-232. https://doi.org/10.1016/S0065-2660(05)54009-4

Hage, C., Hoves, S., Strauss, L., Bissinger, S., Prinz, Y., Poschinger, T., Kiessling, F., & Ries, C. H. (2019). Sorafenib Induces Pyroptosis in Macrophages and Triggers Natural Killer Cell-Mediated Cytotoxicity Against Hepatocellular Carcinoma. *Hepatology*, *70*(4), 1280-1297. https://doi.org/10.1002/hep.30666

Han, X., Han, Y., Jiao, H., & Jie, Y. (2015). 14-3-3zeta regulates immune response through Stat3 signaling in oral squamous cell carcinoma. *Mol Cells*, *38*(2), 112-121. https://doi.org/10.14348/molcells.2015.2101

Han, Y., Chen, Z., Yang, Y., Jiang, Z., Gu, Y., Liu, Y., Lin, C., Pan, Z., Yu, Y., Jiang, M., Zhou, W., & Cao, X. (2014). Human CD14+ CTLA-4+ regulatory dendritic cells suppress T-cell response by cytotoxic T-lymphocyte antigen-4-dependent IL-10 and indoleamine-2,3-dioxygenase production in hepatocellular carcinoma. *Hepatology*, *59*(2), 567-579. https://doi.org/10.1002/hep.26694

Han, Y., Liu, D., & Li, L. (2020). PD-1/PD-L1 pathway: current researches in cancer. *Am J Cancer Res*, *10*(3), 727-742. https://www.ncbi.nlm.nih.gov/pubmed/32266087

Hanks, S. K., & Hunter, T. (1995). Protein kinases 6. The eukaryotic protein kinase superfamily: kinase (catalytic) domain structure and classification. *FASEB J*, *9*(8), 576-596. https://www.ncbi.nlm.nih.gov/pubmed/7768349

Hato, T., Goyal, L., Greten, T. F., Duda, D. G., & Zhu, A. X. (2014). Immune checkpoint blockade in hepatocellular carcinoma: current progress and future directions. *Hepatology*, *60*(5), 1776-1782. https://doi.org/10.1002/hep.27246

He, G., Zhang, H., Zhou, J., Wang, B., Chen, Y., Kong, Y., Xie, X., Wang, X., Fei, R., Wei, L., Chen, H., & Zeng, H. (2015). Peritumoural neutrophils negatively regulate adaptive immunity via the PD-L1/PD-1 signalling pathway in hepatocellular carcinoma. *J Exp Clin Cancer Res*, *34*, 141. https://doi.org/10.1186/s13046-015-0256-0

Heimbach, J. K., Kulik, L. M., Finn, R. S., Sirlin, C. B., Abecassis, M. M., Roberts, L. R., Zhu, A. X., Murad, M. H., & Marrero, J. A. (2018). AASLD guidelines for the treatment of hepatocellular carcinoma. *Hepatology*, *67*(1), 358-380. https://doi.org/10.1002/hep.29086

Hemmer, W., McGlone, M., Tsigelny, I., & Taylor, S. S. (1997). Role of the glycine triad in the ATP-binding site of cAMP-dependent protein kinase. *J Biol Chem*, *272*(27), 16946-16954. https://doi.org/10.1074/jbc.272.27.16946

Heymann, F., & Tacke, F. (2016). Immunology in the liver--from homeostasis to disease. *Nat Rev Gastroenterol Hepatol*, *13*(2), 88-110. https://doi.org/10.1038/nrgastro.2015.200

Hoechst, B., Voigtlaender, T., Ormandy, L., Gamrekelashvili, J., Zhao, F., Wedemeyer, H., Lehner, F., Manns, M. P., Greten, T. F., & Korangy, F. (2009). Myeloid derived suppressor cells inhibit natural killer cells in patients with hepatocellular carcinoma via the NKp30 receptor. *Hepatology*, *50*(3), 799-807. https://doi.org/10.1002/hep.23054

Hsu, I. C., Metcalf, R. A., Sun, T., Welsh, J. A., Wang, N. J., & Harris, C. C. (1991). Mutational hotspot in the p53 gene in human hepatocellular carcinomas. *Nature*, *350*(6317), 427-428. https://doi.org/10.1038/350427a0

Hu, Y., Leo, C., Yu, S., Huang, B. C., Wang, H., Shen, M., Luo, Y., Daniel-Issakani, S., Payan, D. G., & Xu, X. (2004). Identification and functional characterization of a novel human misshapen/Nck interacting kinase-related kinase, hMINK beta. *J Biol Chem*, *279*(52), 54387-54397. https://doi.org/10.1074/jbc.M404497200

Iinuma, K., Kameyama, K., Taniguchi, T., Kawada, K., Ishida, T., Takagi, K., Nagai, S., Enomoto, T., Tomioka, M., Kawase, M., Takeuchi, S., Kato, D., Takai, M., Nakane, K., & Koie, T. (2022). Effectiveness and Safety of Molecular-Targeted Therapy after Nivolumab Plus Ipilimumab for Advanced or Metastatic Renal Cell Carcinoma: A Multicenter, Retrospective Cohort Study. *Cancers (Basel)*, *14*(19). https://doi.org/10.3390/cancers14194579

Ikeguchi, M., & Hirooka, Y. (2005). Interleukin-2 gene expression is a new biological prognostic marker in hepatocellular carcinomas. *Onkologie*, *28*(5), 255-259. https://doi.org/10.1159/000084695

Jansen, R., Embden, J. D., Gaastra, W., & Schouls, L. M. (2002). Identification of genes that are associated with DNA repeats in prokaryotes. *Mol Microbiol*, *43*(6), 1565-1575. https://doi.org/10.1046/j.1365-2958.2002.02839.x

Jia, Z. H., Jia, Y., Guo, F. J., Chen, J., Zhang, X. W., & Cui, M. H. (2017). Phosphorylation of STAT3 at Tyr705 regulates MMP-9 production in epithelial ovarian cancer. *PLoS One*, *12*(8), e0183622. https://doi.org/10.1371/journal.pone.0183622

Jiang, M., He, K., Qiu, T., Sun, J., Liu, Q., Zhang, X., & Zheng, H. (2020). Tumor-targeted delivery of silibinin and IPI-549 synergistically inhibit breast cancer by remodeling the microenvironment. *Int J Pharm*, *581*, 119239. https://doi.org/10.1016/j.ijpharm.2020.119239

Jiang, P., Gu, S., Pan, D., Fu, J., Sahu, A., Hu, X., Li, Z., Traugh, N., Bu, X., Li, B., Liu, J., Freeman, G. J., Brown, M. A., Wucherpfennig, K. W., & Liu, X. S. (2018). Signatures of T cell dysfunction and exclusion predict cancer immunotherapy response. *Nat Med*, *24*(10), 1550-1558. https://doi.org/10.1038/s41591-018-0136-1

Johannessen, L., Sundberg, T. B., O'Connell, D. J., Kolde, R., Berstler, J., Billings, K. J., Khor, B., Seashore-Ludlow, B., Fassl, A., Russell, C. N., Latorre, I. J., Jiang, B., Graham, D. B., Perez, J. R., Sicinski, P., Phillips, A. J., Schreiber, S. L., Gray, N. S., Shamji, A. F., & Xavier, R. J. (2017). Small-molecule studies identify CDK8 as a regulator of IL-10 in myeloid cells. *Nat Chem Biol*, *13*(10), 1102-1108. https://doi.org/10.1038/nchembio.2458

Joung, J., Konermann, S., Gootenberg, J. S., Abudayyeh, O. O., Platt, R. J., Brigham, M. D., Sanjana, N. E., & Zhang, F. (2017). Genome-scale CRISPR-Cas9 knockout and transcriptional activation screening. *Nat Protoc*, *12*(4), 828-863. https://doi.org/10.1038/nprot.2017.016

Ju, H. L., Han, K. H., Lee, J. D., & Ro, S. W. (2016). Transgenic mouse models generated by hydrodynamic transfection for genetic studies of liver cancer and preclinical testing of anti-cancer therapy. *Int J Cancer*, *138*(7), 1601-1608. https://doi.org/10.1002/ijc.29703

Ju, X., Zhang, H., Zhou, Z., Chen, M., & Wang, Q. (2020). Tumor-associated macrophages induce PD-L1 expression in gastric cancer cells through IL-6 and TNF-a signaling. *Exp Cell Res*, *396*(2), 112315. https://doi.org/10.1016/j.yexcr.2020.112315

Kakumu, S., Ito, S., Ishikawa, T., Mita, Y., Tagaya, T., Fukuzawa, Y., & Yoshioka, K. (2000). Decreased function of peripheral blood dendritic cells in patients with hepatocellular carcinoma with hepatitis B and C virus infection. *J Gastroenterol Hepatol*, *15*(4), 431-436. https://doi.org/10.1046/j.1440-1746.2000.02161.x

Kaltenmeier, C., Yazdani, H. O., Morder, K., Geller, D. A., Simmons, R. L., & Tohme, S. (2021). Neutrophil Extracellular Traps Promote T Cell Exhaustion in the Tumor Microenvironment. *Front Immunol*, *12*, 785222. https://doi.org/10.3389/fimmu.2021.785222

Kim, J. M., Nakao, K., Nakamura, K., Saito, I., Katsuki, M., Arai, K., & Masai, H. (2002). Inactivation of Cdc7 kinase in mouse ES cells results in S-phase arrest and p53-dependent cell death. *EMBO J*, *21*(9), 2168-2179.

https://doi.org/10.1093/emboj/21.9.2168

Kimura, T., Kato, Y., Ozawa, Y., Kodama, K., Ito, J., Ichikawa, K., Yamada, K., Hori, Y., Tabata, K., Takase, K., Matsui, J., Funahashi, Y., & Nomoto, K. (2018). Immunomodulatory activity of lenvatinib contributes to antitumor activity in the Hepa1-6 hepatocellular carcinoma model. *Cancer Sci*, *109*(12), 3993-4002. https://doi.org/10.1111/cas.13806

Knighton, D. R., Zheng, J. H., Ten Eyck, L. F., Ashford, V. A., Xuong, N. H., Taylor, S. S., & Sowadski, J. M. (1991). Crystal structure of the catalytic subunit of cyclic adenosine monophosphate-dependent protein kinase. *Science*, *253*(5018), 407-414. https://doi.org/10.1126/science.1862342

Kobayashi, S. D., & DeLeo, F. R. (2009). Role of neutrophils in innate immunity: a systems biology-level approach. *Wiley Interdiscip Rev Syst Biol Med*, *1*(3), 309-333. https://doi.org/10.1002/wsbm.32

Kondili, L. A., Buti, M., Riveiro-Barciela, M., Maticic, M., Negro, F., Berg, T., & Craxi, A. (2022). Impact of the COVID-19 pandemic on hepatitis B and C elimination: An EASL survey. *JHEP Rep*, *4*(9), 100531. https://doi.org/10.1016/j.jhepr.2022.100531

Korbecki, J., Kojder, K., Siminska, D., Bohatyrewicz, R., Gutowska, I., Chlubek, D., & Baranowska-Bosiacka, I. (2020). CC Chemokines in a Tumor: A Review of Pro-Cancer and Anti-Cancer Properties of the Ligands of Receptors CCR1, CCR2, CCR3, and CCR4. *Int J Mol Sci*, *21*(21). https://doi.org/10.3390/ijms21218412

Kuang, D. M., Zhao, Q., Peng, C., Xu, J., Zhang, J. P., Wu, C., & Zheng, L. (2009). Activated monocytes in peritumoral stroma of hepatocellular carcinoma foster immune privilege and disease progression through PD-L1. *J Exp Med*, *206*(6), 1327-1337. https://doi.org/10.1084/jem.20082173

Kudo, M., Finn, R. S., Qin, S., Han, K. H., Ikeda, K., Piscaglia, F., Baron, A., Park, J. W., Han, G., Jassem, J., Blanc, J. F., Vogel, A., Komov, D., Evans, T. R. J., Lopez, C., Dutcus, C., Guo, M., Saito, K., Kraljevic, S., . . . Cheng, A. L. (2018). Lenvatinib versus sorafenib in first-line treatment of patients with unresectable hepatocellular carcinoma: a randomised phase 3 non-inferiority trial. *Lancet*, *391*(10126), 1163-1173. https://doi.org/10.1016/S0140-6736(18)30207-1

Kudo, M., Lim, H. Y., Cheng, A. L., Chao, Y., Yau, T., Ogasawara, S., Kurosaki, M., Morimoto, N., Ohkawa, K., Yamashita, T., Lee, K. H., Chen, E., Siegel, A. B., & Ryoo, B. Y. (2021). Pembrolizumab as Second-Line Therapy for Advanced Hepatocellular Carcinoma: A Subgroup Analysis of Asian Patients in the Phase 3 KEYNOTE-240 Trial. *Liver Cancer*, *10*(3), 275-284. https://doi.org/10.1159/000515553

Kulik, L. M., Fisher, R. A., Rodrigo, D. R., Brown, R. S., Jr., Freise, C. E., Shaked, A., Everhart, J. E., Everson, G. T., Hong, J. C., Hayashi, P. H., Berg, C. L., Lok, A. S., & Group, A. A. S. (2012). Outcomes of living and deceased donor liver transplant recipients with hepatocellular carcinoma: results of the A2ALL cohort. *Am J Transplant*, *12*(11), 2997-3007. https://doi.org/10.1111/j.1600-6143.2012.04272.x

Lan, Y. T., Fan, X. P., Fan, Y. C., Zhao, J., & Wang, K. (2017). Change in the Treg/Th17 cell imbalance in hepatocellular carcinoma patients and its clinical value. *Medicine (Baltimore)*, *96*(32), e7704. https://doi.org/10.1097/MD.0000000000007704

Larhammar, M., Huntwork-Rodriguez, S., Rudhard, Y., Sengupta-Ghosh, A., & Lewcock, J. W. (2017). The Ste20 Family Kinases MAP4K4, MINK1, and TNIK Converge to Regulate Stress-Induced JNK Signaling in Neurons. *J Neurosci*, *37*(46), 11074-11084. https://doi.org/10.1523/JNEUROSCI.0905-17.2017

Lee, J. S. (2015). The mutational landscape of hepatocellular carcinoma. *Clin Mol Hepatol*, *21*(3), 220-229. https://doi.org/10.3350/cmh.2015.21.3.220

Lee, S. E., Chang, S. H., Kim, W. Y., Lim, S. D., Kim, W. S., Hwang, T. S., & Han, H. S. (2016). Frequent somatic TERT promoter mutations and CTNNB1 mutations in hepatocellular carcinoma. *Oncotarget*, *7*(43), 69267-69275. https://doi.org/10.18632/oncotarget.12121

Lencioni, R., Cioni, D., Crocetti, L., Franchini, C., Pina, C. D., Lera, J., & Bartolozzi, C. (2005). Early-stage hepatocellular carcinoma in patients with cirrhosis: long-term results of percutaneous image-guided radiofrequency ablation. *Radiology*, *234*(3), 961-967. https://doi.org/10.1148/radiol.2343040350

Leone, P., Solimando, A. G., Fasano, R., Argentiero, A., Malerba, E., Buonavoglia, A., Lupo, L. G., De Re, V., Silvestris, N., & Racanelli, V. (2021). The Evolving Role of Immune Checkpoint Inhibitors in Hepatocellular Carcinoma Treatment. *Vaccines (Basel)*, *9*(5). https://doi.org/10.3390/vaccines9050532

Li, F., Huang, Q., Luster, T. A., Hu, H., Zhang, H., Ng, W. L., Khodadadi-Jamayran, A., Wang, W., Chen, T., Deng, J., Ranieri, M., Fang, Z., Pyon, V., Dowling, C. M., Bagdatlioglu, E., Almonte, C., Labbe, K., Silver, H., Rabin, A. R., . . . Wong, K. K. (2020). In Vivo Epigenetic CRISPR Screen Identifies Asf1a as an Immunotherapeutic Target in Kras-Mutant Lung Adenocarcinoma. *Cancer Discov*, *10*(2), 270-287. https://doi.org/10.1158/2159-8290.CD-19-0780

Li, G., Hou, C., Dou, S., Zhang, J., Zhang, Y., Liu, Y., Wang, Z., Xiao, H., Wang, R., Chen, G., Li, Y., Feng, J., Shen, B., & Han, G. (2019). Monoclonal antibody against human Tim-3 enhances antiviral immune response. *Scand J Immunol*,

89(2), e12738. https://doi.org/10.1111/sji.12738

Li, L., Yu, R., Cai, T., Chen, Z., Lan, M., Zou, T., Wang, B., Wang, Q., Zhao, Y., & Cai, Y. (2020). Effects of immune cells and cytokines on inflammation and immunosuppression in the tumor microenvironment. *Int Immunopharmacol*, *88*, 106939. https://doi.org/10.1016/j.intimp.2020.106939

Li, N., & Hua, J. (2017). Immune cells in liver regeneration. *Oncotarget*, *8*(2), 3628-3639. https://doi.org/10.18632/oncotarget.12275

Li, T., Yang, Y., Hua, X., Wang, G., Liu, W., Jia, C., Tai, Y., Zhang, Q., & Chen, G. (2012). Hepatocellular carcinoma-associated fibroblasts trigger NK cell dysfunction via PGE2 and IDO. *Cancer Lett*, *318*(2), 154-161. https://doi.org/10.1016/j.canlet.2011.12.020

Li, X., Lian, Z., Wang, S., Xing, L., & Yu, J. (2018). Interactions between EGFR and PD-1/PD-L1 pathway: Implications for treatment of NSCLC. *Cancer Lett*, *418*, 1-9. https://doi.org/10.1016/j.canlet.2018.01.005

Li, X., Yao, W., Yuan, Y., Chen, P., Li, B., Li, J., Chu, R., Song, H., Xie, D., Jiang, X., & Wang, H. (2017). Targeting of tumour-infiltrating macrophages via CCL2/CCR2 signalling as a therapeutic strategy against hepatocellular carcinoma. *Gut*, *66*(1), 157-167. https://doi.org/10.1136/gutjnl-2015-310514

Li, Z., Wu, T., Zheng, B., & Chen, L. (2019). Individualized precision treatment: Targeting TAM in HCC. *Cancer Lett*, *458*, 86-91. https://doi.org/10.1016/j.canlet.2019.05.019

Lieschke, G. J., Grail, D., Hodgson, G., Metcalf, D., Stanley, E., Cheers, C., Fowler, K. J., Basu, S., Zhan, Y. F., & Dunn, A. R. (1994). Mice lacking granulocyte colony-stimulating factor have chronic neutropenia, granulocyte and macrophage progenitor cell deficiency, and impaired neutrophil mobilization. *Blood*, *84*(6), 1737-1746. https://www.ncbi.nlm.nih.gov/pubmed/7521686

Limmer, A., Ohl, J., Wingender, G., Berg, M., Jungerkes, F., Schumak, B., Djandji, D., Scholz, K., Klevenz, A., Hegenbarth, S., Momburg, F., Hammerling, G. J., Arnold, B., & Knolle, P. A. (2005). Cross-presentation of oral antigens by liver sinusoidal endothelial cells leads to CD8 T cell tolerance. *Eur J Immunol*, *35*(10), 2970-2981. https://doi.org/10.1002/eji.200526034

Lin, S. M., Lin, C. J., Lin, C. C., Hsu, C. W., & Chen, Y. C. (2005). Randomised controlled trial comparing percutaneous radiofrequency thermal ablation, percutaneous ethanol injection, and percutaneous acetic acid injection to treat hepatocellular carcinoma of 3 cm or less. *Gut*, *54*(8), 1151-1156. https://doi.org/10.1136/gut.2004.045203

Liu, B., Saber, A., & Haisma, H. J. (2019). CRISPR/Cas9: a powerful tool for identification of new targets for cancer treatment. *Drug Discov Today*, *24*(4),

955-970. https://doi.org/10.1016/j.drudis.2019.02.011

Liu, F., Liu, Y., & Chen, Z. (2018). Tim-3 expression and its role in hepatocellular carcinoma. *J Hematol Oncol*, *11*(1), 126. https://doi.org/10.1186/s13045-018-0667-4

Liu, L., Liu, Y., Yan, X., Zhou, C., & Xiong, X. (2020). The role of granulocyte colony-stimulating factor in breast cancer development: A review. *Mol Med Rep*, *21*(5), 2019-2029. https://doi.org/10.3892/mmr.2020.11017

Liu, W., Xu, H., Ying, X., Zhang, D., Lai, L., Wang, L., Tu, J., & Ji, J. (2020). Radiofrequency Ablation (RFA) Combined with Transcatheter Arterial Chemoembolization (TACE) for Patients with Medium-to-Large Hepatocellular Carcinoma: A Retrospective Analysis of Long-Term Outcome. *Med Sci Monit*, *26*, e923263. https://doi.org/10.12659/MSM.923263

Liu, Y., Poon, R. T., Feng, X., Yu, W. C., Luk, J. M., & Fan, S. T. (2004). Reduced expression of chemokine receptors on peripheral blood lymphocytes in patients with hepatocellular carcinoma. *Am J Gastroenterol*, *99*(6), 1111-1121. https://doi.org/10.1111/j.1572-0241.2004.30265.x

Llovet, J. M., Kelley, R. K., Villanueva, A., Singal, A. G., Pikarsky, E., Roayaie, S., Lencioni, R., Koike, K., Zucman-Rossi, J., & Finn, R. S. (2021). Hepatocellular carcinoma. *Nat Rev Dis Primers*, *7*(1), 6. https://doi.org/10.1038/s41572-020-00240-3

Llovet, J. M., Ricci, S., Mazzaferro, V., Hilgard, P., Gane, E., Blanc, J. F., de Oliveira, A. C., Santoro, A., Raoul, J. L., Forner, A., Schwartz, M., Porta, C., Zeuzem, S., Bolondi, L., Greten, T. F., Galle, P. R., Seitz, J. F., Borbath, I., Haussinger, D., . . . Group, S. I. S. (2008). Sorafenib in advanced hepatocellular carcinoma. *N Engl J Med*, *359*(4), 378-390. https://doi.org/10.1056/NEJMoa0708857

Loomba, R., & Adams, L. A. (2019). The 20% Rule of NASH Progression: The Natural History of Advanced Fibrosis and Cirrhosis Caused by NASH. *Hepatology*, *70*(6), 1885-1888. https://doi.org/10.1002/hep.30946

Lu, C., Rong, D., Zhang, B., Zheng, W., Wang, X., Chen, Z., & Tang, W. (2019). Current perspectives on the immunosuppressive tumor microenvironment in hepatocellular carcinoma: challenges and opportunities. *Mol Cancer*, *18*(1), 130. https://doi.org/10.1186/s12943-019-1047-6

Lu, L. C., Chang, C. J., & Hsu, C. H. (2019). Targeting myeloid-derived suppressor cells in the treatment of hepatocellular carcinoma: current state and future perspectives. *J Hepatocell Carcinoma*, *6*, 71-84. https://doi.org/10.2147/JHC.S159693

Ma, C., Han, M., Heinrich, B., Fu, Q., Zhang, Q., Sandhu, M., Agdashian, D., Terabe, M., Berzofsky, J. A., Fako, V., Ritz, T., Longerich, T., Theriot, C. M., McCulloch,

J. A., Roy, S., Yuan, W., Thovarai, V., Sen, S. K., Ruchirawat, M., . . . Greten, T. F. (2018). Gut microbiome-mediated bile acid metabolism regulates liver cancer via NKT cells. *Science*, *360*(6391). https://doi.org/10.1126/science.aan5931

Ma, C., Kesarwala, A. H., Eggert, T., Medina-Echeverz, J., Kleiner, D. E., Jin, P., Stroncek, D. F., Terabe, M., Kapoor, V., ElGindi, M., Han, M., Thornton, A. M., Zhang, H., Egger, M., Luo, J., Felsher, D. W., McVicar, D. W., Weber, A., Heikenwalder, M., & Greten, T. F. (2016). NAFLD causes selective CD4(+) T lymphocyte loss and promotes hepatocarcinogenesis. *Nature*, *531*(7593), 253-257. https://doi.org/10.1038/nature16969

Ma, C. S., Suryani, S., Avery, D. T., Chan, A., Nanan, R., Santner-Nanan, B., Deenick, E. K., & Tangye, S. G. (2009). Early commitment of naive human CD4(+) T cells to the T follicular helper (T(FH)) cell lineage is induced by IL-12. *Immunol Cell Biol*, *87*(8), 590-600. https://doi.org/10.1038/icb.2009.64

Machairas, N., Tsilimigras, D. I., & Pawlik, T. M. (2021). State-of-the-art surgery for hepatocellular carcinoma. *Langenbecks Arch Surg*, *406*(7), 2151-2162. https://doi.org/10.1007/s00423-021-02298-3

Mahajan, K., & Mahajan, N. P. (2013). WEE1 tyrosine kinase, a novel epigenetic modifier. *Trends Genet*, *29*(7), 394-402. https://doi.org/10.1016/j.tig.2013.02.003

Manguso, R. T., Pope, H. W., Zimmer, M. D., Brown, F. D., Yates, K. B., Miller, B. C., Collins, N. B., Bi, K., LaFleur, M. W., Juneja, V. R., Weiss, S. A., Lo, J., Fisher, D. E., Miao, D., Van Allen, E., Root, D. E., Sharpe, A. H., Doench, J. G., & Haining, W. N. (2017). In vivo CRISPR screening identifies Ptpn2 as a cancer immunotherapy target. *Nature*, *547*(7664), 413-418. https://doi.org/10.1038/nature23270

Matsubara, T., Ono, T., Yamanoi, A., Tachibana, M., & Nagasue, N. (2007). Fractalkine-CX3CR1 axis regulates tumor cell cycle and deteriorates prognosis after radical resection for hepatocellular carcinoma. *J Surg Oncol*, *95*(3), 241-249. https://doi.org/10.1002/jso.20642

Matsui, M., Machida, S., Itani-Yohda, T., & Akatsuka, T. (2002). Downregulation of the proteasome subunits, transporter, and antigen presentation in hepatocellular carcinoma, and their restoration by interferon-gamma. *J Gastroenterol Hepatol*, *17*(8), 897-907. https://doi.org/10.1046/j.1440-1746.2002.02837.x

Matsumura, T., Ito, A., Takii, T., Hayashi, H., & Onozaki, K. (2000). Endotoxin and cytokine regulation of toll-like receptor (TLR) 2 and TLR4 gene expression in murine liver and hepatocytes. *J Interferon Cytokine Res*, *20*(10), 915-921. https://doi.org/10.1089/10799900050163299

Matte, A., Tari, L. W., & Delbaere, L. T. (1998). How do kinases transfer phosphoryl

groups? *Structure*, *6*(4), 413-419. https://doi.org/10.1016/s0969-2126(98)00043-4

Mazzaferro, V., Regalia, E., Doci, R., Andreola, S., Pulvirenti, A., Bozzetti, F., Montalto, F., Ammatuna, M., Morabito, A., & Gennari, L. (1996). Liver transplantation for the treatment of small hepatocellular carcinomas in patients with cirrhosis. *N Engl J Med*, *334*(11), 693-699. https://doi.org/10.1056/NEJM199603143341104

McClendon, C. L., Kornev, A. P., Gilson, M. K., & Taylor, S. S. (2014). Dynamic architecture of a protein kinase. *Proc Natl Acad Sci U S A*, *111*(43), E4623-4631. https://doi.org/10.1073/pnas.1418402111

McFarlane, A. J., Fercoq, F., Coffelt, S. B., & Carlin, L. M. (2021). Neutrophil dynamics in the tumor microenvironment. *J Clin Invest*, *131*(6). https://doi.org/10.1172/JCI143759

McSkimming, D. I., Rasheed, K., & Kannan, N. (2017). Classifying kinase conformations using a machine learning approach. *BMC Bioinformatics*, *18*(1), 86. https://doi.org/10.1186/s12859-017-1506-2

Meng, Z., Moroishi, T., Mottier-Pavie, V., Plouffe, S. W., Hansen, C. G., Hong, A. W., Park, H. W., Mo, J. S., Lu, W., Lu, S., Flores, F., Yu, F. X., Halder, G., & Guan, K. L. (2015). MAP4K family kinases act in parallel to MST1/2 to activate LATS1/2 in the Hippo pathway. *Nat Commun*, *6*, 8357. https://doi.org/10.1038/ncomms9357

Mikryukov, A., & Moss, T. (2012). Agonistic and antagonistic roles for TNIK and MINK in non-canonical and canonical Wnt signalling. *PLoS One*, *7*(9), e43330. https://doi.org/10.1371/journal.pone.0043330

Miller, S. P., Karschnia, E. J., Ikeda, T. P., & LaPorte, D. C. (1996). Isocitrate dehydrogenase kinase/phosphatase. Kinetic characteristics of the wild-type and two mutant proteins. *J Biol Chem*, *271*(32), 19124-19128. https://doi.org/10.1074/jbc.271.32.19124

Modi, V., & Dunbrack, R. L., Jr. (2019). Defining a new nomenclature for the structures of active and inactive kinases. *Proc Natl Acad Sci U S A*, *116*(14), 6818-6827. https://doi.org/10.1073/pnas.1814279116

Moroishi, T., Hayashi, T., Pan, W. W., Fujita, Y., Holt, M. V., Qin, J., Carson, D. A., & Guan, K. L. (2016). The Hippo Pathway Kinases LATS1/2 Suppress Cancer Immunity. *Cell*, *167*(6), 1525-1539 e1517. https://doi.org/10.1016/j.cell.2016.11.005

Morris, K. T., Castillo, E. F., Ray, A. L., Weston, L. L., Nofchissey, R. A., Hanson, J. A., Samedi, V. G., Pinchuk, I. V., Hudson, L. G., & Beswick, E. J. (2015). Anti-G-CSF treatment induces protective tumor immunity in mouse colon cancer by

promoting protective NK cell, macrophage and T cell responses. *Oncotarget*, *6*(26), 22338-22347. https://doi.org/10.18632/oncotarget.4169

Muhanna, N., Doron, S., Wald, O., Horani, A., Eid, A., Pappo, O., Friedman, S. L., & Safadi, R. (2008). Activation of hepatic stellate cells after phagocytosis of lymphocytes: A novel pathway of fibrogenesis. *Hepatology*, *48*(3), 963-977. https://doi.org/10.1002/hep.22413

Munier, C. C., De Maria, L., Edman, K., Gunnarsson, A., Longo, M., MacKintosh, C., Patel, S., Snijder, A., Wissler, L., Brunsveld, L., Ottmann, C., & Perry, M. W. D. (2021). Glucocorticoid receptor Thr524 phosphorylation by MINK1 induces interactions with 14-3-3 protein regulators. *J Biol Chem*, *296*, 100551. https://doi.org/10.1016/j.jbc.2021.100551

Murakami, S. (2004). Soluble interleukin-2 receptor in cancer. *Front Biosci*, *9*, 3085-3090. https://doi.org/10.2741/1461

Nakagawa, H., Mizukoshi, E., Kobayashi, E., Tamai, T., Hamana, H., Ozawa, T., Kishi, H., Kitahara, M., Yamashita, T., Arai, K., Terashima, T., Iida, N., Fushimi, K., Muraguchi, A., & Kaneko, S. (2017). Association Between High-Avidity T-Cell Receptors, Induced by alpha-Fetoprotein-Derived Peptides, and Anti-Tumor Effects in Patients With Hepatocellular Carcinoma. *Gastroenterology*, *152*(6), 1395-1406 e1310. https://doi.org/10.1053/j.gastro.2017.02.001

Nault, J. C., Mallet, M., Pilati, C., Calderaro, J., Bioulac-Sage, P., Laurent, C., Laurent, A., Cherqui, D., Balabaud, C., & Zucman-Rossi, J. (2013). High frequency of telomerase reverse-transcriptase promoter somatic mutations in hepatocellular carcinoma and preneoplastic lesions. *Nat Commun*, *4*, 2218. https://doi.org/10.1038/ncomms3218

Nielsen, S. R., Strobech, J. E., Horton, E. R., Jackstadt, R., Laitala, A., Bravo, M. C., Maltese, G., Jensen, A. R. D., Reuten, R., Rafaeva, M., Karim, S. A., Hwang, C. I., Arnes, L., Tuveson, D. A., Sansom, O. J., Morton, J. P., & Erler, J. T. (2021). Suppression of tumor-associated neutrophils by lorlatinib attenuates pancreatic cancer growth and improves treatment with immune checkpoint blockade. *Nat Commun*, *12*(1), 3414. https://doi.org/10.1038/s41467-021-23731-7

Ninomiya, T., Akbar, S. M., Masumoto, T., Horiike, N., & Onji, M. (1999). Dendritic cells with immature phenotype and defective function in the peripheral blood from patients with hepatocellular carcinoma. *J Hepatol*, *31*(2), 323-331. https://doi.org/10.1016/s0168-8278(99)80231-1

Nolen, B., Taylor, S., & Ghosh, G. (2004). Regulation of protein kinases; controlling activity through activation segment conformation. *Mol Cell*, *15*(5), 661-675. https://doi.org/10.1016/j.molcel.2004.08.024

Okusaka, T., & Ikeda, M. (2018). Immunotherapy for hepatocellular carcinoma: current status and future perspectives. *ESMO Open*, *3*(Suppl 1), e000455. https://doi.org/10.1136/esmoopen-2018-000455

Olson, B., Li, Y., Lin, Y., Liu, E. T., & Patnaik, A. (2018). Mouse Models for Cancer Immunotherapy Research. *Cancer Discov*, *8*(11), 1358-1365. https://doi.org/10.1158/2159-8290.CD-18-0044

Oo, Y. H., Banz, V., Kavanagh, D., Liaskou, E., Withers, D. R., Humphreys, E., Reynolds, G. M., Lee-Turner, L., Kalia, N., Hubscher, S. G., Klenerman, P., Eksteen, B., & Adams, D. H. (2012). CXCR3-dependent recruitment and CCR6-mediated positioning of Th-17 cells in the inflamed liver. *J Hepatol*, *57*(5), 1044-1051. https://doi.org/10.1016/j.jhep.2012.07.008

Ormandy, L. A., Hillemann, T., Wedemeyer, H., Manns, M. P., Greten, T. F., & Korangy, F. (2005). Increased populations of regulatory T cells in peripheral blood of patients with hepatocellular carcinoma. *Cancer Res*, *65*(6), 2457-2464. https://doi.org/10.1158/0008-5472.CAN-04-3232

Ostrand-Rosenberg, S., Sinha, P., Beury, D. W., & Clements, V. K. (2012). Cross-talk between myeloid-derived suppressor cells (MDSC), macrophages, and dendritic cells enhances tumor-induced immune suppression. *Semin Cancer Biol*, *22*(4), 275-281. https://doi.org/10.1016/j.semcancer.2012.01.011

Ou, D. L., Chen, C. W., Hsu, C. L., Chung, C. H., Feng, Z. R., Lee, B. S., Cheng, A. L., Yang, M. H., & Hsu, C. (2021). Regorafenib enhances antitumor immunity via inhibition of p38 kinase/Creb1/Klf4 axis in tumor-associated macrophages. *J Immunother Cancer*, *9*(3). https://doi.org/10.1136/jitc-2020-001657

Owen, K. L., Brockwell, N. K., & Parker, B. S. (2019). JAK-STAT Signaling: A Double-Edged Sword of Immune Regulation and Cancer Progression. *Cancers (Basel)*, *11*(12). https://doi.org/10.3390/cancers11122002

Palacios, F., Abreu, C., Prieto, D., Morande, P., Ruiz, S., Fernandez-Calero, T., Naya, H., Libisch, G., Robello, C., Landoni, A. I., Gabus, R., Dighiero, G., & Oppezzo, P. (2015). Activation of the PI3K/AKT pathway by microRNA-22 results in CLL B-cell proliferation. *Leukemia*, *29*(1), 115-125. https://doi.org/10.1038/leu.2014.158

Park, J., Wysocki, R. W., Amoozgar, Z., Maiorino, L., Fein, M. R., Jorns, J., Schott, A. F., Kinugasa-Katayama, Y., Lee, Y., Won, N. H., Nakasone, E. S., Hearn, S. A., Kuttner, V., Qiu, J., Almeida, A. S., Perurena, N., Kessenbrock, K., Goldberg, M. S., & Egeblad, M. (2016). Cancer cells induce metastasis-supporting neutrophil extracellular DNA traps. *Sci Transl Med*, *8*(361), 361ra138. https://doi.org/10.1126/scitranslmed.aag1711

Pearson, G., Robinson, F., Beers Gibson, T., Xu, B. E., Karandikar, M., Berman, K., &

Cobb, M. H. (2001). Mitogen-activated protein (MAP) kinase pathways: regulation and physiological functions. *Endocr Rev*, *22*(2), 153-183. https://doi.org/10.1210/edrv.22.2.0428

Popow, O., Paulo, J. A., Tatham, M. H., Volk, M. S., Rojas-Fernandez, A., Loyer, N., Newton, I. P., Januschke, J., Haigis, K. M., & Nathke, I. (2019). Identification of Endogenous Adenomatous Polyposis Coli Interaction Partners and beta-Catenin-Independent Targets by Proteomics. *Mol Cancer Res*, *17*(9), 1828-1841. https://doi.org/10.1158/1541-7786.MCR-18-1154

Qin, S., Finn, R. S., Kudo, M., Meyer, T., Vogel, A., Ducreux, M., Macarulla, T. M., Tomasello, G., Boisserie, F., Hou, J., Li, X., Song, J., & Zhu, A. X. (2019). RATIONALE 301 study: tislelizumab versus sorafenib as first-line treatment for unresectable hepatocellular carcinoma. *Future Oncol*, *15*(16), 1811-1822. https://doi.org/10.2217/fon-2019-0097

Qin, S., Ren, Z., Meng, Z., Chen, Z., Chai, X., Xiong, J., Bai, Y., Yang, L., Zhu, H., Fang, W., Lin, X., Chen, X., Li, E., Wang, L., Chen, C., & Zou, J. (2020). Camrelizumab in patients with previously treated advanced hepatocellular carcinoma: a multicentre, open-label, parallel-group, randomised, phase 2 trial. *Lancet Oncol*, *21*(4), 571-580. https://doi.org/10.1016/S1470-2045(20)30011-5

Qiu, M. J., He, X. X., Bi, N. R., Wang, M. M., Xiong, Z. F., & Yang, S. L. (2018). Effects of liver-targeted drugs on expression of immune-related proteins in hepatocellular carcinoma cells. *Clin Chim Acta*, *485*, 103-105. https://doi.org/10.1016/j.cca.2018.06.032

Qu, K., Lu, Y., Lin, N., Singh, R., Xu, X., Payan, D. G., & Xu, D. (2004). Computational and experimental studies on human misshapen/NIK-related kinase MINK-1. *Curr Med Chem*, *11*(5), 569-582. https://doi.org/10.2174/0929867043455873

Que, H., Fu, Q., Lan, T., Tian, X., & Wei, X. (2022). Tumor-associated neutrophils and neutrophil-targeted cancer therapies. *Biochim Biophys Acta Rev Cancer*, *1877*(5), 188762. https://doi.org/10.1016/j.bbcan.2022.188762

Rabinovich, G. A., Gabrilovich, D., & Sotomayor, E. M. (2007). Immunosuppressive strategies that are mediated by tumor cells. *Annu Rev Immunol*, *25*, 267-296. https://doi.org/10.1146/annurev.immunol.25.022106.141609

Rankin, E. B., & Giaccia, A. J. (2016). The Receptor Tyrosine Kinase AXL in Cancer Progression. *Cancers (Basel)*, *8*(11). https://doi.org/10.3390/cancers8110103

Rebouissou, S., & Nault, J. C. (2020). Advances in molecular classification and precision oncology in hepatocellular carcinoma. *J Hepatol*, *72*(2), 215-229. https://doi.org/10.1016/j.jhep.2019.08.017

Reig, M., Forner, A., Rimola, J., Ferrer-Fabrega, J., Burrel, M., Garcia-Criado, A., Kelley, R. K., Galle, P. R., Mazzaferro, V., Salem, R., Sangro, B., Singal, A. G.,

Vogel, A., Fuster, J., Ayuso, C., & Bruix, J. (2022). BCLC strategy for prognosis prediction and treatment recommendation: The 2022 update. *J Hepatol*, *76*(3), 681-693. https://doi.org/10.1016/j.jhep.2021.11.018

Reparaz, D., Aparicio, B., Llopiz, D., Hervas-Stubbs, S., & Sarobe, P. (2022). Therapeutic Vaccines against Hepatocellular Carcinoma in the Immune Checkpoint Inhibitor Era: Time for Neoantigens? *Int J Mol Sci*, *23*(4). https://doi.org/10.3390/ijms23042022

Ribas, A., & Wolchok, J. D. (2018). Cancer immunotherapy using checkpoint blockade. *Science*, *359*(6382), 1350-1355. https://doi.org/10.1126/science.aar4060

Rossetto, A., De Re, V., Steffan, A., Ravaioli, M., Miolo, G., Leone, P., Racanelli, V., Uzzau, A., Baccarani, U., & Cescon, M. (2019). Carcinogenesis and Metastasis in Liver: Cell Physiological Basis. *Cancers (Basel)*, *11*(11). https://doi.org/10.3390/cancers11111731

Rubie, C., Frick, V. O., Wagner, M., Weber, C., Kruse, B., Kempf, K., Konig, J., Rau, B., & Schilling, M. (2006). Chemokine expression in hepatocellular carcinoma versus colorectal liver metastases. *World J Gastroenterol*, *12*(41), 6627-6633. https://doi.org/10.3748/wjg.v12.i41.6627

Rudensky, A. Y. (2011). Regulatory T cells and Foxp3. *Immunol Rev*, *241*(1), 260-268. https://doi.org/10.1111/j.1600-065X.2011.01018.x

Ruggieri, A. N., Yarchoan, M., Goyal, S., Liu, Y., Sharon, E., Chen, H. X., Olson, B. M., Paulos, C. M., El-Rayes, B. F., Maithel, S. K., Azad, N. S., & Lesinski, G. B. (2022). Combined MEK/PD-L1 Inhibition Alters Peripheral Cytokines and Lymphocyte Populations Correlating with Improved Clinical Outcomes in Advanced Biliary Tract Cancer. *Clin Cancer Res*, *28*(19), 4336-4345. https://doi.org/10.1158/1078-0432.CCR-22-1123

Sachdeva, M., Chawla, Y. K., & Arora, S. K. (2015). Immunology of hepatocellular carcinoma. *World J Hepatol*, *7*(17), 2080-2090. https://doi.org/10.4254/wjh.v7.i17.2080

Saito, A., Toyoda, H., Kobayashi, M., Koiwa, Y., Fujii, H., Fujita, K., Maeda, A., Kaneoka, Y., Hazama, S., Nagano, H., Mirza, A. H., Graf, H. P., Cosatto, E., Murakami, Y., & Kuroda, M. (2021). Prediction of early recurrence of hepatocellular carcinoma after resection using digital pathology images assessed by machine learning. *Mod Pathol*, *34*(2), 417-425. https://doi.org/10.1038/s41379-020-00671-z

Sakaguchi, S., Yamaguchi, T., Nomura, T., & Ono, M. (2008). Regulatory T cells and immune tolerance. *Cell*, *133*(5), 775-787. https://doi.org/10.1016/j.cell.2008.05.009

Sang, Y. B., Kim, J. H., Kim, C. G., Hong, M. H., Kim, H. R., Cho, B. C., & Lim, S.

M. (2022). The Development of AXL Inhibitors in Lung Cancer: Recent Progress and Challenges. *Front Oncol*, *12*, 811247. https://doi.org/10.3389/fonc.2022.811247

Sangro, B., Gomez-Martin, C., de la Mata, M., Inarrairaegui, M., Garralda, E., Barrera, P., Riezu-Boj, J. I., Larrea, E., Alfaro, C., Sarobe, P., Lasarte, J. J., Perez-Gracia, J. L., Melero, I., & Prieto, J. (2013). A clinical trial of CTLA-4 blockade with tremelimumab in patients with hepatocellular carcinoma and chronic hepatitis C. *J Hepatol*, *59*(1), 81-88. https://doi.org/10.1016/j.jhep.2013.02.022

Sangro, B., Sarobe, P., Hervas-Stubbs, S., & Melero, I. (2021). Advances in immunotherapy for hepatocellular carcinoma. *Nat Rev Gastroenterol Hepatol*, *18*(8), 525-543. https://doi.org/10.1038/s41575-021-00438-0

Satoh, S., Daigo, Y., Furukawa, Y., Kato, T., Miwa, N., Nishiwaki, T., Kawasoe, T., Ishiguro, H., Fujita, M., Tokino, T., Sasaki, Y., Imaoka, S., Murata, M., Shimano, T., Yamaoka, Y., & Nakamura, Y. (2000). AXIN1 mutations in hepatocellular carcinomas, and growth suppression in cancer cells by virus-mediated transfer of AXIN1. *Nat Genet*, *24*(3), 245-250. https://doi.org/10.1038/73448

Saxena, R., & Kaur, J. (2015). Th1/Th2 cytokines and their genotypes as predictors of hepatitis B virus related hepatocellular carcinoma. *World J Hepatol*, *7*(11), 1572-1580. https://doi.org/10.4254/wjh.v7.i11.1572

Schildberg, F. A., Wojtalla, A., Siegmund, S. V., Endl, E., Diehl, L., Abdullah, Z., Kurts, C., & Knolle, P. A. (2011). Murine hepatic stellate cells veto CD8 T cell activation by a CD54-dependent mechanism. *Hepatology*, *54*(1), 262-272. https://doi.org/10.1002/hep.24352

Seton-Rogers, S. (2017). Immunotherapy: Switching off immune suppression. *Nat Rev Cancer*, *17*(1), 1. https://doi.org/10.1038/nrc.2016.144

Shang, A., Wang, W., Gu, C., Chen, C., Zeng, B., Yang, Y., Ji, P., Sun, J., Wu, J., Lu, W., Sun, Z., & Li, D. (2019). Long non-coding RNA HOTTIP enhances IL-6 expression to potentiate immune escape of ovarian cancer cells by upregulating the expression of PD-L1 in neutrophils. *J Exp Clin Cancer Res*, *38*(1), 411. https://doi.org/10.1186/s13046-019-1394-6

Shaul, M. E., & Fridlender, Z. G. (2017). Neutrophils as active regulators of the immune system in the tumor microenvironment. *J Leukoc Biol*, *102*(2), 343-349. https://doi.org/10.1189/jlb.5MR1216-508R

Shi, D., Shi, Y., Kaseb, A. O., Qi, X., Zhang, Y., Chi, J., Lu, Q., Gao, H., Jiang, H., Wang, H., Yuan, D., Ma, H., Wang, H., Li, Z., & Zhai, B. (2020). Chimeric Antigen Receptor-Glypican-3 T-Cell Therapy for Advanced Hepatocellular Carcinoma: Results of Phase I Trials. *Clin Cancer Res*, *26*(15), 3979-3989. https://doi.org/10.1158/1078-0432.CCR-19-3259

Shi, Y., Zhang, J., Mao, Z., Jiang, H., Liu, W., Shi, H., Ji, R., Xu, W., Qian, H., & Zhang, X. (2020). Extracellular Vesicles From Gastric Cancer Cells Induce PD-L1 Expression on Neutrophils to Suppress T-Cell Immunity. *Front Oncol*, *10*, 629. https://doi.org/10.3389/fonc.2020.00629

Shigeta, K., Matsui, A., Kikuchi, H., Klein, S., Mamessier, E., Chen, I. X., Aoki, S., Kitahara, S., Inoue, K., Shigeta, A., Hato, T., Ramjiawan, R. R., Staiculescu, D., Zopf, D., Fiebig, L., Hobbs, G. S., Quaas, A., Dima, S., Popescu, I., . . . Duda, D. G. (2020). Regorafenib combined with PD1 blockade increases CD8 T-cell infiltration by inducing CXCL10 expression in hepatocellular carcinoma. *J Immunother Cancer*, *8*(2). https://doi.org/10.1136/jitc-2020-001435

Shoji, S., Parmelee, D. C., Wade, R. D., Kumar, S., Ericsson, L. H., Walsh, K. A., Neurath, H., Long, G. L., Demaille, J. G., Fischer, E. H., & Titani, K. (1981). Complete amino acid sequence of the catalytic subunit of bovine cardiac muscle cyclic AMP-dependent protein kinase. *Proc Natl Acad Sci U S A*, *78*(2), 848-851. https://doi.org/10.1073/pnas.78.2.848

Sinha, P., Clements, V. K., Bunt, S. K., Albelda, S. M., & Ostrand-Rosenberg, S. (2007). Cross-talk between myeloid-derived suppressor cells and macrophages subverts tumor immunity toward a type 2 response. *J Immunol*, *179*(2), 977-983. https://doi.org/10.4049/jimmunol.179.2.977

Siveen, K. S., Prabhu, K. S., Achkar, I. W., Kuttikrishnan, S., Shyam, S., Khan, A. Q., Merhi, M., Dermime, S., & Uddin, S. (2018). Role of Non Receptor Tyrosine Kinases in Hematological Malignances and its Targeting by Natural Products. *Mol Cancer*, *17*(1), 31. https://doi.org/10.1186/s12943-018-0788-y

Song, J., Yang, R., Wei, R., Du, Y., He, P., & Liu, X. (2022). Pan-cancer analysis reveals RIPK2 predicts prognosis and promotes immune therapy resistance via triggering cytotoxic T lymphocytes dysfunction. *Mol Med*, *28*(1), 47. https://doi.org/10.1186/s10020-022-00475-8

Spranger, S., & Gajewski, T. F. (2018). Impact of oncogenic pathways on evasion of antitumour immune responses. *Nat Rev Cancer*, *18*(3), 139-147. https://doi.org/10.1038/nrc.2017.117

Sung, H., Ferlay, J., Siegel, R. L., Laversanne, M., Soerjomataram, I., Jemal, A., & Bray, F. (2021). Global Cancer Statistics 2020: GLOBOCAN Estimates of Incidence and Mortality Worldwide for 36 Cancers in 185 Countries. *CA Cancer J Clin*, *71*(3), 209-249. https://doi.org/10.3322/caac.21660

Sutton, A., Friand, V., Brule-Donneger, S., Chaigneau, T., Ziol, M., Sainte-Catherine, O., Poire, A., Saffar, L., Kraemer, M., Vassy, J., Nahon, P., Salzmann, J. L., Gattegno, L., & Charnaux, N. (2007). Stromal cell-derived factor-1/chemokine (C-X-C motif) ligand 12 stimulates human hepatoma cell growth, migration,

and invasion. *Mol Cancer Res*, *5*(1), 21-33. https://doi.org/10.1158/1541-7786.MCR-06-0103

Symeonides, S. N., Anderton, S. M., & Serrels, A. (2017). FAK-inhibition opens the door to checkpoint immunotherapy in Pancreatic Cancer. *J Immunother Cancer*, *5*, 17. https://doi.org/10.1186/s40425-017-0217-6

Tan, W., Luo, X., Li, W., Zhong, J., Cao, J., Zhu, S., Chen, X., Zhou, R., Shang, C., & Chen, Y. (2019). TNF-alpha is a potential therapeutic target to overcome sorafenib resistance in hepatocellular carcinoma. *EBioMedicine*, *40*, 446-456. https://doi.org/10.1016/j.ebiom.2018.12.047

Tian, S. S., Tapley, P., Sincich, C., Stein, R. B., Rosen, J., & Lamb, P. (1996). Multiple signaling pathways induced by granulocyte colony-stimulating factor involving activation of JAKs, STAT5, and/or STAT3 are required for regulation of three distinct classes of immediate early genes. *Blood*, *88*(12), 4435-4444. https://www.ncbi.nlm.nih.gov/pubmed/8977235

Tohumeken, S., Baur, R., Bottcher, M., Stoll, A., Loschinski, R., Panagiotidis, K., Braun, M., Saul, D., Volkl, S., Baur, A. S., Bruns, H., Mackensen, A., Jitschin, R., & Mougiakakos, D. (2020). Palmitoylated Proteins on AML-Derived Extracellular Vesicles Promote Myeloid-Derived Suppressor Cell Differentiation via TLR2/Akt/mTOR Signaling. *Cancer Res*, *80*(17), 3663-3676. https://doi.org/10.1158/0008-5472.CAN-20-0024

Torimura, T., & Iwamoto, H. (2022). Treatment and the prognosis of hepatocellular carcinoma in Asia. *Liver Int*, *42*(9), 2042-2054. https://doi.org/10.1111/liv.15130

Tornesello, M. L., Tornesello, A. L., Starita, N., Cerasuolo, A., Izzo, F., Buonaguro, L., & Buonaguro, F. M. (2022). Telomerase: a good target in hepatocellular carcinoma? An overview of relevant preclinical data. *Expert Opin Ther Targets*, *26*(9), 767-780. https://doi.org/10.1080/14728222.2022.2147062

Totoki, Y., Tatsuno, K., Covington, K. R., Ueda, H., Creighton, C. J., Kato, M., Tsuji, S., Donehower, L. A., Slagle, B. L., Nakamura, H., Yamamoto, S., Shinbrot, E., Hama, N., Lehmkuhl, M., Hosoda, F., Arai, Y., Walker, K., Dahdouli, M., Gotoh, K., . . . Shibata, T. (2014). Trans-ancestry mutational landscape of hepatocellular carcinoma genomes. *Nat Genet*, *46*(12), 1267-1273. https://doi.org/10.1038/ng.3126

Vendetti, F. P., Karukonda, P., Clump, D. A., Teo, T., Lalonde, R., Nugent, K., Ballew, M., Kiesel, B. F., Beumer, J. H., Sarkar, S. N., Conrads, T. P., O'Connor, M. J., Ferris, R. L., Tran, P. T., Delgoffe, G. M., & Bakkenist, C. J. (2018). ATR kinase inhibitor AZD6738 potentiates CD8+ T cell-dependent antitumor activity following radiation. *J Clin Invest*, *128*(9), 3926-3940.

https://doi.org/10.1172/JCI96519

Villanueva, A. (2019). Hepatocellular Carcinoma. *N Engl J Med*, *380*(15), 1450-1462. https://doi.org/10.1056/NEJMra1713263

Vonwirth, V., Bulbul, Y., Werner, A., Echchannaoui, H., Windschmitt, J., Habermeier, A., Ioannidis, S., Shin, N., Conradi, R., Bros, M., Tenzer, S., Theobald, M., Closs, E. I., & Munder, M. (2020). Inhibition of Arginase 1 Liberates Potent T Cell Immunostimulatory Activity of Human Neutrophil Granulocytes. *Front Immunol*, *11*, 617699. https://doi.org/10.3389/fimmu.2020.617699

Wang, H., Wang, X., Li, X., Fan, Y., Li, G., Guo, C., Zhu, F., Zhang, L., & Shi, Y. (2014). CD68(+)HLA-DR(+) M1-like macrophages promote motility of HCC cells via NF-kappaB/FAK pathway. *Cancer Lett*, *345*(1), 91-99. https://doi.org/10.1016/j.canlet.2013.11.013

Wang, T. T., Zhao, Y. L., Peng, L. S., Chen, N., Chen, W., Lv, Y. P., Mao, F. Y., Zhang, J. Y., Cheng, P., Teng, Y. S., Fu, X. L., Yu, P. W., Guo, G., Luo, P., Zhuang, Y., & Zou, Q. M. (2017). Tumour-activated neutrophils in gastric cancer foster immune suppression and disease progression through GM-CSF-PD-L1 pathway. *Gut*, *66*(11), 1900-1911. https://doi.org/10.1136/gutjnl-2016-313075

Wang, X., Tokheim, C., Gu, S. S., Wang, B., Tang, Q., Li, Y., Traugh, N., Zeng, Z., Zhang, Y., Li, Z., Zhang, B., Fu, J., Xiao, T., Li, W., Meyer, C. A., Chu, J., Jiang, P., Cejas, P., Lim, K., . . . Liu, X. S. (2021). In vivo CRISPR screens identify the E3 ligase Cop1 as a modulator of macrophage infiltration and cancer immunotherapy target. *Cell*, *184*(21), 5357-5374 e5322. https://doi.org/10.1016/j.cell.2021.09.006

Watanabe, Y., Fukuda, T., Hayashi, C., Nakao, Y., Toyoda, M., Kawakami, K., Shinjo, T., Iwashita, M., Yamato, H., Yotsumoto, K., Taketomi, T., Uchiumi, T., Sanui, T., & Nishimura, F. (2022). Extracellular vesicles derived from GMSCs stimulated with TNF-alpha and IFN-alpha promote M2 macrophage polarization via enhanced CD73 and CD5L expression. *Sci Rep*, *12*(1), 13344. https://doi.org/10.1038/s41598-022-17692-0

Weber, A., Boege, Y., Reisinger, F., & Heikenwalder, M. (2011). Chronic liver inflammation and hepatocellular carcinoma: persistence matters. *Swiss Med Wkly*, *141*, w13197. https://doi.org/10.4414/smw.2011.13197

Weber, R., Groth, C., Lasser, S., Arkhypov, I., Petrova, V., Altevogt, P., Utikal, J., & Umansky, V. (2021). IL-6 as a major regulator of MDSC activity and possible target for cancer immunotherapy. *Cell Immunol*, *359*, 104254. https://doi.org/10.1016/j.cellimm.2020.104254

Wong, M., Hyodo, T., Asano, E., Funasaka, K., Miyahara, R., Hirooka, Y., Goto, H., Hamaguchi, M., & Senga, T. (2014). Silencing of STRN4 suppresses the

malignant characteristics of cancer cells. *Cancer Sci*, *105*(12), 1526-1532. https://doi.org/10.1111/cas.12541

Wong, V. W., Yu, J., Cheng, A. S., Wong, G. L., Chan, H. Y., Chu, E. S., Ng, E. K., Chan, F. K., Sung, J. J., & Chan, H. L. (2009). High serum interleukin-6 level predicts future hepatocellular carcinoma development in patients with chronic hepatitis B. *Int J Cancer*, *124*(12), 2766-2770. https://doi.org/10.1002/ijc.24281

Woo, H. G., Park, E. S., Cheon, J. H., Kim, J. H., Lee, J. S., Park, B. J., Kim, W., Park, S. C., Chung, Y. J., Kim, B. G., Yoon, J. H., Lee, H. S., Kim, C. Y., Yi, N. J., Suh, K. S., Lee, K. U., Chu, I. S., Roskams, T., Thorgeirsson, S. S., & Kim, Y. J. (2008). Gene expression-based recurrence prediction of hepatitis B virus-related human hepatocellular carcinoma. *Clin Cancer Res*, *14*(7), 2056-2064. https://doi.org/10.1158/1078-0432.CCR-07-1473

Wu, K., Kryczek, I., Chen, L., Zou, W., & Welling, T. H. (2009). Kupffer cell suppression of CD8+ T cells in human hepatocellular carcinoma is mediated by B7-H1/programmed death-1 interactions. *Cancer Res*, *69*(20), 8067-8075. https://doi.org/10.1158/0008-5472.CAN-09-0901

Wu, Z., Weng, L., Zhang, T., Tian, H., Fang, L., Teng, H., Zhang, W., Gao, J., Hao, Y., Li, Y., Zhou, H., & Wang, P. (2019). Identification of Glutaminyl Cyclase isoenzyme isoQC as a regulator of SIRPalpha-CD47 axis. *Cell Res*, *29*(6), 502-505. https://doi.org/10.1038/s41422-019-0177-0

Xiao, Y., Cong, M., Li, J., He, D., Wu, Q., Tian, P., Wang, Y., Yang, S., Liang, C., Liang, Y., Wen, J., Liu, Y., Luo, W., Lv, X., He, Y., Cheng, D. D., Zhou, T., Zhao, W., Zhang, P., . . . Hu, G. (2021). Cathepsin C promotes breast cancer lung metastasis by modulating neutrophil infiltration and neutrophil extracellular trap formation. *Cancer Cell*, *39*(3), 423-437 e427. https://doi.org/10.1016/j.ccell.2020.12.012

Xu, J., Zhang, Y., Jia, R., Yue, C., Chang, L., Liu, R., Zhang, G., Zhao, C., Zhang, Y., Chen, C., Wang, Y., Yi, X., Hu, Z., Zou, J., & Wang, Q. (2019). Anti-PD-1 Antibody SHR-1210 Combined with Apatinib for Advanced Hepatocellular Carcinoma, Gastric, or Esophagogastric Junction Cancer: An Open-label, Dose Escalation and Expansion Study. *Clin Cancer Res*, *25*(2), 515-523. https://doi.org/10.1158/1078-0432.CCR-18-2484

Xue, J., Ge, X., Zhao, W., Xue, L., Dai, C., Lin, F., & Peng, W. (2019). PIPKIgamma Regulates CCL2 Expression in Colorectal Cancer by Activating AKT-STAT3 Signaling. *J Immunol Res*, *2019*, 3690561. https://doi.org/10.1155/2019/3690561

Yang, Q., Modi, P., Newcomb, T., Queva, C., & Gandhi, V. (2015). Idelalisib: First-in-Class PI3K Delta Inhibitor for the Treatment of Chronic Lymphocytic Leukemia,

Small Lymphocytic Leukemia, and Follicular Lymphoma. *Clin Cancer Res*, *21*(7), 1537-1542. https://doi.org/10.1158/1078-0432.CCR-14-2034

Yau, T., Kang, Y. K., Kim, T. Y., El-Khoueiry, A. B., Santoro, A., Sangro, B., Melero, I., Kudo, M., Hou, M. M., Matilla, A., Tovoli, F., Knox, J. J., Ruth He, A., El-Rayes, B. F., Acosta-Rivera, M., Lim, H. Y., Neely, J., Shen, Y., Wisniewski, T., . . . Hsu, C. (2020). Efficacy and Safety of Nivolumab Plus Ipilimumab in Patients With Advanced Hepatocellular Carcinoma Previously Treated With Sorafenib: The CheckMate 040 Randomized Clinical Trial. *JAMA Oncol*, *6*(11), e204564. https://doi.org/10.1001/jamaoncol.2020.4564

Yau, T., Park, J. W., Finn, R. S., Cheng, A. L., Mathurin, P., Edeline, J., Kudo, M., Harding, J. J., Merle, P., Rosmorduc, O., Wyrwicz, L., Schott, E., Choo, S. P., Kelley, R. K., Sieghart, W., Assenat, E., Zaucha, R., Furuse, J., Abou-Alfa, G. K., . . . Sangro, B. (2022). Nivolumab versus sorafenib in advanced hepatocellular carcinoma (CheckMate 459): a randomised, multicentre, open-label, phase 3 trial. *Lancet Oncol*, *23*(1), 77-90. https://doi.org/10.1016/S1470-2045(21)00604-5

Yi, C., Chen, L., Lin, Z., Liu, L., Shao, W., Zhang, R., Lin, J., Zhang, J., Zhu, W., Jia, H., Qin, L., Lu, L., & Chen, J. (2021). Lenvatinib Targets FGF Receptor 4 to Enhance Antitumor Immune Response of Anti-Programmed Cell Death-1 in HCC. *Hepatology*, *74*(5), 2544-2560. https://doi.org/10.1002/hep.31921

Yoong, K. F., Afford, S. C., Jones, R., Aujla, P., Qin, S., Price, K., Hubscher, S. G., & Adams, D. H. (1999). Expression and function of CXC and CC chemokines in human malignant liver tumors: a role for human monokine induced by gamma-interferon in lymphocyte recruitment to hepatocellular carcinoma. *Hepatology*, *30*(1), 100-111. https://doi.org/10.1002/hep.510300147

Yue, M., Luo, D., Yu, S., Liu, P., Zhou, Q., Hu, M., Liu, Y., Wang, S., Huang, Q., Niu, Y., Lu, L., & Hu, H. (2016). Misshapen/NIK-related kinase (MINK1) is involved in platelet function, hemostasis, and thrombus formation. *Blood*, *127*(7), 927-937. https://doi.org/10.1182/blood-2015-07-659185

Zahran, A. M., Hetta, H. F., Rayan, A., Eldin, A. S., Hassan, E. A., Fakhry, H., Soliman, A., & El-Badawy, O. (2020). Differential expression of Tim-3, PD-1, and CCR5 on peripheral T and B lymphocytes in hepatitis C virus-related hepatocellular carcinoma and their impact on treatment outcomes. *Cancer Immunol Immunother*, *69*(7), 1253-1263. https://doi.org/10.1007/s00262-019-02465-y

Zecca, A., Barili, V., Olivani, A., Biasini, E., Boni, C., Fisicaro, P., Montali, I., Tiezzi, C., Dalla Valle, R., Ferrari, C., Cariani, E., & Missale, G. (2022). Targeting Stress Sensor Kinases in Hepatocellular Carcinoma-Infiltrating Human NK Cells as a Novel Immunotherapeutic Strategy for Liver Cancer. *Front Immunol*,

13, 875072. https://doi.org/10.3389/fimmu.2022.875072

Zhang, J., Lei, H., & Li, X. (2021). LncRNA SNHG14 contributes to proinflammatory cytokine production in rheumatoid arthritis via the regulation of the miR-17-5p/MINK1-JNK pathway. *Environ Toxicol*, *36*(12), 2484-2492. https://doi.org/10.1002/tox.23361

Zhang, M., Pang, H. J., Zhao, W., Li, Y. F., Yan, L. X., Dong, Z. Y., & He, X. F. (2018). VISTA expression associated with CD8 confers a favorable immune microenvironment and better overall survival in hepatocellular carcinoma. *BMC Cancer*, *18*(1), 511. https://doi.org/10.1186/s12885-018-4435-1

Zhang, Q. B., Jia, Q. A., Wang, H., Hu, C. X., Sun, D., Jiang, R. D., & Zhang, Z. L. (2016). High-mobility group protein box1 expression correlates with peritumoral macrophage infiltration and unfavorable prognosis in patients with hepatocellular carcinoma and cirrhosis. *BMC Cancer*, *16*(1), 880. https://doi.org/10.1186/s12885-016-2883-z

Zhang, R., Zhang, Z., Liu, Z., Wei, D., Wu, X., Bian, H., & Chen, Z. (2019). Adoptive cell transfer therapy for hepatocellular carcinoma. *Front Med*, *13*(1), 3-11. https://doi.org/10.1007/s11684-019-0684-x

Zhang, X., & Xu, W. (2017). Neutrophils diminish T-cell immunity to foster gastric cancer progression: the role of GM-CSF/PD-L1/PD-1 signalling pathway. *Gut*, *66*(11), 1878-1880. https://doi.org/10.1136/gutjnl-2017-313923

Zhang, Z., Lee, J. C., Lin, L., Olivas, V., Au, V., LaFramboise, T., Abdel-Rahman, M., Wang, X., Levine, A. D., Rho, J. K., Choi, Y. J., Choi, C. M., Kim, S. W., Jang, S. J., Park, Y. S., Kim, W. S., Lee, D. H., Lee, J. S., Miller, V. A., . . . Bivona, T. G. (2012). Activation of the AXL kinase causes resistance to EGFR-targeted therapy in lung cancer. *Nat Genet*, *44*(8), 852-860. https://doi.org/10.1038/ng.2330

Zhao, H., Wu, L., Yan, G., Chen, Y., Zhou, M., Wu, Y., & Li, Y. (2021). Inflammation and tumor progression: signaling pathways and targeted intervention. *Signal Transduct Target Ther*, *6*(1), 263. https://doi.org/10.1038/s41392-021-00658-5

Zheng, Y., Liu, Y., Zhang, F., Su, C., Chen, X., Zhang, M., Sun, M., Sun, Y., & Xing, L. (2023). Radiation combined with KRAS-MEK inhibitors enhances anticancer immunity in KRAS-mutated tumor models. *Transl Res*, *252*, 79-90. https://doi.org/10.1016/j.trsl.2022.08.005

Zhou, J., Ding, T., Pan, W., Zhu, L. Y., Li, L., & Zheng, L. (2009). Increased intratumoral regulatory T cells are related to intratumoral macrophages and poor prognosis in hepatocellular carcinoma patients. *Int J Cancer*, *125*(7), 1640-1648. https://doi.org/10.1002/ijc.24556

Zhou, J., Sun, H., Wang, Z., Cong, W., Wang, J., Zeng, M., Zhou, W., Bie, P., Liu, L.,

Wen, T., Han, G., Wang, M., Liu, R., Lu, L., Ren, Z., Chen, M., Zeng, Z., Liang, P., Liang, C., . . . Fan, J. (2020). Guidelines for the Diagnosis and Treatment of Hepatocellular Carcinoma (2019 Edition). *Liver Cancer*, *9*(6), 682-720. https://doi.org/10.1159/000509424

Zhou, S. L., Zhou, Z. J., Hu, Z. Q., Huang, X. W., Wang, Z., Chen, E. B., Fan, J., Cao, Y., Dai, Z., & Zhou, J. (2016). Tumor-Associated Neutrophils Recruit Macrophages and T-Regulatory Cells to Promote Progression of Hepatocellular Carcinoma and Resistance to Sorafenib. *Gastroenterology*, *150*(7), 1646-1658 e1617. https://doi.org/10.1053/j.gastro.2016.02.040

Zhou, Z., Qin, H., Weng, L., & Ni, Y. (2019). Clinical efficacy of DC-CIK combined with sorafenib in the treatment of advanced hepatocellular carcinoma. *J BUON*, *24*(2), 615-621. https://www.ncbi.nlm.nih.gov/pubmed/31128014

Zhu, A. X., Finn, R. S., Edeline, J., Cattan, S., Ogasawara, S., Palmer, D., Verslype, C., Zagonel, V., Fartoux, L., Vogel, A., Sarker, D., Verset, G., Chan, S. L., Knox, J., Daniele, B., Webber, A. L., Ebbinghaus, S. W., Ma, J., Siegel, A. B., . . . investigators, K.-. (2018). Pembrolizumab in patients with advanced hepatocellular carcinoma previously treated with sorafenib (KEYNOTE-224): a non-randomised, open-label phase 2 trial. *Lancet Oncol*, *19*(7), 940-952. https://doi.org/10.1016/S1470-2045(18)30351-6

Zhu, H., Ye, B., Qiao, Z., Zeng, L., & Li, Q. (2019). Hepatectomy combined with sorafenib in patients with intermediate-advanced hepatocellullar carcinoma. *J BUON*, *24*(4), 1382-1389. https://www.ncbi.nlm.nih.gov/pubmed/31646781

Zhu, J., Fang, P., Wang, C., Gu, M., Pan, B., Guo, W., Yang, X., & Wang, B. (2021). The immunomodulatory activity of lenvatinib prompts the survival of patients with advanced hepatocellular carcinoma. *Cancer Med*, *10*(22), 7977-7987. https://doi.org/10.1002/cam4.4312

Zhu, K., Jin, X., Chi, Z., Chen, S., Wu, S., Sloan, R. D., Lin, X., Neculai, D., Wang, D., Hu, H., & Lu, L. (2021). Priming of NLRP3 inflammasome activation by Msn kinase MINK1 in macrophages. *Cell Mol Immunol*, *18*(10), 2372-2382. https://doi.org/10.1038/s41423-021-00761-1

Zhu, K. L., L. (2020). Enhanced anti-tumor response upon deficiency of Msn kinase MINK1 in mice. *J Immunol*, *204*(165), 28.

Zucman-Rossi, J., Villanueva, A., Nault, J. C., & Llovet, J. M. (2015). Genetic Landscape and Biomarkers of Hepatocellular Carcinoma. *Gastroenterology*, *149*(5), 1226-1239 e1224. https://doi.org/10.1053/j.gastro.2015.05.061